AD_____

Award Number: DAMD17-99-1-9226

TITLE: New Transfer Theory Relationships for Signal and Noise Analyses of X-ray Detectors

PRINCIPAL INVESTIGATOR: Ian A. Cunningham, Ph.D.

CONTRACTING ORGANIZATION: The John P. Robarts Research Institute
London, Ontario Canada N6A 5K8

REPORT DATE: November 2000

TYPE OF REPORT: Annual

PREPARED FOR: U.S. Army Medical Research and Materiel Command
Fort Detrick, Maryland 21702-5012

REPORT DOCUMENTATION PAGE

Form Approved
OMB No. 074-0188

1. AGENCY USE ONLY (Leave blank)	2. REPORT DATE	3. REPORT TYPE AND DATES COVERED
	November 2000	Annual (1 Oct 99 - 30 Sep 00)

4. TITLE AND SUBTITLE
New Transfer Theory Relationships for Signal and Noise Analyses of X-ray Detectors

5. FUNDING NUMBERS
DAMD17-99-1-9226

6. AUTHOR(S)
Ian A. Cunningham, Ph.D.

7. PERFORMING ORGANIZATION NAME(S) AND ADDRESS(ES)
The John P. Robarts Research Institute
London, Ontario, Canada N6A 5K8

E-MAIL:
icunning@irus.rri.on.ca

8. PERFORMING ORGANIZATION REPORT NUMBER

9. SPONSORING / MONITORING AGENCY NAME(S) AND ADDRESS(ES)
U.S. Army Medical Research and Materiel Command
Fort Detrick, Maryland 21702-5012

10. SPONSORING / MONITORING AGENCY REPORT NUMBER

11. SUPPLEMENTARY NOTES

12a. DISTRIBUTION / AVAILABILITY STATEMENT
Approved for public release; Distribution unlimited

12b. DISTRIBUTION CODE

13. ABSTRACT ***(Maximum 200 Words)***

X-ray mammography is currently the most reliable method available for the detection of breast cancer in screening programs, but it still does not detect all cancers. A great deal of research effort over the past several decades has been directed towards the development of better and more effective imaging systems. These new systems must be designed carefully to ensure they can produce images of the highest quality possible. Fourier-based linear-systems transfer theory is often used to develop theoretical models of the signal and noise performance of new system designs. While it has been used successfully in a number of new system designs, only relatively simple systems can be analyzed using this approach. We are developing new Fourier-based transfer relationships that will extend the capabilities of linear-systems theory so that it can be used in the design of increasingly complex systems.

The most important outcome of the first year of progress has been development of the idea of parallel cascaded of amplified point processes. Using it, linear-systems transfer theory can be used to predict the detective quantum efficiency (DQE) during the design of complex x-ray detectors being developed for digital mammography, to ensure optimal design of these detectors that will maximize image quality for any specified radiation dose to the patient.

14. SUBJECT TERMS
x-ray mammography, diagnostic imaging physics, linear-systems theory, imaging theory

15. NUMBER OF PAGES
50

16. PRICE CODE

17. SECURITY CLASSIFICATION OF REPORT	18. SECURITY CLASSIFICATION OF THIS PAGE	19. SECURITY CLASSIFICATION OF ABSTRACT	20. LIMITATION OF ABSTRACT
Unclassified	Unclassified	Unclassified	Unlimited

Table of Contents

Introduction

While x-ray mammography is the most reliable method available at present for the detection of breast cancer in screening programs, it still does not detect all cancers. A great deal of research effort over the past several decades has been directed towards the development of better and more effective imaging systems. These new systems must be designed carefully to ensure they can produce images of the highest quality possible for a specified radiation dose to the patient.

Fourier-based linear-systems transfer theory is often used to develop theoretical models of the signal and noise performance of new system designs. While it has been used successfully in a number of new system designs, only relatively simple systems can be analyzed using this approach. We are developing new theoretical relationships that will extend the capabilities of linear-systems theory so that it can be used in the design of increasingly complex systems. ***In particular, we are developing new Fourier-based transfer relationships for the description of: a) complex parallel cascades; and, b) digital detector systems. The result of our research will be a generalized resource "library" of transfer relationships to be used by scientists and engineers to achieve optimal designs of new imaging systems for mammography.***

Body

The following four tasks correspond to the four tasks outlined for Year 1 in the Statement of Work of our grant application. A statement of our progress on each task to date is summarized in this section.

Task 1. Develop Expertise in Stochastic Point-Process Theory

Stochastic point-process theory has been adopted as our primary means of mathematically representing the distribution of image quanta that collectively form a quantum image. This includes both x-ray images and optical images. In our work this year, we have also used this approach to represent the spatial distribution of particular events that take place within an imaging system, such as the distribution of photoelectric events, or the distribution of sites where characteristic x rays are re-absorbed. The use of stochastic point-process theory in medical imaging was recently pioneered by H.H. Barrett, and he remains one of only a few such experts in the world on this material.[1,2,3] Drs. Barrett and Myers are currently writing a new book scheduled for publication in 2001 that describes the fundamentals of this method.[3] The use of stochastic point-process theory is complex and requires more mathematical expertise in random processes than most scientists and engineers who design imaging systems can achieve in a reasonable time. However, use of the transfer-theory relationships can generally be accomplished by non-mathematicians, making the benefits of the complex statistical analysis available to system designers.

In the past year, we have developed our own expertise in the use of point-process theory to a level adequate for the analysis of medical imaging systems. Using this approach, each quantum is represented as a Dirac delta function distributed somewhere within the image and a quantum image is described as a spatial distribution of many such delta functions. What we call "image noise" is the impact of statistical correlations between these quanta. The mathematical relationship between these statistical correlations in the input x-ray image and the output digital image is described in terms of signal and noise "transfer-theory" relationships.

Task 2. Develop Expertise in Moment-Generating Function Theory

An additional skill needed for this work is expertise in moment-generating functions for this research. This has also be completed but was significantly easier than developing expertise in random point processes.

Task 3. Develop Concept of Cross Spectral Density of Parallel Cascades

A generalized approach to describing transfer of the noise power spectrum (NPS) through medical imaging systems has been developed over the past several years in which image-forming processes are represented in terms of a cascade of amplified point processes. Until recently, this approach has been restricted to serial cascades only. The development of a general expression for the cross spectral density of parallel cascades was the major task identified for the first year. This has been completed using the random point-process approach, and enables the use of parallel cascades of image-forming processes. A manuscript has been submitted for publication in Medical Physics[4] and a copy is included as Appendix I of this report. The final result of this work can be expressed as a single equation: the general expression for the cross covariance of amplified point processes and an expression for the cross spectral density for wide-sense stationary conditions is given by Eq. 81 in Appendix I.

These results extend the generalized transfer-theory approach to include the description of more complex image-forming processes involving parallel cascades of quantum amplification processes. This parallel-cascade approach has been used to develop a theoretical expression for noise-power transfer in a simple radiographic screen that includes the effect of characteristic x-ray reabsorption. The result confirms earlier work by Metz and Vyborny5 who showed that reabsorption increases image noise and decreases the detective quantum efficiency (DQE) at some spatial frequencies. Use of the transfer-theory approach facilitates a straightforward generalization to many new digital imaging systems including conventional angiographic and active-matrix flat-panel systems.

Task 4. Design and Construct Mono-Energetic X-Ray System

Task 4 was the development of a mono-energetic x-ray source based on a secondary lanthanum target. This has been designed and construction completed. This system is required to generate experimental proof of the correctness of the results described in Task 3 for reabsorption of characteristic radiation in a digital imaging system using a CsI input phosphor. During year II, experiments will be performed using both a conventional x-ray image intensifier system as well as a flat-panel detector using the General

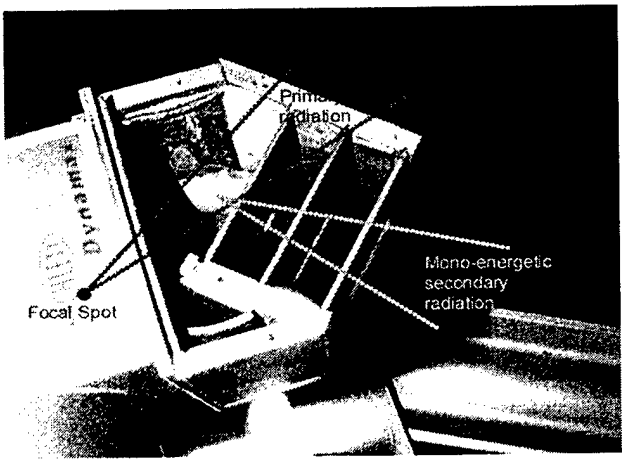

Figure 1. Photograph of mono-energetic x-ray source with top removed.

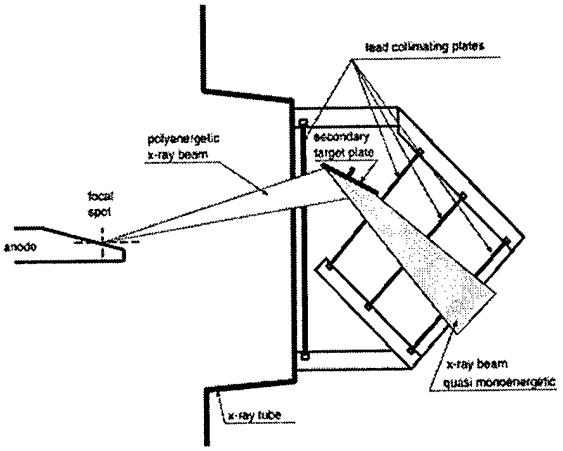

Figure 2. Schematic illustration of mono-energetic x-ray source.

Electric digital mammography system. Figure 1 shows a photograph of the mono-energetic source and Fig. 2 shows a schematic drawing of the design. It will be used to measure the DQE of the CsI-based systems just above and just below the iodine k edge. The difference in the DQE is due to the effects of reabsorption.

The results described here are consistent with the tasks identified in the approved grant application. No insurmountable difficulties are expected to prevent us from achieving the tasks identified for year II.

Key Research Accomplishments

The key research accomplishments are itemized here, consistent with the tasks identified above plus two additional accomplishments directly related to the current grant:

1. Develop expertise in stochastic point-process theory.

2. Develop concept of cross spectral density of amplified point processes. This has been the missing link preventing the use of parallel cascades in the design of complex digital imaging systems for mammography. A manuscript describing this result has been submitted for publication and is attached as Appendix I.

3. Design and build mono-energetic x-ray source for experimental verification of the parallel cascaded approach to understand the effects of self reabsorption in detectors.

4. Completion and submission of a paper describing how linear systems theory can be used to describe x-ray scatter in terms of a scatter operator, attached as Appendix II.[6]

5. A review chapter has been written in the past year and recently published by the Society for Optical Engineering.[7] This chapter consists of approximately 100 pages and describes the use of linear systems transfer theory in the design of digital x-ray detectors. Approximately 25% of this chapter is based on research completed during the first year of the current grant. This investigator has been invited to give a course on this material during the SPIE meeting in San Diego, February 2001.

Reportable Outcomes

Publications

(students working under my direct supervision indicated with •)

1. •J. Yao, •T.E. Moschandreou and I.A. Cunningham. *Parallel cascades: New ways to describe noise transfer in medical imaging systems*, Medical Physics [submitted].

2. I.A. Cunningham, •M.S. Westmore and A. Fenster. *Unified representation of image blur and noise in linear-systems transfer theory using a scatter operator*, Medical Physics [submitted].

3. I.A. Cunningham. *Applied linear-systems theory*, Chapter 2, Handbook of Medical Imaging, Vol 1.

Physics and Psychophysics, Eds. J. Beutel, H.L. Kundel and R.L. Van Metter, pp. 79-159 (The International Society for Optical Engineering, Bellingham, Washington, 2000).

Abstracts and Presentations

(students working under my direct supervision indicated with ●)

1. *Understanding radiologic image quality: From basic concepts to a practical tool-kit for scientists and engineers*, American Association of Physicists in Medicine and World Congress of Medical Physics and Biomedical Engineering, Chicago, July 2000.

2. ●J. Yao, ●T. Moschandreou and I.A. Cunningham, Cross Covariance of Correlated Point Processes for use in Linear-Systems Theory, World Congress of Medical Physics and Biomedical Engineering, Chicago, July 2000.

3. ●T. Moschandreou, ●J. Yao and I.A. Cunningham, Use of the Cross Covariance in Linear-Systems Theory to Model the DQE of Detectors with Fluorescence Reabsorption, World Congress of Medical Physics and Biomedical Engineering, Chicago, July 2000.

Conclusions

The most important outcome of the first year of progress has been development of the idea of parallel cascaded of amplified point processes. In particular, Eq. (81) of Appendix I describes the cross spectral density which has been the missing link preventing prior use of this approach. Using it, linear-systems transfer theory can be used to predict the detective quantum efficiency (DQE) during the design of complex x-ray detectors being developed for digital mammography, to ensure optimal design of these detectors that will maximize image quality for any specified radiation dose to the patient.

References

1. Papoulis,A."Probability, random variables, and stochastic processes," 3 (1991).

2. Snyder,D.L. and Miller,M.I."Random Point Processes in Time and Space," (1991).

3. Barrett,H.H. and Myers,K.J."Foundations of Image Science," (in preparation) (2001).

4. Yao,J., Moschandreou,T.E., and Cunningham,I.A."Parallel cascades: new ways to describe noise transfer in medical imaging systems," Medical Physics[submitted] (2000).

5. Metz,C.E. and Vyborny,C.J."Wiener spectral effects of spatial correlation between the sites of characteristic x-ray emission and reabsorption in radiographic screen-film systems," Physics in Medicine & Biology 28 547-564 (1983).

6. Cunningham,I.A., Westmore,M.S., and Fenster,A."Unified representation of image blur and noise using a scatter operator in linear-systems transfer theory using a scatter operator," Medical Physics[submitted] (2000).

7. Cunningham,I.A."Applied linear-systems theory," 79-159 (2000).

Appendix I: Parallel Cascades

This appendix consists of a copy of a manuscript submitted to Medical Physics. It describes the concept of parallel cascades in linear-systems transfer theory and is the primary outcome for year I.

Parallel cascades: New ways to describe noise transfer in medical imaging systems

J. Yao, T.E. Moschandreou
Imaging Research Laboratories, The John P. Robarts Research Institute, London, Ontario N6A 5K8, Canada

and I.A. Cunningham
Imaging Research Laboratories, The John P. Robarts Research Institute and Department of Diagnostic Radiology, London Health Sciences Center and The University of Western Ontario, London, Ontario, Canada

(November 16, 2000)

A generalized approach to describing transfer of the noise power spectrum (NPS) through medical imaging systems has been developed over the past several years in which image-forming processes are represented in terms of a cascade of amplified point processes. Until recently, this approach has been restricted to serial cascades only. Here, we develop a generalized expression for the cross covariance of amplified point processes and an expression for the cross spectral density for wide-sense stationary conditions. These results extend the generalized transfer-theory approach to include the description of more complex image-forming processes involving *parallel* cascades of quantum amplification processes.

This parallel-cascade approach is used to develop a theoretical expression for noise-power transfer in a simple radiographic screen that includes the effect of characteristic x-ray reabsorption. The result confirms earlier work by Metz and Vyborny who showed that reabsorption increases image noise and decreases the detective quantum efficiency (DQE) at low spatial frequencies. Use of the transfer-theory approach facilitates a straightforward generalization to many new digital imaging systems including conventional angiographic and active-matrix flat-panel systems.

Key words: random point processes, amplified point processes, cross covariance, cross spectral density, noise power spectrum, transfer theory

Submitted to Medical Physics May 2000

I. INTRODUCTION

Medical x-ray imaging systems must be designed to ensure that maximum image quality is obtained for a specified radiation dose to the patient. While there are many aspects of "image quality", one important consideration is image noise as described by the Wiener spectrum, or noise power spectrum (NPS) [1–3]. The NPS describes the spectral decomposition of second-moment statistics in terms of spatial frequencies under wide-sense stationary (WSS) conditions [2,3]. It is required for the determination of other image-quality metrics used to quantify image quality and system performance including the noise-equivalent number of quanta (NEQ) [1,4,5], which describes an equivalent number of quanta forming an image, and the detective quantum efficiency (DQE) [4–9], which describes the ability of an imaging system to make efficient use of the incident image quanta.

Over the past several years, a generalized transfer-theory approach [10–12] has been developed to describe how the NPS is transferred from the input of an imaging system to the output image [13–18]. Of particular significance in this development was a description of how the NPS is transferred through quantum gain and quantum scattering stages by Rabbani, Shaw and Van Metter [13] and by Barrett, Wagner and Myers [19,20]. This generalized description of image noise has resulted in a comprehensive frame-work for the understanding of system performance built upon a communication theory based approach.

Using this approach, many imaging systems can be represented in terms of serial cascades of three elementary processes: i) quantum amplification; ii) quantum scattering; and, iii) linear filters. Transfer of signal and noise through these models can be described by cascading transfer relationships of each elementary process. In Appendix A, transfer properties of these three elementary processes are summarized. This approach has been used recently to describe signal and noise transfer and the DQE of a number of x-ray medical imaging systems, including film screen systems [21–23], active-matrix flat-panel systems for digital radiography [24–26], video-based systems for portal imaging and radiation therapy verification [27,28], and other new system designs [29–32].

We are developing a number of new transfer-theory relationships to describe noise transfer through processes where the three elementary processes described above are inadequate. These new relationships form the basis of new theoretical "tools" that can be used by scientists and engineers developing or assessing new system designs. Of particular practical importance is the spatial-frequency-dependent form of these tools for

WSS conditions. They can be used to make a theoretical prediction of the NEQ or DQE of a particular system design.

One such current limitation of the transfer-theory approach is that it has been restricted to *serial* cascades of the elementary processes. This excludes the situation where more than one image-forming process must be summed to form an image [16]. For example, x rays interacting in a radiographic screen generally do so by the photo-electric interaction. This process often results in the emission of a characteristic x ray that may be reabsorbed elsewhere in the screen. Light is generated at both the primary-interaction and reabsorption sites, but with different intensities. In addition, the reabsorption site is randomly located but spatially correlated with the primary-interaction site. Light from both sites contribute to production of the final radiographic image recorded on film. However, it is not possible to describe image noise as the sum of these correlated image-forming processes using a simple serial cascade, and hence the effect of reabsorption has not been included in any transfer-theory analysis.

In this article, we extend the capabilities of the transfer-theory approach so that more complex systems requiring both serial and parallel cascades of these elementary processes can be represented. This is accomplished by developing a general expression for the cross covariance and cross spectral density of noise processes that can be incorporated into the transfer-theory analysis (see Appendix B). Use is made of random point process theory, where a quantum image is represented as a two-dimensional spatial point process in which each quantum is represented as a point impulse [19,20,33]. A general expression is derived for the cross covariance of two correlated random point processes. This is then simplified for the special case of wide-sense stationary random point processes where the cross spectral density function is derived.

We derive here a general expression for the cross covariance of a pair of correlated point processes. Of practical importance for applications in medical imaging is the special case where each point process represents a subset of a common input point distribution. The cross covariance of these two subsets is derived, and then generalized to describe the cross covariance of the two distributions after they subsequently undergo an arbitrary cascade of quantum amplification and scattering processes. It is shown that a very simple closed-form expression for the cross covariance and cross spectral density exists under WSS conditions, where the cross spectral density is the Fourier transform of the cross covariance. Use of the cross spectral density is then demonstrated in an analysis of noise in a radiographic screen with reabsorption. This problem was first solved by Metz and Vyborny [34] using a very different type of statistical analysis. Our work confirms their result, and is of a more general nature that is readily extended to describe reabsorption in other imaging systems including digital flat-panel radiographic systems.

Throughout the following description, we use a notation where the overhead tilde (eg. $\widetilde{N}$) indicates a random variable, overline (e.g. $\bar{q}$) indicates a mean value and bold face (eg. $\boldsymbol{r}$) indicates a vector.

II. THEORY

The framework of this analysis is based in part on earlier works by Barrett *et al.* [19,20] who developed the use of random point process theory for studying noise in imaging systems. A random point process is any random process for which all sample functions can be represented as a distribution of points, and we will represent each point as a spatial Dirac δ function. For instance, a quantum image is described as a spatial distribution of δ functions. However, these points may also represent a spatial distribution of certain events, such as a distribution of photo-electric events, or a distribution of photo-electric events when a K x ray is reabsorbed.

A random point process is associated with two important quantities: the location of points in space where events occur and the number of such points [33]. The mathematical realization of a spatial point process can be expressed as a sequence of random impulses, given by

$$\tilde{q}(\boldsymbol{r}) = \sum_{n=1}^{\widetilde{N}} \delta(\boldsymbol{r} - \tilde{\boldsymbol{r}}_n), \tag{1}$$

where $\boldsymbol{r}$ is a multidimensional spatial coordinate vector in space $\mathcal{S}$ where the point process is defined, $\tilde{\boldsymbol{r}}_n$ is a continuous random vector describing the location of the n^{th} point falling in $\mathcal{S}$ and $\widetilde{N}$ is a random variable describing the number of points. The ensemble of random vectors describing the positions of all $\widetilde{N}$ points is $\{\tilde{\boldsymbol{r}}_n : n = 1, 2, \cdots, \widetilde{N}\}$. In this section, we derive a general expression for the cross covariance of two correlated point processes drawing on previous work by Barrett *et al.* [19,20].

A quantum image is represented as a sample $q(\boldsymbol{r})$ of the random point process given by Eq. (1), where the space $\mathcal{S}$ of points denotes the two-dimensional image area. Our analysis is also applicable to higher dimensional space. Although the size of $\mathcal{S}$ is arbitrary, an infinite size is required for the analysis under WSS conditions, and hence we consider $\mathcal{S}$ to be infinite in size.

A. Cross covariance of point processes

For the general case, we consider two random spatial point processes,

$$\tilde{q}_A(\boldsymbol{r}) = \sum_{n=1}^{\widetilde{N}^A} \delta\Big(\boldsymbol{r} - \tilde{\boldsymbol{r}}_n^A\Big), \tag{2}$$

and

$$\tilde{q}_B(\boldsymbol{r}) = \sum_{j=1}^{\widetilde{N}^B} \delta\Big(\boldsymbol{r} - \tilde{\boldsymbol{r}}_j^B\Big), \tag{3}$$

which may or may not be statistically correlated. The cross correlation of $\tilde{q}_A(\boldsymbol{r})$ and $\tilde{q}_B(\boldsymbol{r})$ is the mean of the product $q_A(\boldsymbol{r})q_B^*(\boldsymbol{r}')$ [2], i.e.,

$$\mathrm{R}_{AB}(\boldsymbol{r},\boldsymbol{r}') = \Big\langle \tilde{q}_A(\boldsymbol{r})\tilde{q}_B^*(\boldsymbol{r}') \Big\rangle, \tag{4}$$

where * denotes a complex conjugate and $\langle\ \rangle$ represents an expectation operator. The cross covariance of $\tilde{q}_A(\boldsymbol{r})$ and $\tilde{q}_B(\boldsymbol{r})$ is given by

$$\mathrm{K}_{AB}(\boldsymbol{r},\boldsymbol{r}') = \mathrm{R}_{AB}(\boldsymbol{r},\boldsymbol{r}') - \Big\langle \tilde{q}_A(\boldsymbol{r}) \Big\rangle \Big\langle \tilde{q}_B^*(\boldsymbol{r}') \Big\rangle. \tag{5}$$

Barrett *et al.* [19,20] have shown that the mean of $\tilde{q}_A(\boldsymbol{r})$ in Eq. (2) is given by

$$\bar{q}_A(\boldsymbol{r}) = \Big\langle \tilde{q}_A(\boldsymbol{r}) \Big\rangle = \left\langle \sum_{n=1}^{\widetilde{N}^A} \mathrm{pr}_{\tilde{\boldsymbol{r}}_n^A}(\boldsymbol{r}|N^A) \right\rangle_{\widetilde{N}^A}, \tag{6}$$

where $\mathrm{pr}_{\tilde{\boldsymbol{r}}_n^A}(\boldsymbol{r}|N^A)$ is the conditional probability density function of the n^{th} point of the process $\tilde{q}_A(\boldsymbol{r})$ evaluated at $\boldsymbol{r}_n = \boldsymbol{r}$ for a specified value of N^A, and we denote by $\langle\ \rangle_{\widetilde{N}^A}$ the average over $\widetilde{N}^A$. Similarly,

$$\bar{q}_B(\boldsymbol{r}) = \Big\langle \tilde{q}_B(\boldsymbol{r}) \Big\rangle = \left\langle \sum_{j=1}^{\widetilde{N}^B} \mathrm{pr}_{\tilde{\boldsymbol{r}}_j^B}(\boldsymbol{r}|N^B) \right\rangle_{\widetilde{N}^B}. \tag{7}$$

If $\tilde{q}_A(\boldsymbol{r})$ is statistically independent of $\tilde{q}_B(\boldsymbol{r})$, the cross correlation $\mathrm{R}_{AB}(\boldsymbol{r},\boldsymbol{r}')$ is equal to the product of their means, and the cross covariance $\mathrm{K}_{AB}(\boldsymbol{r},\boldsymbol{r}')$ in Eq. (5) becomes zero. Spatial point processes $\tilde{q}_A(\boldsymbol{r})$ and $\tilde{q}_B(\boldsymbol{r})$ are then called uncorrelated.

In order to calculate the mean of the product $\tilde{q}_A(\boldsymbol{r})\tilde{q}_B^*(\boldsymbol{r}')$ in Eq. (4) where $\tilde{q}_A(\boldsymbol{r})$ and $\tilde{q}_B(\boldsymbol{r})$ may be statistically correlated, we must average over all random quantities $\{\tilde{\boldsymbol{r}}_n^A\}$, $\{\tilde{\boldsymbol{r}}_j^B\}$, $\widetilde{N}^A$ and $\widetilde{N}^B$ in processes $\tilde{q}_A(\boldsymbol{r})$ and $\tilde{q}_B(\boldsymbol{r}')$. The procedure is divided into two steps [19]. The first one is to take the conditional expectation of the continuous random quantities $\{\tilde{\boldsymbol{r}}_n^A\}$ and $\{\tilde{\boldsymbol{r}}_j^B\}$ for fixed N^A and N^B. By definition of the statistical average over a continuous random variable, shown in Appendix C, we have

$$\begin{aligned}
&\mathrm{E}\Big\{\tilde{q}_A(\boldsymbol{r})\tilde{q}_B^*(\boldsymbol{r}')|N^A,N^B\Big\} \\
&= \int_\infty d\boldsymbol{r}_1^A \cdots \int_\infty d\boldsymbol{r}_{N^B}^B \Bigg\{ \sum_{n=1}^{N^A} \delta\Big(\boldsymbol{r} - \boldsymbol{r}_n^A\Big) \sum_{j=1}^{N^B} \delta\Big(\boldsymbol{r}' - \boldsymbol{r}_j^B\Big) \\
&\qquad \times \mathrm{pr}\Big(\Big\{\boldsymbol{r}_n^A\Big\},\Big\{\boldsymbol{r}_j^B\Big\}\Big|N^A,N^B\Big)\Bigg\} \\
&= \sum_{n=1}^{N^A}\sum_{j=1}^{N^B} \int_\infty d\boldsymbol{r}_1^A \cdots \int_\infty d\boldsymbol{r}_{N^B}^B \Big\{ \delta\Big(\boldsymbol{r} - \boldsymbol{r}_n^A\Big)\delta\Big(\boldsymbol{r}' - \boldsymbol{r}_j^B\Big) \\
&\qquad \times \mathrm{pr}\Big(\Big\{\boldsymbol{r}_n^A\Big\},\Big\{\boldsymbol{r}_j^B\Big\}\Big|N^A,N^B\Big)\Big\},
\end{aligned} \tag{8}$$

where $\mathrm{pr}(\{\boldsymbol{r}_n^A\},\{\boldsymbol{r}_j^B\}|N^A,N^B)$ is the conditional joint density function of random variables $\{\tilde{\boldsymbol{r}}_n^A\}$ and $\{\tilde{\boldsymbol{r}}_j^B\}$ given N^A and N^B, and we use the symbol $\int_\infty$ to denote a multidimensional integral over all $\mathcal{S}$. Using the property of marginal densities, shown in Appendix C, we obtain

$$\begin{aligned}
&\mathrm{E}\Big\{\tilde{q}_A(\boldsymbol{r})\tilde{q}_B^*(\boldsymbol{r}')|N^A,N^B\Big\} \\
&= \sum_{n=1}^{N^A}\sum_{j=1}^{N^B} \int_\infty d\boldsymbol{r}_n^A \int_\infty d\boldsymbol{r}_j^B \Big\{ \delta\Big(\boldsymbol{r} - \boldsymbol{r}_n^A\Big)\delta\Big(\boldsymbol{r}' - \boldsymbol{r}_j^B\Big) \\
&\qquad \times \mathrm{pr}_{\tilde{\boldsymbol{r}}_n^A,\tilde{\boldsymbol{r}}_j^B}\Big(\boldsymbol{r}_n^A,\boldsymbol{r}_j^B|N^A,N^B\Big)\Big\}.
\end{aligned} \tag{9}$$

It follows from the sifting property of delta functions that

$$\begin{aligned}
&\mathrm{E}\Big\{\tilde{q}_A(\boldsymbol{r})\tilde{q}_B^*(\boldsymbol{r}')|N^A,N^B\Big\} \\
&= \sum_{n=1}^{N^A}\sum_{j=1}^{N^B} \mathrm{pr}_{\tilde{\boldsymbol{r}}_n^A,\tilde{\boldsymbol{r}}_j^B}\Big(\boldsymbol{r},\boldsymbol{r}'|N^A,N^B\Big),
\end{aligned} \tag{10}$$

where $\mathrm{pr}_{\tilde{\boldsymbol{r}}_n^A,\tilde{\boldsymbol{r}}_j^B}(\boldsymbol{r},\boldsymbol{r}'|N^A,N^B)$ is the conditional joint density function of $\tilde{\boldsymbol{r}}_n^A$ and $\tilde{\boldsymbol{r}}_j^B$ for fixed N^A and N^B, evaluated at $\boldsymbol{r}_n^A = \boldsymbol{r}$ and $\boldsymbol{r}_j^B = \boldsymbol{r}'$. Next, by averaging Eq. (10) over $\widetilde{N}^A$ and $\widetilde{N}^B$, we obtain the cross correlation of $\tilde{q}_A(\boldsymbol{r})$ and $\tilde{q}_B(\boldsymbol{r})$ given by

$$\mathrm{R}_{AB}(\boldsymbol{r},\boldsymbol{r}') = \left\langle \sum_{n=1}^{\widetilde{N}^A}\sum_{j=1}^{\widetilde{N}^B} \mathrm{pr}_{\tilde{\boldsymbol{r}}_n^A,\tilde{\boldsymbol{r}}_j^B}\Big(\boldsymbol{r},\boldsymbol{r}'|N^A,N^B\Big) \right\rangle_{\widetilde{N}^A,\widetilde{N}^B}. \tag{11}$$

From Eqs. (5)–(7) and (11), therefore, the cross covariance of $\tilde{q}_A(\boldsymbol{r})$ and $\tilde{q}_B(\boldsymbol{r})$ is given by

$$\begin{aligned}
\mathrm{K}_{AB}(\boldsymbol{r},\boldsymbol{r}') &= \left\langle \sum_{n=1}^{\widetilde{N}^A}\sum_{j=1}^{\widetilde{N}^B} \mathrm{pr}_{\tilde{\boldsymbol{r}}_n^A,\tilde{\boldsymbol{r}}_j^B}\Big(\boldsymbol{r},\boldsymbol{r}'|N^A,N^B\Big) \right\rangle_{\widetilde{N}^A,\widetilde{N}^B} \\
&\quad - \left\langle \sum_{n=1}^{\widetilde{N}^A} \mathrm{pr}_{\tilde{\boldsymbol{r}}_n^A}\Big(\boldsymbol{r}|N^A\Big) \right\rangle_{\widetilde{N}^A} \left\langle \sum_{j=1}^{\widetilde{N}^B} \mathrm{pr}_{\tilde{\boldsymbol{r}}_j^B}\Big(\boldsymbol{r}'|N^B\Big) \right\rangle_{\widetilde{N}^B}.
\end{aligned} \tag{12}$$

Without loss of generality we assume that each point has the same conditional probability density function

for given N^A or N^B. The probability density functions are therefore independent of the indices n and j and we simplify our notation by using $\tilde{\boldsymbol{r}}^A$ and $\tilde{\boldsymbol{r}}^B$ instead of $\tilde{\boldsymbol{r}}_n^A$ and $\tilde{\boldsymbol{r}}_j^B$. Thus, Eq. (12) becomes

$$\mathrm{K}_{AB}(\boldsymbol{r},\boldsymbol{r}') = \left\langle \widetilde{N}^A \widetilde{N}^B \mathrm{pr}_{\tilde{\boldsymbol{r}}^A,\tilde{\boldsymbol{r}}^B}\left(\boldsymbol{r},\boldsymbol{r}'|N^A,N^B\right)\right\rangle_{\widetilde{N}^A,\widetilde{N}^B} - \left\langle \widetilde{N}^A \mathrm{pr}_{\tilde{\boldsymbol{r}}^A}\left(\boldsymbol{r}|N^A\right)\right\rangle_{\widetilde{N}^A} \left\langle \widetilde{N}^B \mathrm{pr}_{\tilde{\boldsymbol{r}}^B}\left(\boldsymbol{r}'|N^B\right)\right\rangle_{\widetilde{N}^B} \quad (13)$$

where the $\widetilde{N}^A \times \widetilde{N}^B$ terms in the double sum over n and j are identical.

Equation (13) is a general expression for the cross covariance of two random point processes. It is valid for both stationary and non-stationary random processes. For imaging applications where, in general, $\widetilde{N}^A, \widetilde{N}^B \gg 1$ and the probability density and the joint density functions are independent of N^A and N^B, the statistical nature of $\widetilde{N}^A$ and $\widetilde{N}^B$ can often be ignored and the cross covariance of two quantum images is then given by

$$\mathrm{K}_{AB}(\boldsymbol{r},\boldsymbol{r}') \approx N^A N^B \left[\mathrm{pr}_{\tilde{\boldsymbol{r}}^A,\tilde{\boldsymbol{r}}^B}(\boldsymbol{r},\boldsymbol{r}') - \mathrm{pr}_{\tilde{\boldsymbol{r}}^A}(\boldsymbol{r})\mathrm{pr}_{\tilde{\boldsymbol{r}}^B}(\boldsymbol{r}')\right]. \quad (14)$$

B. Cross covariance of random subsets of a random point process

If the quanta in two images are independent of each other, the cross covariance of the two images will be zero. This is certainly the case when two images are acquired independently of each other. However, we are interested in the special case where two point distributions (images) are not independent. A simple example of this occurs when the two point distributions are each random subsets of a common input point distribution or image. If quanta in the input image are statistically correlated, there will in general be a nonzero cross covariance between the two subsets. In this section, the cross covariance of two point distributions is determined when each represents a random subset of a correlated input image.

The process of randomly selecting points from a distribution is illustrated in Fig. 1. This random point-selection process represents a sequence of independent trials in which each trial makes a random determination for each point in the input distribution. The point is selected to path A with probability $\bar{\xi}$, and path B with probability $\bar{\zeta}$. That is, each trial is described in terms of two binomial random variables, denoted by $\tilde{\xi}_n$ and $\tilde{\zeta}_n$ for the n^{th} trial, where each random variable can have a value of 0 or 1 only. Each trial is independent of all others, but we will allow statistical relationships between variables $\tilde{\xi}_n$ and $\tilde{\zeta}_n$ for a given

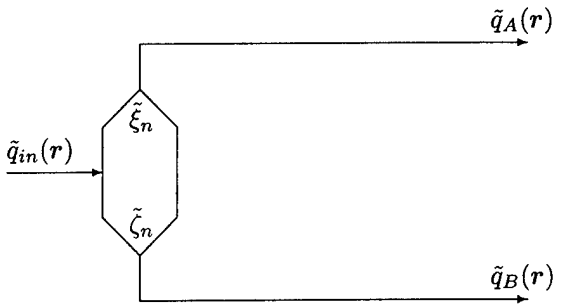

FIG. 1. Illustration of randomly selecting points from a random point process.

trial n. For N trials, the set of random variables $\tilde{\xi}_n$ and $\tilde{\zeta}_n$ required to describe a single image is given by $\{\tilde{\xi}_n, \tilde{\zeta}_n : n = 1, 2, \cdots, N\}$.

Similar to Eq. (1), the input is a general spatial point process rewritten as

$$\tilde{q}_{in}(\boldsymbol{r}) = \sum_{n=1}^{\widetilde{N}} \delta(\boldsymbol{r} - \widetilde{\boldsymbol{R}}_n), \quad (15)$$

where $\widetilde{\boldsymbol{R}}_n$ is a random vector describing the position of the n^{th} quantum in the input image. The point selection process is assumed to be independent of $\tilde{q}_{in}(\boldsymbol{r})$. The outputs $\tilde{q}_A(\boldsymbol{r})$ and $\tilde{q}_B(\boldsymbol{r})$ can therefore be written in terms of the random variables $\tilde{\xi}_n$ and $\tilde{\zeta}_n$ as

$$\begin{cases} \tilde{q}_A(\boldsymbol{r}) = \displaystyle\sum_{n=1}^{\widetilde{N}} \tilde{\xi}_n \, \delta(\boldsymbol{r} - \widetilde{\boldsymbol{R}}_n) \\ \tilde{q}_B(\boldsymbol{r}) = \displaystyle\sum_{n=1}^{\widetilde{N}} \tilde{\zeta}_n \, \delta(\boldsymbol{r} - \widetilde{\boldsymbol{R}}_n) \end{cases} . \quad (16)$$

In Eq. (16), the point processes $\tilde{q}_A(\boldsymbol{r})$ and $\tilde{q}_B(\boldsymbol{r})$ are random subsets of $\tilde{q}_{in}(\boldsymbol{r})$. We are interested in the cross covariance of $\tilde{q}_A(\boldsymbol{r})$ and $\tilde{q}_B(\boldsymbol{r})$. In the following, we examine both first-order and second-order statistics of $\tilde{q}_A(\boldsymbol{r})$ and $\tilde{q}_B(\boldsymbol{r})$.

1. Mean

We calculate the mean of $\tilde{q}_A(\boldsymbol{r})$ in Eq. (16), in two steps. The first step is to take the conditional expectation of $\tilde{q}_A(\boldsymbol{r})$ for fixed $\{\boldsymbol{R}_n\}$ and N, i.e., for fixed $q_{in}(\boldsymbol{r})$ refering to the sample space of $\tilde{q}_{in}(\boldsymbol{r})$, and then to average over $\tilde{q}_{in}(\boldsymbol{r})$. Thus, we have

$$\mathrm{E}\Big\{\tilde{q}_A(\boldsymbol{r})|q_{in}(\boldsymbol{r})\Big\} = \Big\langle \sum_{n=1}^{\widetilde{N}} \tilde{\xi}_n \delta(\boldsymbol{r}-\widetilde{\boldsymbol{R}}_n)\Big| q_{in}(\boldsymbol{r})\Big\rangle_{\tilde{\xi}_n}$$
$$= \sum_{n=1}^{N} \mathrm{E}\Big\{\tilde{\xi}_n\Big\}\delta(\boldsymbol{r}-\boldsymbol{R}_n)\Big|_{q_{in}(\boldsymbol{r})}$$
$$= \bar{\xi}\sum_{n=1}^{N}\delta(\boldsymbol{r}-\boldsymbol{R}_n) = \bar{\xi}\, q_{in}(\boldsymbol{r}). \quad (17)$$

where $\tilde{\xi}_n$ has the same mean value for all n, given by $\bar{\xi}$, and we use the symbol $|_{q_{in}(\boldsymbol{r})}$ to denote the computation condition, i.e., for fixed $q_{in}(\boldsymbol{r})$. Next, by averaging over $\tilde{q}_{in}(\boldsymbol{r})$, we can obtain the mean of $\tilde{q}_A(\boldsymbol{r})$ given by

$$\bar{q}_A(\boldsymbol{r}) = \mathrm{E}\Big\{\tilde{q}_A(\boldsymbol{r})\Big\} = \bar{\xi}\,\bar{q}_{in}(\boldsymbol{r}). \quad (18)$$

Similarly,

$$\bar{q}_B(\boldsymbol{r}) = \mathrm{E}\Big\{\tilde{q}_B(\boldsymbol{r})\Big\} = \bar{\zeta}\,\bar{q}_{in}(\boldsymbol{r}). \quad (19)$$

2. Cross correlation and cross covariance

The cross correlation of $\tilde{q}_A(\boldsymbol{r})$ and $\tilde{q}_B(\boldsymbol{r})$, $\mathrm{R}_{AB}(\boldsymbol{r},\boldsymbol{r}')$, is the mean of the product $\tilde{q}_A(\boldsymbol{r})\tilde{q}_B^*(\boldsymbol{r}')$, i.e.,

$$\mathrm{R}_{AB}(\boldsymbol{r},\boldsymbol{r}') = \mathrm{E}\Big\{\tilde{q}_A(\boldsymbol{r})\tilde{q}_B^*(\boldsymbol{r}')\Big\}$$
$$= \Big\langle \sum_{n=1}^{\widetilde{N}} \tilde{\xi}_n\,\delta(\boldsymbol{r}-\widetilde{\boldsymbol{R}}_n)\sum_{j=1}^{\widetilde{N}}\tilde{\zeta}_j\,\delta(\boldsymbol{r}'-\widetilde{\boldsymbol{R}}_j)\Big\rangle. \quad (20)$$

Again, using an approach similar to Barrett *et al.* [19], computation of the expectation in Eq. (20) is divided into two steps. That is, the first one is to average over $\{\tilde{\xi}_n\}$ and $\{\tilde{\zeta}_n\}$ for fixed input $q_{in}(\boldsymbol{r})$, and then average over $\tilde{q}_{in}(\boldsymbol{r})$. There are two cases to be considered in Eq. (20), corresponding to $n=j$ and $n\neq j$. When $n=j$, which has N terms,

$$\mathrm{E}\Big\{\tilde{q}_A(\boldsymbol{r})\tilde{q}_B^*(\boldsymbol{r}')|q_{in}(\boldsymbol{r})\Big\}\Big|_{n=j}$$
$$= \Big\langle \sum_{n=1}^{\widetilde{N}} \tilde{\xi}_n\tilde{\zeta}_n\,\delta(\boldsymbol{r}-\widetilde{\boldsymbol{R}}_n)\delta(\boldsymbol{r}'-\widetilde{\boldsymbol{R}}_n)\Big| q_{in}(\boldsymbol{r})\Big\rangle_{\tilde{\xi}_n,\tilde{\zeta}_n}\Big|_{n=j}. \quad (21)$$

It is convenient to denote the cross correlation of $\tilde{\xi}_n$ and $\tilde{\zeta}_n$ for $n=1,2,\cdots,N$ as $\mathrm{R}_{\xi\zeta} = \mathrm{E}\{\tilde{\xi}_n\tilde{\zeta}_n\}$. It is non-zero when the two random variables are non-orthogonal. For instance, if the two images A and B represent identical subsets of the input distribution, where $\tilde{\zeta}_n = \tilde{\xi}_n$, they are correlated and the cross correlation of $\tilde{\xi}_n$ and $\tilde{\zeta}_n$ is $\mathrm{R}_{\xi\zeta}$. If the two images represent complementary subsets, where there are no common points in A and B, then $\tilde{\zeta}_n$ is orthogonal with $\tilde{\xi}_n$, i.e., $\tilde{\zeta}_n = (1-\tilde{\xi}_n)$ and $\mathrm{R}_{\xi\zeta}=0$. With this notation, we have

$$\mathrm{E}\Big\{\tilde{q}_A(\boldsymbol{r})\tilde{q}_B^*(\boldsymbol{r}')|q_{in}(\boldsymbol{r})\Big\}\Big|_{n=j}$$
$$= \mathrm{R}_{\xi\zeta}\sum_{n=1}^{N}\delta(\boldsymbol{r}-\boldsymbol{R}_n)\delta(\boldsymbol{r}'-\boldsymbol{R}_n)\Big|_{n=j}$$
$$= \mathrm{R}_{\xi\zeta}\, q_{in}(\boldsymbol{r})q_{in}(\boldsymbol{r}')\Big|_{n=j}. \quad (22)$$

When $n\neq j$, random variable $\tilde{\xi}_n$ is independent of $\tilde{\zeta}_j$ and $\mathrm{E}\{\tilde{\xi}_n\tilde{\zeta}_j\} = \bar{\xi}\,\bar{\zeta}$. In this case, we have

$$\mathrm{E}\Big\{\tilde{q}_A(\boldsymbol{r})\tilde{q}_B^*(\boldsymbol{r}')|q_{in}(\boldsymbol{r})\Big\}\Big|_{n\neq j}$$
$$= \Big\langle \sum_{n=1}^{\widetilde{N}}\sum_{j=1}^{\widetilde{N}} \tilde{\xi}_n\tilde{\zeta}_j\,\delta(\boldsymbol{r}-\widetilde{\boldsymbol{R}}_n)\delta(\boldsymbol{r}'-\widetilde{\boldsymbol{R}}_j)\Big| q_{in}(\boldsymbol{r})\Big\rangle_{\tilde{\xi}_n,\tilde{\zeta}_j}\Big|_{n\neq j}$$
$$= \bar{\xi}\,\bar{\zeta}\sum_{n=1}^{N}\sum_{j=1}^{N}\delta(\boldsymbol{r}-\boldsymbol{R}_n)\delta(\boldsymbol{r}'-\boldsymbol{R}_j)\Big|_{n\neq j}$$
$$= \bar{\xi}\,\bar{\zeta}\, q_{in}(\boldsymbol{r})q_{in}(\boldsymbol{r}')\Big|_{n\neq j}. \quad (23)$$

Adding Eqs. (22) and (23), the conditional expectation of the product $\tilde{q}_A(\boldsymbol{r})\tilde{q}_B^*(\boldsymbol{r}')$ is given by

$$\mathrm{E}\Big\{\tilde{q}_A(\boldsymbol{r})\tilde{q}_B^*(\boldsymbol{r}')|q_{in}(\boldsymbol{r})\Big\}$$
$$= \mathrm{R}_{\xi\zeta}\, q_{in}(\boldsymbol{r})q_{in}(\boldsymbol{r}')\Big|_{n=j} + \bar{\xi}\,\bar{\zeta}\, q_{in}(\boldsymbol{r})q_{in}(\boldsymbol{r}')\Big|_{n\neq j} \quad (24)$$

which after averaging over $\tilde{q}_{in}(\boldsymbol{r})$ yields

$$\mathrm{R}_{AB}(\boldsymbol{r},\boldsymbol{r}') = \mathrm{R}_{\xi\zeta}\mathrm{R}_{in}(\boldsymbol{r},\boldsymbol{r}')\Big|_{n=j} + \bar{\xi}\,\bar{\zeta}\,\mathrm{R}_{in}(\boldsymbol{r},\boldsymbol{r}')\Big|_{n\neq j}, \quad (25)$$

where $\mathrm{R}_{in}(\boldsymbol{r},\boldsymbol{r}') = \mathrm{E}\{\tilde{q}_{in}(\boldsymbol{r})\tilde{q}_{in}^*(\boldsymbol{r}')\}$ is the autocorrelation of $\tilde{q}_{in}(\boldsymbol{r})$ and is given by

$$\mathrm{R}_{in}(\boldsymbol{r},\boldsymbol{r}') = \mathrm{R}_{in}(\boldsymbol{r},\boldsymbol{r}')\Big|_{n=j} + \mathrm{R}_{in}(\boldsymbol{r},\boldsymbol{r}')\Big|_{n\neq j}. \quad (26)$$

Equation (25) can be further simplified. Note that for a general point process as in Eq. (15), we have [19,20]

$$\mathrm{R}_{in}(\boldsymbol{r},\boldsymbol{r}')\Big|_{n=j} = \bar{q}_{in}(\boldsymbol{r})\delta(\boldsymbol{r}-\boldsymbol{r}'). \quad (27)$$

From Eqs. (25)–(27), therefore, the cross correlation of $\tilde{q}_A(\boldsymbol{r})$ and $\tilde{q}_B(\boldsymbol{r})$ becomes

$$\mathrm{R}_{AB}(\boldsymbol{r},\boldsymbol{r}') = (\mathrm{R}_{\xi\zeta} - \bar{\xi}\bar{\zeta})\bar{q}_{in}(\boldsymbol{r})\delta(\boldsymbol{r}-\boldsymbol{r}') + \bar{\xi}\,\bar{\zeta}\,\mathrm{R}_{in}(\boldsymbol{r},\boldsymbol{r}')$$
$$= \mathrm{K}_{\xi\zeta}\,\bar{q}_{in}(\boldsymbol{r})\delta(\boldsymbol{r}-\boldsymbol{r}') + \bar{\xi}\,\bar{\zeta}\,\mathrm{R}_{in}(\boldsymbol{r},\boldsymbol{r}'), \quad (28)$$

where $K_{\xi\zeta}$ is the cross covariance of random variables $\tilde{\xi}_n$ and $\tilde{\zeta}_n$, given by $K_{\xi\zeta} = R_{\xi\zeta} - \bar{\xi}\,\bar{\zeta}$.

Finally, the cross covariance of $\tilde{q}_A(\boldsymbol{r})$ and $\tilde{q}_B(\boldsymbol{r})$ is given by

$$\begin{aligned} K_{AB}(\boldsymbol{r},\boldsymbol{r}') &= R_{AB}(\boldsymbol{r},\boldsymbol{r}') - \bar{q}_A(\boldsymbol{r})\bar{q}_B(\boldsymbol{r}') \\ &= K_{\xi\zeta}\,\bar{q}_{in}(\boldsymbol{r})\delta(\boldsymbol{r}-\boldsymbol{r}') + \bar{\xi}\,\bar{\zeta}\,K_{in}(\boldsymbol{r},\boldsymbol{r}'), \quad (29) \end{aligned}$$

where $K_{in}(\boldsymbol{r},\boldsymbol{r}')$ is the autocovariance of the input point process $\tilde{q}_{in}(\boldsymbol{r})$.

Equation (29) is a general expression for the cross covariance of $\tilde{q}_A(\boldsymbol{r})$ and $\tilde{q}_B(\boldsymbol{r})$, where each is a random subset of the input point process. It consists of two components. The first represents uncorrelated noise power given as a δ function scaled by the cross covariance $K_{\xi\zeta}$ of the two binomial random variables and the mean number $\bar{q}_{in}(\boldsymbol{r})$ of quanta per unit area in the input. This component is zero when A and B represent independent subsets of the input, and non-zero otherwise. The second component represents correlated noise and is proportional to the cross covariance of the input point process $K_{in}(\boldsymbol{r},\boldsymbol{r}')$.

C. Cross covariance following an amplified point process

A more general case involves the cross covariance of two point processes that undergo an amplified point process subsequent to selection as illustrated in Fig. 2. Following the work of Rabbani, Shaw and Van Metter [13], and Barrett *et al.* [19,20], an amplified point process is considered to be a random point process where each point is converted into a random "cluster" of $\tilde{k}_n$ secondary points randomly distributed by the random vectors $\{\widetilde{\boldsymbol{\Delta}}_{nk} : k = 1,2,\cdots,\tilde{k}_n\}$, which is the cascade of the elementary processes, quantum gain and quantum scatter, described in Appendix A. If each amplification process is independent of all others, the point processes $\tilde{q}_A(\boldsymbol{r})$ and $\tilde{q}_B(\boldsymbol{r})$ in Fig. 2 can be written as

$$\begin{cases} \tilde{q}_A(\boldsymbol{r}) = \displaystyle\sum_{n=1}^{\widetilde{N}} \tilde{\xi}_n \sum_{k=1}^{\tilde{k}_n^A} \delta\Big(\boldsymbol{r} - \widetilde{\boldsymbol{R}}_n - \widetilde{\boldsymbol{\Delta}}_{nk}^{\,A}\Big) \\ \tilde{q}_B(\boldsymbol{r}) = \displaystyle\sum_{n=1}^{\widetilde{N}} \tilde{\zeta}_n \sum_{k=1}^{\tilde{k}_n^B} \delta\Big(\boldsymbol{r} - \widetilde{\boldsymbol{R}}_n - \widetilde{\boldsymbol{\Delta}}_{nk}^{\,B}\Big) \end{cases}, \quad (30)$$

where the n^{th} input quantum randomly located at $\widetilde{\boldsymbol{R}}_n$, if passed to paths A and B produce $\tilde{k}_n^A$ and $\tilde{k}_n^B$ quanta respectively, and

$$\tilde{\boldsymbol{r}}_{nk}^{\,A} \triangleq \widetilde{\boldsymbol{R}}_n + \widetilde{\boldsymbol{\Delta}}_{nk}^{\,A}$$

and

$$\tilde{\boldsymbol{r}}_{nk}^{\,B} \triangleq \widetilde{\boldsymbol{R}}_n + \widetilde{\boldsymbol{\Delta}}_{nk}^{\,B}$$

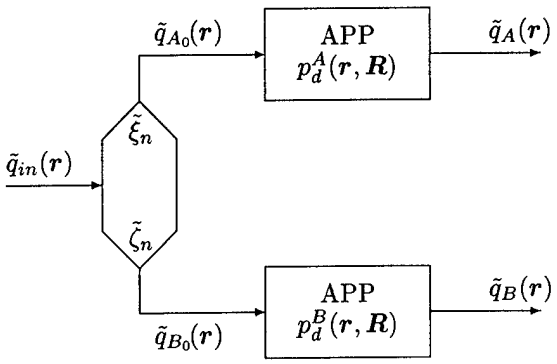

†APP: Amplified Point Process

FIG. 2. Two point processes following an amplified point process subsequent to selection of a random point process.

are random vectors describing the positions of the k^{th} quantum produced by the n^{th} primary in the image plane for each path. As assumed by Barrett *et al.* [19,20], we assume the random displacements $\widetilde{\boldsymbol{\Delta}}_{nk}^{\,A}$ and $\widetilde{\boldsymbol{\Delta}}_{nk}^{\,B}$ are independent of all others, possibly depending on the position of the primary for non-stationary processes.

Denote by $\mathrm{pr}_{\widetilde{\boldsymbol{\Delta}}}^{A}(\boldsymbol{\Delta}_{nk}^{A}|\boldsymbol{R}_n)$ the univariate probability density function of

$$\Big\{\widetilde{\boldsymbol{\Delta}}_{nk}^{\,A} : k = 1,2,\cdots,\tilde{k}_n;\ n = 1,2,\cdots,\tilde{N}\Big\}$$

given the primary $\boldsymbol{R}_n$. The following relationship is then known [19,20],

$$\mathrm{pr}_{\widetilde{\boldsymbol{\Delta}}}^{A}\Big(\boldsymbol{\Delta}_{nk}^{A}|\boldsymbol{R}_n\Big) = \Big[\bar{k}_n^A(\boldsymbol{R}_n)\Big]^{-1} p_d^A\Big(\boldsymbol{\Delta}_{nk}^{A} + \boldsymbol{R}_n, \boldsymbol{R}_n\Big), \quad (31)$$

where the mean number $\bar{k}_n^A(\boldsymbol{R}_n)$ of secondaries resulting from primary $\boldsymbol{R}_n$ in path A is

$$\bar{k}_n^A(\boldsymbol{R}_n) = \int_{\infty} d\boldsymbol{r}\, p_d^A(\boldsymbol{r},\boldsymbol{R}_n), \quad (32)$$

and $p_d^A(\boldsymbol{r},\boldsymbol{R}_n)$, for path A, is defined as the mean distribution of secondaries at $\boldsymbol{r}$ when a primary is absorbed at $\boldsymbol{R}_n$. Similarly for path B, we have

$$\mathrm{pr}_{\widetilde{\boldsymbol{\Delta}}}^{B}\Big(\boldsymbol{\Delta}_{nk}^{B}|\boldsymbol{R}_n\Big) = \Big[\bar{k}_n^B(\boldsymbol{R}_n)\Big]^{-1} p_d^B\Big(\boldsymbol{\Delta}_{nk}^{B} + \boldsymbol{R}_n, \boldsymbol{R}_n\Big), \quad (33)$$

where $\mathrm{pr}_{\widetilde{\boldsymbol{\Delta}}}^{B}(\boldsymbol{\Delta}_{nk}^{B}|\boldsymbol{R}_n)$ is the univariate probability density function of $\{\widetilde{\boldsymbol{\Delta}}_{nk}^{\,B}\}$ given $\boldsymbol{R}_n$, and

$$\bar{k}_n^B(\boldsymbol{R}_n) = \int_{\infty} d\boldsymbol{r}\, p_d^B(\boldsymbol{r},\boldsymbol{R}_n). \quad (34)$$

We now examine the means and cross covariance of $\tilde{q}_A(\boldsymbol{r})$ and $\tilde{q}_B(\boldsymbol{r})$ for these amplification processes.

1. Mean

The mean of the point processes $\tilde{q}_A(\boldsymbol{r})$ and $\tilde{q}_B(\boldsymbol{r})$ are calculated using an approach similar to that described by Barrett *et al.* [19]. For path A, the procedure is as follows.

(a) Average over displacements $\{\tilde{\boldsymbol{\Delta}}_{nk}^{A}\}$ for fixed $\boldsymbol{R}_n$;

(b) average over number $\tilde{k}_n^A$ of secondaries for fixed $\boldsymbol{R}_n$;

(c) average over binomial random variables $\tilde{\xi}_n$ for fixed $q_{in}(\boldsymbol{r})$;

(d) average over positions $\{\tilde{\boldsymbol{R}}_n\}$ of input quanta for fixed N; and,

(e) average over total number $\tilde{N}$ of input quanta to get the result $\mathrm{E}\{\tilde{q}_A(\boldsymbol{r})\}$.

Steps (a) and (b) calculate the conditional expectation of secondary points given a primary. Step (c) averages over the selection of quanta entering path A for fixed input. An average over the input point process is obtained in steps (d) and (e). In an attempt to simplify the notation, we will use the step label as a subscript to express the result of a step (a)–(e). For example, denote by $\mathrm{E}_{(a)}\{\tilde{q}_A(\boldsymbol{r})\}$ the result of step (a).

Step (a) is the statistical average over the continuous random vectors $\{\boldsymbol{\Delta}_{nk}^{A}\}$ given $\boldsymbol{R}_n$. In a similar way to Eqs. (8)–(10), we can obtain

$$\mathrm{E}_{(a)}\Big\{\tilde{q}_A(\boldsymbol{r})\Big\} = \sum_{n=1}^{N} \xi_n \sum_{k=1}^{k_n^A} \Big[\bar{k}_n(\boldsymbol{R}_n)\Big]^{-1} p_d^A(\boldsymbol{r}, \boldsymbol{R}_n), \quad (35)$$

where the probability density function $\mathrm{pr}_{\tilde{\boldsymbol{\Delta}}}^{A}(\boldsymbol{\Delta}_{nk}^{A}|\boldsymbol{R}_n)$ has been expressed in terms of $p_d^A(\boldsymbol{r}, \boldsymbol{R}_n)$ from Eq. (31). We can simplify Eq. (35) into

$$\mathrm{E}_{(a)}\Big\{\tilde{q}_A(\boldsymbol{r})\Big\} = \sum_{n=1}^{N} \xi_n k_n^A \Big[\bar{k}_n^A(\boldsymbol{R}_n)\Big]^{-1} p_d^A(\boldsymbol{r}, \boldsymbol{R}_n), \quad (36)$$

since the kernel in the sum over k is independent of k.

Step (b) requires the average of Eq. (36) over discrete value $\tilde{k}_n^A$ given $\boldsymbol{R}_n$. This leads to cancellation of $[\bar{k}_n^A(\boldsymbol{R}_n)]^{-1}$ in Eq. (36) because of the conditional expectation of $\tilde{k}_n^A$ given $\boldsymbol{R}_n$ as shown by $\mathrm{E}_{(b)}\{\tilde{k}_n^A\} = \bar{k}_n^A(\boldsymbol{R}_n)$. Thus

$$\mathrm{E}_{(b)}\Big\{\tilde{q}_A(\boldsymbol{r})\Big\} = \mathrm{E}_{(b)}\Big\{\mathrm{E}_{(a)}\Big\{\tilde{q}_A(\boldsymbol{r})\Big\}\Big\} = \sum_{n=1}^{N} \xi_n p_d^A(\boldsymbol{r}, \boldsymbol{R}_n). \quad (37)$$

Step (c) can be obtained simply by replacing ξ_n in Eq. (37) with $\bar{\xi}$, i.e.,

$$\mathrm{E}_{(c)}\Big\{\tilde{q}_A(\boldsymbol{r})\Big\} = \mathrm{E}_{(c)}\Big\{\mathrm{E}_{(b)}\Big\{\tilde{q}_A(\boldsymbol{r})\Big\}\Big\} = \sum_{n=1}^{N} \bar{\xi}\, p_d^A(\boldsymbol{r}, \boldsymbol{R}_n). \quad (38)$$

Step (d), for the continuous random variables $\{\tilde{\boldsymbol{R}}_n\}$ with the univariate conditional density function $\mathrm{pr}_{\tilde{\boldsymbol{R}}_n}(\boldsymbol{R}_n|N)$ given N, requires the computation of

$$\begin{aligned}
&\mathrm{E}_{(d)}\Big\{\tilde{q}_A(\boldsymbol{r})\Big\} \\
&= \int_\infty d\boldsymbol{R}_1 \cdots \int_\infty d\boldsymbol{R}_N \sum_{n=1}^{N} \bar{\xi}\, p_d^A(\boldsymbol{r}, \boldsymbol{R}_n)\, \mathrm{pr}_{\{\tilde{\boldsymbol{R}}_n\}}\Big(\{\boldsymbol{R}_n\}|N\Big) \\
&= \sum_{n=1}^{N} \bar{\xi} \int_\infty d\boldsymbol{R}_n\, p_d^A(\boldsymbol{r}, \boldsymbol{R}_n)\, \mathrm{pr}_{\tilde{\boldsymbol{R}}_n}(\boldsymbol{R}_n|N) \\
&= \sum_{n=1}^{N} \bar{\xi} \int_\infty d\boldsymbol{R}\, p_d^A(\boldsymbol{r}, \boldsymbol{R})\, \mathrm{pr}_{\tilde{\boldsymbol{R}}_n}(\boldsymbol{R}|N), \quad (39)
\end{aligned}$$

where the property of marginal densities was invoked and the integration variable $\boldsymbol{R}_n$ is renamed $\boldsymbol{R}$. Since the conditional expectation of $\tilde{q}_{in}(\boldsymbol{r})$ for fixed N is given by (see Eq. (6))

$$\mathrm{E}\Big\{\tilde{q}_{in}(\boldsymbol{r})|N\Big\} = \sum_{n=1}^{N} \mathrm{pr}_{\tilde{\boldsymbol{R}}_n}(\boldsymbol{r}|N), \quad (40)$$

then Eq. (39) becomes

$$\mathrm{E}_{(d)}\Big\{\tilde{q}_A(\boldsymbol{r})\Big\} = \bar{\xi} \int_\infty d\boldsymbol{R}\, p_d^A(\boldsymbol{r}, \boldsymbol{R})\, \mathrm{E}\Big\{\tilde{q}_{in}(\boldsymbol{R})|N\Big\}. \quad (41)$$

Step (e), the average of Eq. (41) over $\tilde{N}$, yields

$$\mathrm{E}\Big\{\tilde{q}_A(\boldsymbol{r})\Big\} = \bar{\xi} \int_\infty d\boldsymbol{R}\, p_d^A(\boldsymbol{r}, \boldsymbol{R})\, \bar{q}_{in}(\boldsymbol{R}), \quad (42)$$

where $\mathrm{E}\{\tilde{q}_{in}(\boldsymbol{R})|N\}$ is averaged over $\tilde{N}$. Since $\bar{q}_{A_0}(\boldsymbol{r}) = \bar{\xi}\,\bar{q}_{in}(\boldsymbol{r})$, where point process $\tilde{q}_{A_0}(\boldsymbol{r})$ is the output of the point-selection process for path A (see Fig. 2), we obtain

$$\mathrm{E}\Big\{\tilde{q}_A(\boldsymbol{r})\Big\} = \int_\infty d\boldsymbol{R}\, p_d^A(\boldsymbol{r}, \boldsymbol{R})\, \bar{q}_{A_0}(\boldsymbol{R}). \quad (43)$$

Equations (42) and (43) are general expressions for the mean of an amplified point process. Similarly, the mean of $\tilde{q}_B(\boldsymbol{r})$ is given by

$$\begin{aligned}
\mathrm{E}\Big\{\tilde{q}_B(\boldsymbol{r})\Big\} &= \bar{\zeta} \int_\infty d\boldsymbol{R}\, p_d^B(\boldsymbol{r}, \boldsymbol{R})\, \bar{q}_{in}(\boldsymbol{R}) \\
&= \int_\infty d\boldsymbol{R}\, p_d^B(\boldsymbol{r}, \boldsymbol{R})\, \bar{q}_{B_0}(\boldsymbol{R}). \quad (44)
\end{aligned}$$

2. Cross Correlation and Cross Covariance

We now calculate the cross correlation for the output point processes $\tilde{q}_A(\boldsymbol{r})$ and $\tilde{q}_B(\boldsymbol{r})$. By definition, $\mathrm{R}_{AB}(\boldsymbol{r},\boldsymbol{r}')$ is given by

$$\mathrm{R}_{AB}(\boldsymbol{r},\boldsymbol{r}') = \mathrm{E}\Big\{\tilde{q}_A(\boldsymbol{r})\tilde{q}_B^*(\boldsymbol{r}')\Big\}$$
$$= \left\langle \sum_{n=1}^{\widetilde{N}} \tilde{\xi}_n \sum_{k=1}^{\tilde{k}_n^A} \delta\Big(\boldsymbol{r}-\widetilde{\boldsymbol{R}}_n-\widetilde{\boldsymbol{\Delta}}_{nk}^{\,A}\Big) \sum_{n=1}^{\widetilde{N}} \tilde{\zeta}_n \sum_{k=1}^{\tilde{k}_n^B} \delta\Big(\boldsymbol{r}'-\widetilde{\boldsymbol{R}}_n-\widetilde{\boldsymbol{\Delta}}_{nk}^{\,B}\Big) \right\rangle. \tag{45}$$

Similar to the computation of the mean of $\tilde{q}_A(\boldsymbol{r})$, we calculate the expectation in Eq. (45) by the five steps (a)–(e) shown above. Step (a) is to average over displacements $\{\widetilde{\boldsymbol{\Delta}}_{nk}^{\,A}\}$ in $\tilde{q}_A(\boldsymbol{r})$ and $\{\widetilde{\boldsymbol{\Delta}}_{nk}^{\,B}\}$ in $\tilde{q}_B(\boldsymbol{r})$ for fixed $\{\boldsymbol{R}_n\}$, denoted by $\mathrm{E}_{(a)}\{\tilde{q}_A(\boldsymbol{r})\tilde{q}_B(\boldsymbol{r}')\}$. Step (b) is to average over $\tilde{k}_n^A$ and $\tilde{k}_n^B$ for fixed $\{\boldsymbol{R}_n\}$, denoted by $\mathrm{E}_{(b)}\{\tilde{q}_A(\boldsymbol{r})\tilde{q}_B(\boldsymbol{r}')\}$. We assume the point amplification processes in paths A and B may depend on incident locations $\{\boldsymbol{R}_n\}$, but are independent of all other terms. That is, both the gain factors $\{\tilde{k}_n^A\}$ and $\{\tilde{k}_n^B\}$ are independent for all n and the scatter vectors $\{\widetilde{\boldsymbol{\Delta}}_{nk}^{\,A}\}$ and $\{\widetilde{\boldsymbol{\Delta}}_{nk}^{\,B}\}$ are independent for all n and k. Therefore, we can write down the results for steps (a) and (b) as

$$\mathrm{E}_{(a)}\Big\{\tilde{q}_A(\boldsymbol{r})\tilde{q}_B(\boldsymbol{r}')\Big\} = \mathrm{E}_{(a)}\Big\{\tilde{q}_A(\boldsymbol{r})\Big\}\,\mathrm{E}_{(a)}\Big\{\tilde{q}_B(\boldsymbol{r}')\Big\} \tag{46}$$

and

$$\mathrm{E}_{(b)}\Big\{\tilde{q}_A(\boldsymbol{r})\tilde{q}_B(\boldsymbol{r}')\Big\} = \mathrm{E}_{(b)}\Big\{\tilde{q}_A(\boldsymbol{r})\Big\}\,\mathrm{E}_{(b)}\Big\{\tilde{q}_B(\boldsymbol{r}')\Big\} \tag{47}$$

respectively. From Eq. (37) and

$$\mathrm{E}_{(b)}\Big\{\tilde{q}_B(\boldsymbol{r}')\Big\} = \sum_{j=1}^{N} \zeta_j\, p_d^B(\boldsymbol{r}',\boldsymbol{R}_j), \tag{48}$$

we can obtain the following result,

$$\mathrm{E}_{(b)}\Big\{\tilde{q}_A(\boldsymbol{r})\tilde{q}_B(\boldsymbol{r}')\Big\} = \sum_{n=1}^{N}\sum_{j=1}^{N} \xi_n\zeta_j\, p_d^A(\boldsymbol{r},\boldsymbol{R}_n)\, p_d^B(\boldsymbol{r}',\boldsymbol{R}_j). \tag{49}$$

In order to average over $\{\tilde{\xi}_n\}$ and $\{\tilde{\zeta}_j\}$ for fixed $q_{in}(\boldsymbol{r})$ in step (c), we must consider two cases, denoted by $\mathrm{E}_{(c)}\{\tilde{q}_A(\boldsymbol{r})\tilde{q}_B(\boldsymbol{r}')\}|_{n=j}$ when $n=j$ and, by $\mathrm{E}_{(c)}\{\tilde{q}_A(\boldsymbol{r})\tilde{q}_B(\boldsymbol{r}')\}|_{n\neq j}$ when $n\neq j$. For the double sum over n and j in Eq. (49), there are N terms with $n=j$. Averaging these N terms in Eq. (49), yields

$$\mathrm{E}_{(c)}\Big\{\tilde{q}_A(\boldsymbol{r})\tilde{q}_B(\boldsymbol{r}')\Big\}\Big|_{n=j}$$
$$= \left\langle \sum_{n=1}^{\widetilde{N}} \tilde{\xi}_n\tilde{\zeta}_n\, p_d^A(\boldsymbol{r},\boldsymbol{R}_n)\, p_d^B(\boldsymbol{r}',\boldsymbol{R}_n) \right\rangle_{(c)}\Bigg|_{n=j}$$
$$= \sum_{n=1}^{N} \mathrm{E}\Big\{\tilde{\xi}_n\tilde{\zeta}_n\Big\}\, p_d^A(\boldsymbol{r},\boldsymbol{R}_n)\, p_d^B(\boldsymbol{r}',\boldsymbol{R}_n)$$
$$= \mathrm{R}_{\xi\zeta} \sum_{n=1}^{N} p_d^A(\boldsymbol{r},\boldsymbol{R}_n)\, p_d^B(\boldsymbol{r}',\boldsymbol{R}_n). \tag{50}$$

The calculation for Steps (d) and (e) on Eq. (50) is now similar to what was done in Eqs. (39)–(42). Thus, the result is given by

$$\mathrm{E}_{(e)}\Big\{\tilde{q}_A(\boldsymbol{r})\tilde{q}_B(\boldsymbol{r}')\Big\}\Big|_{n=j}$$
$$= \mathrm{R}_{\xi\zeta} \int_{\infty} d\boldsymbol{R}\, p_d^A(\boldsymbol{r},\boldsymbol{R}) p_d^B(\boldsymbol{r}',\boldsymbol{R})\, \bar{q}_{in}(\boldsymbol{R}). \tag{51}$$

Next, consider the case of $n\neq j$ for step (c). From Eq. (49), we have

$$\mathrm{E}_{(c)}\Big\{\tilde{q}_A(\boldsymbol{r})\tilde{q}_B(\boldsymbol{r}')\Big\}\Big|_{n\neq j}$$
$$= \left\langle \sum_{n=1}^{\widetilde{N}}\sum_{j=1}^{\widetilde{N}} \tilde{\xi}_n\tilde{\zeta}_j\, p_d^A(\boldsymbol{r},\boldsymbol{R}_n)\, p_d^B(\boldsymbol{r}',\boldsymbol{R}_j) \right\rangle_{(c)}\Bigg|_{n\neq j}$$
$$= \sum_{n=1}^{N}\sum_{j=1}^{N} \mathrm{E}\Big\{\tilde{\xi}_n\tilde{\zeta}_j\Big\}\, p_d^A(\boldsymbol{r},\boldsymbol{R}_n)\, p_d^B(\boldsymbol{r}',\boldsymbol{R}_j)\Big|_{n\neq j}$$
$$= \bar{\xi}\,\bar{\zeta} \sum_{n=1}^{N}\sum_{j=1}^{N} p_d^A(\boldsymbol{r},\boldsymbol{R}_n)\, p_d^B(\boldsymbol{r}',\boldsymbol{R}_j)\Big|_{n\neq j}. \tag{52}$$

Again, similarly as in Eq. (39), step (d) applied to Eq. (52) now gives

$$\mathrm{E}_{(d)}\Big\{\tilde{q}_A(\boldsymbol{r})\tilde{q}_B(\boldsymbol{r}')\Big\}\Big|_{n\neq j} = \bar{\xi}\,\bar{\zeta} \int_{\infty} d\boldsymbol{R} \int_{\infty} d\boldsymbol{R}' \Big\{ p_d^{(A)}(\boldsymbol{r},\boldsymbol{R}) \times p_d^{(B)}(\boldsymbol{r}',\boldsymbol{R}') \sum_{n=1}^{N}\sum_{j=1}^{N} \mathrm{pr}_{\tilde{\boldsymbol{R}}_n,\tilde{\boldsymbol{R}}_j}(\boldsymbol{R},\boldsymbol{R}'|N) \Big\}\Big|_{n\neq j}. \tag{53}$$

Based on the work by Barrett *et al.* [19], it can be shown that

$$\mathrm{E}\Big\{\tilde{q}_{in}(\boldsymbol{R})\tilde{q}_{in}(\boldsymbol{R}')|N\Big\}\Big|_{n\neq j} = \sum_{n=1}^{N}\sum_{j=1}^{N} \mathrm{pr}_{\tilde{\boldsymbol{R}}_n,\tilde{\boldsymbol{R}}_j}(\boldsymbol{R},\boldsymbol{R}'|N)\Big|_{n\neq j}. \tag{54}$$

Substituting Eq. (54) into Eq. (53), we have

$$\mathrm{E}_{(d)}\Big\{\tilde{q}_A(\boldsymbol{r})\tilde{q}_B(\boldsymbol{r}')\Big\}\Big|_{n\neq j} = \bar{\xi}\,\bar{\zeta} \int_{\infty} d\boldsymbol{R} \int_{\infty} d\boldsymbol{R}' \Big\{ p_d^A(\boldsymbol{r},\boldsymbol{R}) \times p_d^B(\boldsymbol{r}',\boldsymbol{R}')\, \mathrm{E}\Big\{\tilde{q}_{in}(\boldsymbol{R})\tilde{q}_{in}(\boldsymbol{R}')|N\Big\}\Big|_{n\neq j} \Big\}. \tag{55}$$

Now it is easily shown that step (e) applied to Eq. (55), to obtain the average over $\widetilde{N}$, gives

$$\mathrm{E}_{(e)}\Big\{\tilde{q}_A(\boldsymbol{r})\tilde{q}_B(\boldsymbol{r}')\Big\}\Big|_{n\neq j}$$
$$= \bar{\xi}\,\bar{\zeta}\int_\infty d\boldsymbol{R}\int_\infty d\boldsymbol{R}' p_d^A(\boldsymbol{r},\boldsymbol{R})p_d^B(\boldsymbol{r}',\boldsymbol{R}')\mathrm{E}\Big\{\tilde{q}_{in}(\boldsymbol{R})\tilde{q}_{in}(\boldsymbol{R}')\Big\}\Big|_{n\neq j}$$
$$= \bar{\xi}\,\bar{\zeta}\int_\infty d\boldsymbol{R}\int_\infty d\boldsymbol{R}'\, p_d^A(\boldsymbol{r},\boldsymbol{R})p_d^B(\boldsymbol{r}',\boldsymbol{R}')\mathrm{R}_{in}(\boldsymbol{R},\boldsymbol{R}')\Big|_{n\neq j}. \quad (56)$$

To replace $\mathrm{R}_{in}(\boldsymbol{R},\boldsymbol{R}')|_{n\neq j}$ in Eq. (56) with $\mathrm{R}_{in}(\boldsymbol{R},\boldsymbol{R}')$, we invoke Eqs. (26)–(27) again. Thus Eq. (56) becomes

$$\mathrm{E}_{(e)}\Big\{\tilde{q}_A(\boldsymbol{r})\tilde{q}_B(\boldsymbol{r}')\Big\}\Big|_{n\neq j}$$
$$= \bar{\xi}\,\bar{\zeta}\int_\infty d\boldsymbol{R}\int_\infty d\boldsymbol{R}'\, p_d^A(\boldsymbol{r},\boldsymbol{R})p_d^B(\boldsymbol{r}',\boldsymbol{R}')\mathrm{R}_{in}(\boldsymbol{R},\boldsymbol{R}')$$
$$-\bar{\xi}\,\bar{\zeta}\int_\infty d\boldsymbol{R}\, p_d^A(\boldsymbol{r},\boldsymbol{R})p_d^B(\boldsymbol{r}',\boldsymbol{R})\,\bar{q}_{in}(\boldsymbol{R}). \quad (57)$$

Adding Eqs. (51) and (57), the cross correlation of $\tilde{q}_A(\boldsymbol{r})$ and $\tilde{q}_B(\boldsymbol{r})$ is given by

$$\mathrm{R}_{AB}(\boldsymbol{r},\boldsymbol{r}') = \mathrm{K}_{\xi\zeta}\int_\infty d\boldsymbol{R}\, p_d^A(\boldsymbol{r},\boldsymbol{R})p_d^B(\boldsymbol{r}',\boldsymbol{R})\,\bar{q}_{in}(\boldsymbol{R})$$
$$+\bar{\xi}\,\bar{\zeta}\int_\infty d\boldsymbol{R}\int_\infty d\boldsymbol{R}'\, p_d^A(\boldsymbol{r},\boldsymbol{R})p_d^B(\boldsymbol{r}',\boldsymbol{R}')\mathrm{R}_{in}(\boldsymbol{R},\boldsymbol{R}'), \quad (58)$$

which is a general expression for the non-stationary cross correlation of two amplified point processes following a stochastic input selection. The cross covariance of $\tilde{q}_A(\boldsymbol{r})$ and $\tilde{q}_B(\boldsymbol{r})$ is given by subtracting the product of means from the cross correlation. From Eqs. (42), (44) and (58), finally, we have

$$\mathrm{K}_{AB}(\boldsymbol{r},\boldsymbol{r}') = \mathrm{K}_{\xi\zeta}\int_\infty d\boldsymbol{R}\, p_d^A(\boldsymbol{r},\boldsymbol{R})p_d^B(\boldsymbol{r}',\boldsymbol{R})\,\bar{q}_{in}(\boldsymbol{R})$$
$$+\bar{\xi}\,\bar{\zeta}\int_\infty d\boldsymbol{R}\int_\infty d\boldsymbol{R}'\, p_d^A(\boldsymbol{r},\boldsymbol{R})p_d^B(\boldsymbol{r}',\boldsymbol{R}')\mathrm{K}_{in}(\boldsymbol{R},\boldsymbol{R}'), \quad (59)$$

which is the desired result. For the case illustrated in Fig. 2, the expressions given by Eqs. (58) and (59) show that: a) the correlation in $\tilde{q}_A(\boldsymbol{r})$ and $\tilde{q}_B(\boldsymbol{r})$ is proportional to the cross correlation of the binomial random variables $\tilde{\xi}_n$ and $\tilde{\zeta}_n$ describing the point selection as given by the first term on the right-hand side of Eqs. (58) and (59); and, b) any correlation in the random source $\tilde{q}_{in}(\boldsymbol{r})$ is transferred to the outputs through paths A and B as shown by the second term.

D. Cross Covariance Following Multiple Amplified Point Processes

We now generalize the result of Eq. (59) derived in the above section to an arbitrary number of cascaded amplification stages in each of the two paths A and B, as illustrated in Fig. 3. In doing so, it is important to note that there are no random variables in Eq. (59), the cross covariance is expressed only in terms of mean values and the cross covariance of $\tilde{\xi}_n$ and $\tilde{\zeta}_n$.

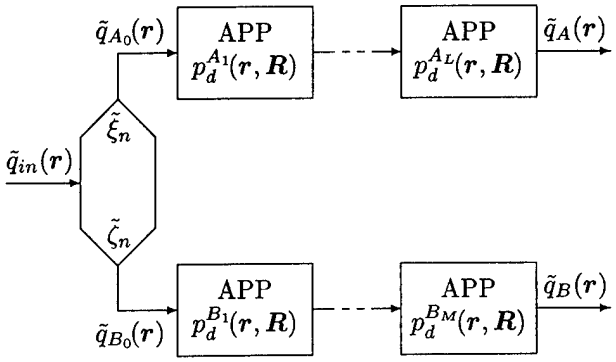

†APP: Amplified Point Process

FIG. 3. Two point processes following multiple amplified point processes subsequent to selection of a random point process.

1. Transfer Function of Mean

We approach the generalization of Eq. (59) by first considering the general expression Eq. (43) for the mean of an amplified point process with any input point process. Without loss of generality, we define a transfer function $H(\cdot)$, an integral operator, in terms of Eq. (43), as

$$H\Big(\bar{q}_{in}(\boldsymbol{R})\Big) = \int_\infty d\boldsymbol{R}\, p_d(\boldsymbol{r},\boldsymbol{R})\,\bar{q}_{in}(\boldsymbol{R}), \quad (60)$$

which describes the propagation of the mean of a point process passing through an amplification stage. As shown in Fig. 4(a), given an amplification stage with transfer function $H(\cdot)$, the mean of the amplified point process $\bar{q}_{out}(\boldsymbol{r})$ resulting from any point process input $\tilde{q}_{in}(\boldsymbol{r})$ can be uniquely determined, i.e., $\bar{q}_{out}(\boldsymbol{r}) = H(\bar{q}_{in}(\boldsymbol{R}))$, where $\boldsymbol{R}$ and $\boldsymbol{r}$ represent the position vectors of input and output quanta, respectively. The mathematical operation in Eq. (60) that maps the mean of input at $\boldsymbol{R}$ to the output at $\boldsymbol{r}$ is a convolution of the input $\bar{q}_{in}(\boldsymbol{R})$ with the function $p_d(\boldsymbol{r},\boldsymbol{R})$. For convenience, denote $*_v$ to represent the "shift variant" convolution integral such that

$$H\Big(\bar{q}_{in}(\boldsymbol{R})\Big) = \int_\infty d\boldsymbol{R}\, p_d(\boldsymbol{r},\boldsymbol{R})\,\bar{q}_{in}(\boldsymbol{R})$$
$$\triangleq p_d(\boldsymbol{r},\boldsymbol{R}) *_v \bar{q}_{in}(\boldsymbol{R}), \quad (61)$$

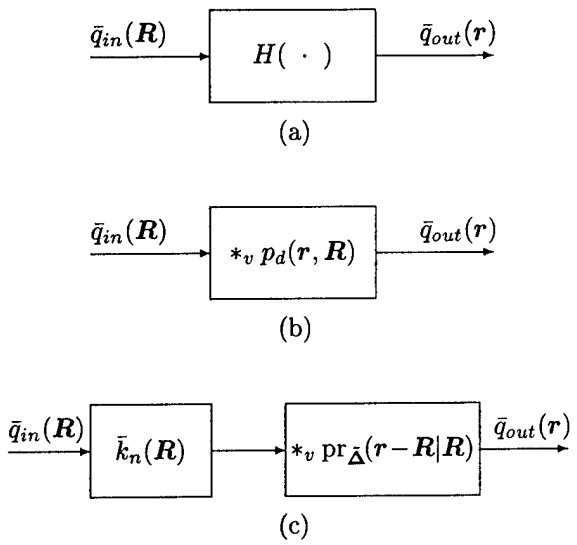

FIG. 4. Transfer functions of mean for an amplified point process.

where the subscript v of the symbol $*$ is used to make a distinction between shift invariant and variant systems. Fig. 4(b) is the block-diagram representation of Eq. (61). From the relationship between function $p_d(\boldsymbol{r},\boldsymbol{R})$ and the probability density function $\mathrm{pr}_{\tilde{\Delta}}(\boldsymbol{r}-\boldsymbol{R}|\boldsymbol{R})$ given by Eq. (31), we have

$$H\Big(\bar{q}_{in}(\boldsymbol{R})\Big) = \int_{\infty} d\boldsymbol{R}\,\mathrm{pr}_{\tilde{\Delta}}(\boldsymbol{r}-\boldsymbol{R}|\boldsymbol{R})\bar{k}_n(\boldsymbol{R})\,\bar{q}_{in}(\boldsymbol{R}) = \mathrm{pr}_{\tilde{\Delta}}(\boldsymbol{r}-\boldsymbol{R}|\boldsymbol{R}) *_v \Big(\bar{k}_n(\boldsymbol{R})\,\bar{q}_{in}(\boldsymbol{R})\Big), \quad (62)$$

which is an equivalent expression of the mean for an amplified point process. As illustrated in Fig. 4(c), an input point process $\tilde{q}_{in}(\boldsymbol{R})$ is first amplified with mean gain $\bar{k}_n(\boldsymbol{R})$ and then scattered with the density function $\mathrm{pr}_{\tilde{\Delta}}(\boldsymbol{r}-\boldsymbol{R}|\boldsymbol{R})$. This result can be found in [13] developed by Rabbani *et al.* from the view of multivariate moment-generating functions.

If the amplified point process is shift-invariant, then the mean gain and density function are independent of position $\boldsymbol{R}$, where $\bar{k}_n(\boldsymbol{R}) = \bar{k}$ and $\mathrm{pr}_{\tilde{\Delta}}(\boldsymbol{r}-\boldsymbol{R}|\boldsymbol{R}) = \mathrm{pr}_{\tilde{\Delta}}(\boldsymbol{r}-\boldsymbol{R})$. In this case, Eq. (62) becomes

$$H\Big(\bar{q}_{in}(\boldsymbol{R})\Big) = \int_{\infty} d\boldsymbol{R}\,\mathrm{pr}_{\tilde{\Delta}}(\boldsymbol{r}-\boldsymbol{R})\,\bar{k}\,\bar{q}_{in}(\boldsymbol{R}) = \bar{k}\,\mathrm{pr}_{\tilde{\Delta}}(\boldsymbol{r}) * \bar{q}_{in}(\boldsymbol{r}). \quad (63)$$

2. Cross Covariance

Now consider the case illustrated in Fig. 3, where there are L and M cascaded amplification stages in paths A and B, respectively. The output of each amplification stage forms a virtual input to the next.

First, using an approach similar to the procedure discussed previously, we calculate the cross covariance of the outputs for the case of two cascaded amplification stages in each of the paths A and B. In other words, we may make the calculation, for that case, by considering the five steps shown in the previous section. Then, by the method of induction, the cross covariance for the output of the system shown in Fig. 3 can be obtained. However, this procedure becomes tedious due to the conditional average over multiple amplification processes. Rather, cascaded amplification stages in each path can be thought of as an entire amplified point process if we consider only linear systems where the spatial pattern of each amplification stage depends only on the position of the primary interaction. To obtain the statistical characteristic for the entire amplified point process, consider the calculation of the mean of the output point process $\tilde{q}_A(\boldsymbol{r})$ by cascading Eq. (61) with the L amplification stages in path A. In Fig. 5, the mean $\bar{q}_A(\boldsymbol{r})$ of the output at $\boldsymbol{r}$ is the convolution of $\bar{q}_{A_{L-1}}(\boldsymbol{R}^{A_{L-1}})$ with the function $p_d^{A_L}(\boldsymbol{r},\boldsymbol{R}^{A_{L-1}})$ and then of $\bar{q}_{A_{L-2}}(\boldsymbol{R}^{A_{L-2}})$ with the function $p_d^{A_{L-1}}(\boldsymbol{R}^{A_{L-1}},\boldsymbol{R}^{A_{L-2}})$, $\cdots$, finally of input at $\boldsymbol{R}$ with the function $p_d^{A_1}(\boldsymbol{R}^{A_1},\boldsymbol{R})$. This lead to

$$\begin{aligned}
\bar{q}_A(\boldsymbol{r}) &= p_d^{A_L}\Big(\boldsymbol{r},\boldsymbol{R}^{A_{L-1}}\Big) *_v \bar{q}_{A_{L-1}}\Big(\boldsymbol{R}^{A_{L-1}}\Big) \\
&= p_d^{A_L}\Big(\boldsymbol{r},\boldsymbol{R}^{A_{L-1}}\Big) *_v \Big[p_d^{A_{L-1}}\Big(\boldsymbol{R}^{A_{L-1}},\boldsymbol{R}^{A_{L-2}}\Big) *_v \bar{q}_{A_{L-2}}\Big(\boldsymbol{R}^{A_{L-2}}\Big)\Big] \\
&= \cdots\cdots \\
&= p_d^{A_L}\Big(\boldsymbol{r},\boldsymbol{R}^{A_{L-1}}\Big) *_v \cdots *_v p_d^{A_1}\Big(\boldsymbol{R}^{A_1},\boldsymbol{R}\Big) *_v \bar{q}_{A_0}(\boldsymbol{R}) \\
&\triangleq p_d^{A}(\boldsymbol{r},\boldsymbol{R}) *_v \bar{q}_{A_0}(\boldsymbol{R}),
\end{aligned} \quad (64)$$

where we define $p_d^A(\boldsymbol{r},\boldsymbol{R})$ as the statistical characteristic function for the cascade of all stages along path A given by

$$p_d^A(\boldsymbol{r},\boldsymbol{R}) \triangleq p_d^{A_L}\Big(\boldsymbol{r},\boldsymbol{R}^{A_{L-1}}\Big) *_v \cdots *_v p_d^{A_1}\Big(\boldsymbol{R}^{A_1},\boldsymbol{R}\Big). \quad (65)$$

Now we can say that the mean of the output $\tilde{q}(\boldsymbol{r})$ is the convolution of the mean of the input at $\boldsymbol{R}$ with the function $p_d^A(\boldsymbol{r},\boldsymbol{R})$.

Similarly, for path B, we obtain that the mean of $\tilde{q}_B(\boldsymbol{r})$ is given by

$$\bar{q}_B(\boldsymbol{r}) = p_d^B(\boldsymbol{r},\boldsymbol{R}) *_v \bar{q}_{B_0}(\boldsymbol{R}), \quad (66)$$

where point process $\tilde{q}_{B_0}(\boldsymbol{r})$ is the output of the point-selection process for path B (see Fig. 3) and

$$p_d^B(\boldsymbol{r},\boldsymbol{R}) \triangleq p_d^{B_M}\Big(\boldsymbol{r},\boldsymbol{R}^{B_{M-1}}\Big) *_v \cdots *_v p_d^{B_1}\Big(\boldsymbol{R}^{B_1},\boldsymbol{R}\Big). \quad (67)$$

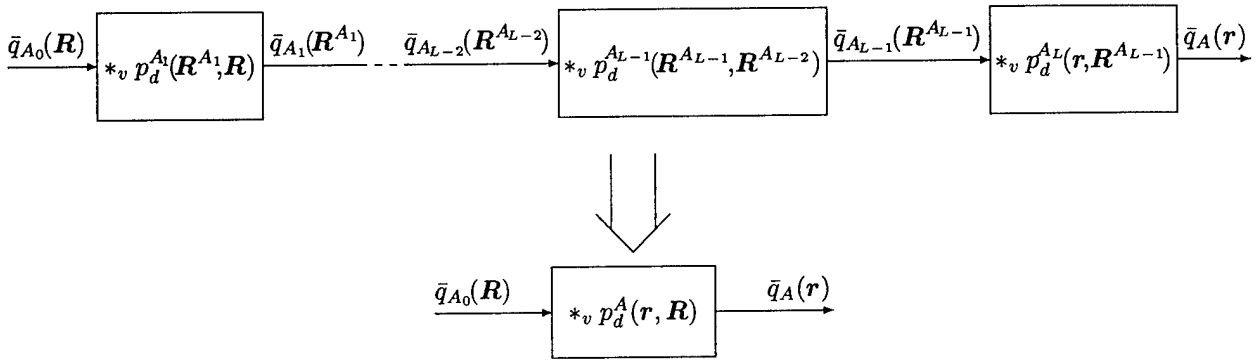

FIG. 5. Transfer function of mean for multiple amplified point processes.

This result shows that multiple cascaded amplified point processes can be expressed as a single amplified point process with the appropriate statistical characteristic function for the purpose of describing transfer of mean value. Since calculation of the cross covariance in Eq. (59) involves integrals in which amplification is represented in terms of the statistical characteristic only, we conclude that the cross covariance for $\tilde{q}_A(\boldsymbol{r})$ and $\tilde{q}_B(\boldsymbol{r})$ is also given by Eq. (59), where $p_d^A(\boldsymbol{r},\boldsymbol{R})$ is described by Eq. (65) and $p_d^B(\boldsymbol{r},\boldsymbol{R})$ is described by Eq. (67).

E. Important Special Cases

1. Doubly Stochastic Poisson Impulses Source

In medical imaging systems, the incident x rays at the detector form a quantum image which is a distribution of quanta, and can be expressed as a sample function of a spatial point process $\tilde{q}_{in}(\boldsymbol{r})$ as in Eq. (15). Barrett [19] has shown that such a point process may be described in terms of doubly stochastic Poisson impulses with intensity process $\tilde{b}(\boldsymbol{r})$, which he calls the random input fluence. In x ray imaging, for instance, random changes of the radiation source makes $b(\boldsymbol{r})$ spatially random.

For the input point process $\tilde{q}_{in}(\boldsymbol{r})$ of doubly stochastic Poisson impulses, Barrett shows that the mean is given by

$$\bar{q}_{in}(\boldsymbol{r}) = \bar{b}(\boldsymbol{r}), \tag{68}$$

where $\bar{b}(\boldsymbol{r})$ is the mean of random input fluence, and the autocovariance is

$$\mathrm{K}_{in}(\boldsymbol{r},\boldsymbol{r}') = \bar{b}(\boldsymbol{r})\delta(\boldsymbol{r}-\boldsymbol{r}') + \mathrm{K}_b(\boldsymbol{r},\boldsymbol{r}'), \tag{69}$$

where $\mathrm{K}_b(\boldsymbol{r},\boldsymbol{r}')$ is the autocovariance of $\tilde{b}(\boldsymbol{r})$. Substituting Eqs. (68)–(69) into Eq. (29), we obtain (see Fig. 1)

$$\mathrm{K}_{AB}(\boldsymbol{r},\boldsymbol{r}') = \mathrm{R}_{\xi\zeta}\,\bar{b}(\boldsymbol{r})\delta(\boldsymbol{r}-\boldsymbol{r}') + \bar{\xi}\,\bar{\zeta}\,\mathrm{K}_b(\boldsymbol{r},\boldsymbol{r}'), \tag{70}$$

where $\mathrm{R}_{\xi\zeta} = \mathrm{K}_{\xi\zeta} + \bar{\xi}\,\bar{\zeta}$ is the cross correlation of random binomial variables $\tilde{\xi}_n$ and $\tilde{\zeta}_n$. Similarly, substituting Eqs. (68) and (69) into Eq. (59), after some algebraic manipulations, the cross covariance becomes

$$\mathrm{K}_{AB}(\boldsymbol{r},\boldsymbol{r}') = \mathrm{R}_{\xi\zeta}\int_\infty d\boldsymbol{R}\, p_d^A(\boldsymbol{r},\boldsymbol{R}) p_d^B(\boldsymbol{r}',\boldsymbol{R})\,\bar{b}(\boldsymbol{R})$$
$$+\bar{\xi}\,\bar{\zeta}\int_\infty d\boldsymbol{R}\int_\infty d\boldsymbol{R}'\, p_d^A(\boldsymbol{r},\boldsymbol{R}) p_d^B(\boldsymbol{r}',\boldsymbol{R}')\mathrm{K}_b(\boldsymbol{R},\boldsymbol{R}'), \tag{71}$$

which is the result of Fig. 2 for the input process of doubly stochastic Poisson impulses. Eqs (70) and (71) are given to show the relationship to Barrett's work, but are not required to obtain the following special cases.

2. Shift-Invariant System with Multiple Amplified Point Processes

If the system shown in Fig. 3 is shift-invariant, which requires that the mean gain and the probability density function for each amplification stage be independent of position, then the propagation of the mean of the input point process is shown in Fig. 6. From Fig. 6 and Eq. (63), it is easily shown that

$$\begin{cases} \bar{q}_A(\boldsymbol{r}) = \bar{k}^A\,\mathrm{pr}_{\tilde{\Delta}}^A(\boldsymbol{r}) * \bar{q}_{A_0}(\boldsymbol{r}) \\ \bar{q}_B(\boldsymbol{r}) = \bar{k}^B\,\mathrm{pr}_{\tilde{\Delta}}^B(\boldsymbol{r}) * \bar{q}_{B_0}(\boldsymbol{r}) \end{cases}, \tag{72}$$

where the probability density functions $\mathrm{pr}_{\tilde{\Delta}}^A(\boldsymbol{r})$ and $\mathrm{pr}_{\tilde{\Delta}}^B(\boldsymbol{r})$ for the entire amplified point processes along paths A and B, respectively, are expressed as convolutions of the density functions of sub-stages in its path, i.e.,

$$\begin{cases} \mathrm{pr}_{\tilde{\Delta}}^A(\boldsymbol{r}) = \mathrm{pr}_{\tilde{\Delta}}^{A_L}(\boldsymbol{r}) * \mathrm{pr}_{\tilde{\Delta}}^{A_{L-1}}(\boldsymbol{r}) * \cdots * \mathrm{pr}_{\tilde{\Delta}}^{A_1}(\boldsymbol{r}) \\ \mathrm{pr}_{\tilde{\Delta}}^B(\boldsymbol{r}) = \mathrm{pr}_{\tilde{\Delta}}^{B_M}(\boldsymbol{r}) * \mathrm{pr}_{\tilde{\Delta}}^{B_{M-1}}(\boldsymbol{r}) * \cdots * \mathrm{pr}_{\tilde{\Delta}}^{B_1}(\boldsymbol{r}) \end{cases}, \tag{73}$$

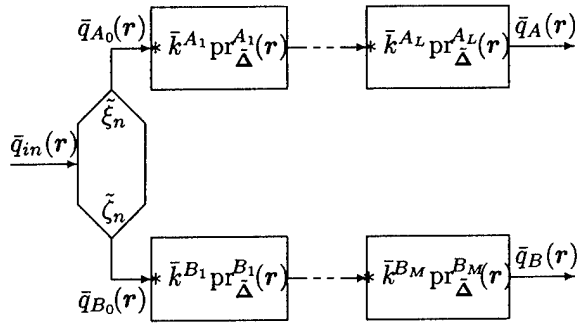

FIG. 6. Shift-invariant system with multiple amplified point processes.

and the mean gains $\bar{k}^A$ and $\bar{k}^B$ for the entire amplified point processes of paths A and B, respectively, are given by

$$\begin{cases} \bar{k}^A = \prod_{i=1}^{L} \bar{k}^{A_i} \\ \bar{k}^B = \prod_{j=1}^{M} \bar{k}^{B_j} \end{cases} . \tag{74}$$

From Eq. (31), we obtain the function $p_d^A(\boldsymbol{r}, \boldsymbol{R})$ for the entire amplified point process of path A, i.e.,

$$p_d^A(\boldsymbol{r}, \boldsymbol{R}) = \bar{k}^A \,\mathrm{pr}^A_{\tilde{\Delta}}(\boldsymbol{r} - \boldsymbol{R}). \tag{75}$$

Similarly, we have

$$p_d^B(\boldsymbol{r}, \boldsymbol{R}) = \bar{k}^B \,\mathrm{pr}^B_{\tilde{\Delta}}(\boldsymbol{r} - \boldsymbol{R}). \tag{76}$$

Substituting Eqs. (75) and (76) into Eq. (59), the cross covariance function of $\tilde{q}_A(\boldsymbol{r})$ and $\tilde{q}_B(\boldsymbol{r})$ is given by

$$\begin{aligned} &\mathrm{K}_{AB}(\boldsymbol{r}, \boldsymbol{r}') \\ &= \mathrm{K}_{\xi\zeta} \bar{k}^A \bar{k}^B \int_\infty d\boldsymbol{R}\, \mathrm{pr}^A_{\tilde{\Delta}}(\boldsymbol{r} - \boldsymbol{R})\, \mathrm{pr}^B_{\tilde{\Delta}}(\boldsymbol{r}' - \boldsymbol{R})\, \bar{q}_{in}(\boldsymbol{R}) \\ &+ \bar{\xi}\,\bar{\zeta}\, \bar{k}^A \bar{k}^B \int_\infty d\boldsymbol{R} \int_\infty d\boldsymbol{R}'\, \mathrm{pr}^A_{\tilde{\Delta}}(\boldsymbol{r} - \boldsymbol{R})\, \mathrm{pr}^B_{\tilde{\Delta}}(\boldsymbol{r}' - \boldsymbol{R}')\, \mathrm{K}_{in}(\boldsymbol{R}, \boldsymbol{R}') \end{aligned} \tag{77}$$

which is the desired result for the case when the system is shift invariant.

3. Cross Covariance and Cross Spectral Density Under WSS Conditions

If the outputs of point processes $\tilde{q}_A(\boldsymbol{r})$ and $\tilde{q}_B(\boldsymbol{r})$ in Fig. 2 are wide-sense stationary (WSS), we can describe the correlation between two paths A and B in the frequency domain by their cross spectral density [3] which is equal to the Fourier transform of the cross covariance $\mathrm{K}_{AB}(\boldsymbol{r}, \boldsymbol{r}')$. For the wide-sense stationary conditions, the input process must be stationary in the wide sense and, the amplification processes must be shift-invariant with uniform mean gains of quanta in an infinite imaging plane. Thus, under WSS conditions, let $\bar{q}_{in}(\boldsymbol{R}) = \bar{q}_{in}$ be constant, and $\mathrm{K}_{in}(\boldsymbol{R}, \boldsymbol{R}') = K_{in}(\boldsymbol{R} - \boldsymbol{R}')$. Moreover, the functions $p_d^A(\boldsymbol{r}, \boldsymbol{R})$ and $p_d^B(\boldsymbol{r}', \boldsymbol{R}')$ in Eq. (59) are replaced with the products of their corresponding constant mean gains and shift-invariant density functions as in Eqs. (75) and (76), respectively. We obtain

$$\begin{aligned} &\mathrm{K}_{AB}(\boldsymbol{r}, \boldsymbol{r}') = \mathrm{K}_{AB}(\boldsymbol{r} - \boldsymbol{r}') \\ &= \mathrm{K}_{\xi\zeta} \bar{k}^A \bar{k}^B\, \bar{q}_{in} \int_\infty d\boldsymbol{R}\, \mathrm{pr}^A_{\tilde{\Delta}}(\boldsymbol{r} - \boldsymbol{R})\, \mathrm{pr}^B_{\tilde{\Delta}}(\boldsymbol{r}' - \boldsymbol{R}) \\ &+ \bar{\xi}\,\bar{\zeta}\, \bar{k}^A \bar{k}^B \int_\infty d\boldsymbol{R} \int_\infty d\boldsymbol{R}'\, \mathrm{pr}^A_{\tilde{\Delta}}(\boldsymbol{r} - \boldsymbol{R})\, \mathrm{pr}^B_{\tilde{\Delta}}(\boldsymbol{r}' - \boldsymbol{R}')\, \mathrm{K}_{in}(\boldsymbol{R} - \boldsymbol{R}'), \end{aligned} \tag{78}$$

By changing the integral variable $\boldsymbol{R}$ such that $\boldsymbol{\tau}' = \boldsymbol{r}' - \boldsymbol{R}$, the integral of the first term in Eq. (78) can be rewritten as

$$\int_\infty d\boldsymbol{\tau}'\, \mathrm{pr}^A_{\tilde{\Delta}}(\boldsymbol{r} - \boldsymbol{r}' + \boldsymbol{\tau}')\, \mathrm{pr}^B_{\tilde{\Delta}}(\boldsymbol{\tau}')$$

which is the correlation integral of two functions $\mathrm{pr}^A_{\tilde{\Delta}}(\boldsymbol{\tau})$ and $\mathrm{pr}^B_{\tilde{\Delta}}(\boldsymbol{\tau})$ over $\boldsymbol{\tau}'$, denoted in short form by $\mathrm{pr}^A_{\tilde{\Delta}}(\boldsymbol{\tau}) \star \mathrm{pr}^B_{\tilde{\Delta}}(\boldsymbol{\tau})$, where $\boldsymbol{\tau} = \boldsymbol{r} - \boldsymbol{r}'$. Moreover, for the double integral of the second term in Eq. (78), we perform the changes of $\boldsymbol{\tau}'' = \boldsymbol{r}' - \boldsymbol{R}'$ in the $\boldsymbol{R}'$ integral and $\boldsymbol{\tau}''' + \boldsymbol{\tau}'' = \boldsymbol{r} - \boldsymbol{R}$ in the $\boldsymbol{R}$ integral, yielding

$$\int_\infty d\boldsymbol{\tau}''' \left[\int_\infty d\boldsymbol{\tau}'' \mathrm{pr}^A_{\tilde{\Delta}}(\boldsymbol{\tau}''' + \boldsymbol{\tau}'')\, \mathrm{pr}^B_{\tilde{\Delta}}(\boldsymbol{\tau}'') \right] \mathrm{K}_{in}(\boldsymbol{r} - \boldsymbol{r}' - \boldsymbol{\tau}''').$$

The integral over $\boldsymbol{\tau}''$ is the correlation integral of $\mathrm{pr}^A_{\tilde{\Delta}}(\boldsymbol{\tau}''')$ and $\mathrm{pr}^B_{\tilde{\Delta}}(\boldsymbol{\tau}''')$, and the integral over $\boldsymbol{\tau}'''$ is the convolution integral of the correlation integral and $\mathrm{K}_{in}(\boldsymbol{\tau})$. At this point we simplify our notation and let $\mathrm{pr}(\boldsymbol{\tau}) = \mathrm{pr}_{\tilde{\Delta}}(\boldsymbol{\tau})$. Therefore, Eq. (78) becomes

$$\begin{aligned} \mathrm{K}_{AB}(\boldsymbol{\tau}) &= \mathrm{K}_{\xi\zeta} \bar{k}^A \bar{k}^B \bar{q}_{in}\, \mathrm{pr}^A(\boldsymbol{\tau}) \star \mathrm{pr}^B(\boldsymbol{\tau}) \\ &+ \bar{\xi}\,\bar{\zeta}\, \bar{k}^A \bar{k}^B \left[\mathrm{pr}^A(\boldsymbol{\tau}) \star \mathrm{pr}^B(\boldsymbol{\tau}) \right] * \mathrm{K}_{in}(\boldsymbol{\tau}), \end{aligned} \tag{79}$$

which is the desired expression of the cross covariance for wide-sense stationary $\tilde{q}_A(\boldsymbol{r})$ and $\tilde{q}_B(\boldsymbol{r})$.

The cross spectral density for paths A and B is defined as the Fourier transform of the cross covariance $\mathrm{K}_{AB}(\boldsymbol{\tau})$, given by

$$\begin{aligned} &\mathrm{NPS}_{AB}(\boldsymbol{\nu}) = \mathcal{F}\left\{ \mathrm{K}_{AB}(\boldsymbol{\tau}) \right\} \\ &= \mathrm{K}_{\xi\zeta} \bar{k}^A \bar{k}^B \bar{q}_{in}\, \mathcal{F}\left\{ \mathrm{pr}^A(\boldsymbol{\tau}) \star \mathrm{pr}^B(\boldsymbol{\tau}) \right\} \\ &+ \bar{\xi}\,\bar{\zeta}\, \bar{k}^A \bar{k}^B \mathcal{F}\left\{ \left[\mathrm{pr}^A(\boldsymbol{\tau}) \star \mathrm{pr}^B(\boldsymbol{\tau}) \right] * \mathrm{K}_{in}(\boldsymbol{\tau}) \right\}. \end{aligned} \tag{80}$$

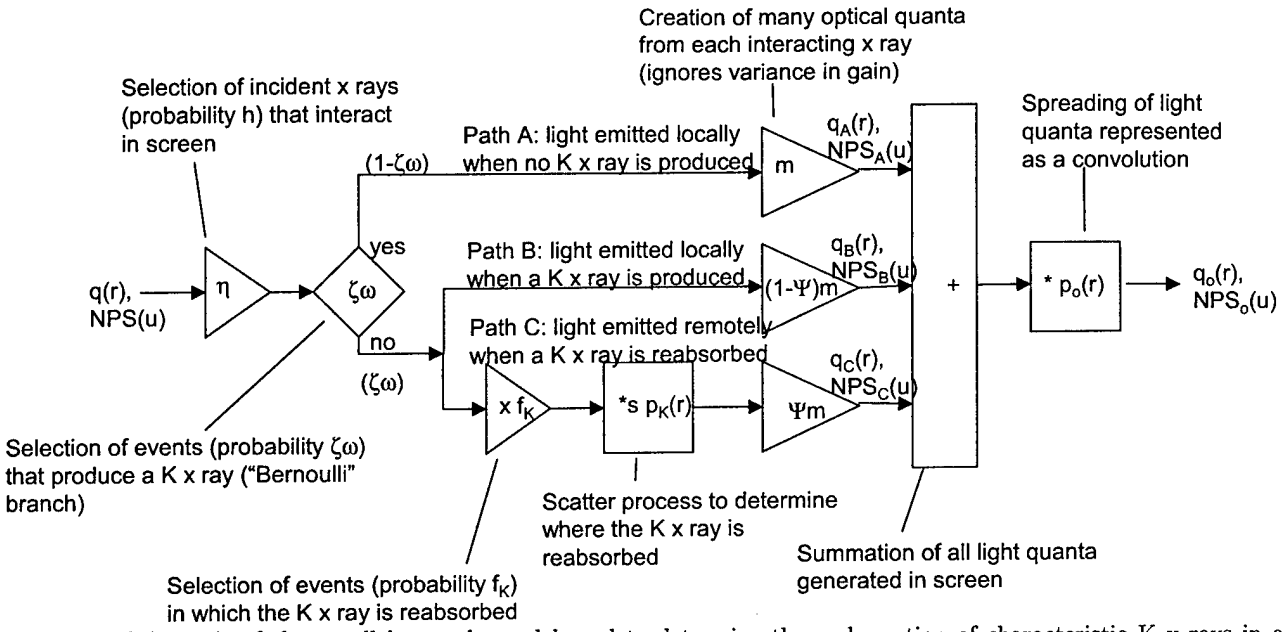

FIG. 7. Schematic of the parallel cascade model used to determine the reabsorption of characteristic K x rays in a radiographic screen.

Then the final result for the cross spectral density under WSS conditions is

$$\mathrm{NPS}_{AB}(\nu)=\bar{k}^A\bar{k}^B\,\mathrm{T}^A(\nu)\mathrm{T}^{B*}(\nu)\left[\bar{\xi}\,\bar{\zeta}\,\mathrm{NPS}_{in}(\nu)+\mathrm{K}_{\xi\zeta}\bar{q}_{in}\right] \tag{81}$$

where $\mathrm{NPS}_{in}(\nu)$ is the NPS of the input point process (the Fourier transform of $\mathrm{K}_{in}(\tau)$), $\mathrm{T}^A(\nu)$ and $\mathrm{T}^B(\nu)$ are Fourier transforms of $\mathrm{pr}^A(\tau)$ and $\mathrm{pr}^B(\tau)$ respectively. When paths A and B represent a cascade of multiple amplified point processes, the mean gains $\bar{k}^A$ and $\bar{k}^B$ are the product of mean gains along each path as given by Eq. (74), and $\mathrm{pr}^A(\tau)$ and $\mathrm{pr}^B(\tau)$ represent the cascaded probability density functions for each path as given by Eq. (73). Taking the Fourier transform of both sides of Eq. (73) shows that $\mathrm{T}^A(\nu)$ and $\mathrm{T}^B(\nu)$ represent the product of all scatter transfer functions along each path, as given by

$$\begin{cases} \mathrm{T}^A(\nu)=\prod_{i=1}^{L}\mathrm{T}^{A_i}(\nu) \\ \mathrm{T}^B(\nu)=\prod_{j=1}^{M}\mathrm{T}^{B_j}(\nu) \end{cases}, \tag{82}$$

where $\mathrm{T}^{A_i}(\nu)$ is the Fourier transform of the probability density function of the ith sub-stage in path A. The probability density functions always have unity area, and hence the transfer functions $\mathrm{T}^A(\nu)$ and $\mathrm{T}^B(\nu)$ always have a value of unity at $\nu = 0$. While the transfer functions are complex in general, as shown in Appendix B, the sum of any cross term pair, $\mathrm{NPS}_{AB}(\nu)+\mathrm{NPS}_{BA}(\nu)$, will always be real only.

III. APPLICATIONS

Equation (81) is the general expression for the WSS cross spectral density of two parallel cascaded amplified point processes descending from a single input point process. It is in a particularly simple and convenient form for application in a linear-systems model as it is expressed solely in terms of the NPS and mean value of the input point process, the selection probabilities and corresponding cross covariance, and mean gains and mean scatter transfer functions for each path. In this section, this result is used in a description of characteristic reabsorption in a radiographic screen.

A. Application to Reabsorption of Characteristic X Rays in a Radiographic Screen

We examine here the effects on image noise of fluorescence reabsorption in a radiographic screen, where light is emitted at both the primary photo-electric interaction site and at the reabsorption site. This problem was studied previously by Metz and Vyborny [34] using a relatively sophisticated statistical analysis. We show that the same result can be obtained using a simpler linear transfer-theory model that includes parallel cascades and the cross spectral density derived in the previous section.

Figure 7 illustrates a "flow diagram" showing the sequence of events leading to light production in the Metz-Vyborny model. WSS conditions are assumed throughout so that each position in this diagram represents an intermediate step between input and output

characterized in terms of a two-dimensional distribution of quanta (points) $q(\boldsymbol{r})$. The processes included in Fig. 7 are based on three "elementary processes" (see Appendix A) in the serial cascades plus branch-points that give rise to the parallel cascades.

Several simplifying assumptions are made in order to be consistent with Metz and Vyborny [34] and with earlier work of Rossmann [35,36]. They include: a) incident x rays are assumed monoenergetic; b) differences in light emission due to different x ray interaction depths are ignored; and c) only photo-electric interactions are considered. Metz and Vyborny also ignored the statistical nature of light generation in the screen.

At the input of the model in Fig. 7, a uniform x-ray distribution consisting of $\bar{q}$ quanta/mm^2, each with energy E_x, is incident on the radiographic screen. These quanta are Poisson distributed, and hence have an associated NPS given by $\mathrm{NPS}(\boldsymbol{\nu}) = \bar{q}$ [37]. A fraction η of these incident quanta will result in a photo-electric interaction in the screen. Selection of these events is represented as a stochastic selection or binary gain stage, where gain is represented by a random variable $\tilde{\eta}$ that can have a value of 0 or 1 only and mean of η. The output from this gain stage is the two-dimensional distribution of photo-electric events in the screen.

As described by Metz and Vyborny, there are three possible sequences of events whereby light can be generated for each photo-electric interaction: 1) absorption of the primary x-ray photon at the primary interaction site without emission of a characteristic K x ray; 2) absorption of the primary x ray accompanied by emission of a K x ray; and 3) reabsorption of the K x ray at a remote location. These three sequences correspond to paths A, B and C in Fig. 7.

Path A describes the emission of light at the primary interaction location when no K x ray is produced. For each photo-electric interaction, there is a probability $\varsigma\omega$ that a K x ray will be generated, and therefore a probability $(1-\varsigma\omega)$ that a K x ray is not generated where ς is the probability that, when an incident photon interacts in the screen, it undergoes a K-shell interaction, and ω is the fluorescent yield of K-shell photo-electric interactions. This branching is represented in Fig. 7 as the diamond-shaped "Bernoulli branch". It is to be interpreted as a Bernoulli trial [2,37] that, for each interaction, determines the outcome "yes" or "no" where "yes" is obtained randomly with a probability $\varsigma\omega$, and "no" otherwise. If a K x ray is not produced, corresponding to path A in Fig. 7, it is assumed that the incident x-ray energy E_x is absorbed locally producing the number m optical quanta (the gain factor m is assumed to be proportional to the absorbed energy) which will be emitted from the screen. Metz and Vyborny ignore the statistical nature of light emission, and hence m is modeled as a deterministic gain factor. Note that the gain factor m only describes generation of the number of light quanta that are *emitted* from the screen.

Path B describes light emission at the site of the photo-electric interaction when a K x ray *is* emitted (which may or may not be reabsorbed). In this case, the energy $E_K = \psi E_x$ is carried away in the K x ray, and the remaining energy $E_x - E_K$ is deposited at the primary interaction site. Thus, only $(1-\psi)m$ optical quanta are emitted at the primary interaction site for each photo-electric interaction where $\psi = E_K/E_x$ and $E_K \approx 59.3$ kev for tungsten in the calcium tungstate screens.

Path C describes the light emitted from the screen at a remote site due to reabsorption of the K x ray, where f_K is the probability of reabsorption somewhere in the screen for each photo-electric interaction producing a K x ray. The location of reabsorption is random, but the point-spread function $p_K(\boldsymbol{r})$, which has unity area, describes the probability density that the K x ray is reabsorbed at a distance $\boldsymbol{r}$ from the photo-electric interaction site. The process representing this random relocation of the K x ray is a quantum scatter stage as described in Appendix A. At the reabsorption site, the K x ray is converted to optical quanta with a conversion factor ψm. Events are selected for both paths B and C for every "no" event in the Bernoulli branch. We call the point of separation of paths B and C a "cascade fork."

Due to geometrical spread and possibly light scatter in the screen, optical quanta are distributed spatially with a point spread function (normalized to unity area) given by $p_o(\boldsymbol{r})$, Metz and Vyborny ignore the statistical nature of light scatter and this redistribution of light is represented as a linear filter (convolution) with a kernel $p_o(\boldsymbol{r})$.

The total light emitted from the screen is therefore the sum of contributions from each path, resulting in

$$\bar{q}_o = |T_o(0)|[\bar{q}_A + \bar{q}_B + \bar{q}_C] \tag{83}$$

quanta per unit area, where we have used Eq. (A9) for the output linear filter in Fig. 7, and the function $T_o(\boldsymbol{\nu})$ is the Fourier transform of $p_o(\boldsymbol{r})$. The contributions from each path can be obtained by cascadeing the elementary processes (see Appendix A) included in each path and considering the outcome probability of the Bernoulli branch. Then, we have

$$\bar{q}_A = m(1-\varsigma\omega)\eta\,\bar{q}, \tag{84}$$

$$\bar{q}_B = (1-\psi)m\varsigma\omega\eta\,\bar{q}, \tag{85}$$

$$\bar{q}_C = \psi m f_K \varsigma\omega\eta\,\bar{q}. \tag{86}$$

Substituting Eqs. (84)–(86) into Eq. (83), we can obtain

$$\bar{q}_o = \bar{q}\eta m[1-\varsigma\omega\psi(1-f_K)]|T_o(0)|. \tag{87}$$

The NPS of light emitted from the screen, denoted by $\mathrm{NPS}_o(u)$, is therefore given by (see Appendix B)

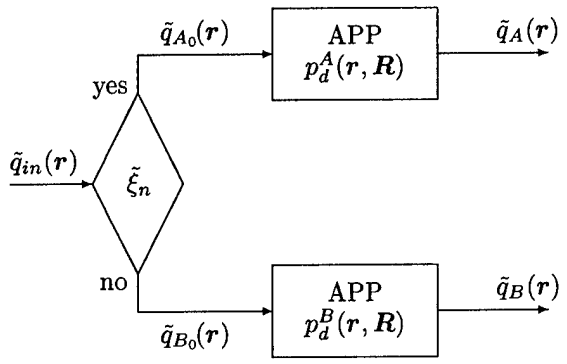

†APP: Amplified Point Process

FIG. 8. The Bernoulli branch with amplified point processes.

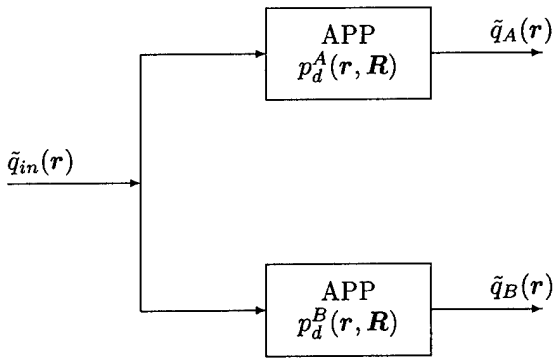

†APP: Amplified Point Process

FIG. 9. The cascade fork with amplified point processes.

$$\begin{aligned}\mathrm{NPS}_o(\nu) = \Big[&\mathrm{NPS}_A(\nu) + \mathrm{NPS}_B(\nu) + \mathrm{NPS}_C(\nu) \\ &+\mathrm{NPS}_{AB}(\nu) + \mathrm{NPS}_{BA}(\nu) + \mathrm{NPS}_{AC}(\nu) \\ &+\mathrm{NPS}_{CA}(\nu) + \mathrm{NPS}_{BC}(\nu) + \mathrm{NPS}_{CB}(\nu)\Big]|T_o(\nu)|^2 \quad (88)\end{aligned}$$

consisting of the NPS from each of the paths A, B and C plus corresponding cross terms as described below for the parallel paths with "Bernoulli branch" and "cascade fork" selection processes.

1. Bernoulli Branch

The Bernoulli branch with amplified point processes is illustrated in Fig. 8. Each quantum in the input point process is selected for path A, denoted by "yes", when $\tilde{\xi}_n = 1$ and for path B, denoted by "no" when $\tilde{\xi}_n = 0$. The Bernoulii branch is a special case of the point selection process described in Fig. 2 where the two binomial random variables are related to $\tilde{\zeta} = (1 - \tilde{\xi})$. This results in the cross covariance of these random variables given by

$$\mathrm{K}_{\xi\zeta} = \mathrm{E}\Big\{\tilde{\xi}_n\tilde{\zeta}_n\Big\} - \mathrm{E}\Big\{\tilde{\xi}_n\Big\}\mathrm{E}\Big\{\tilde{\zeta}_n\Big\} = -\bar{\xi}\,\bar{\zeta} = -\bar{\xi}(1-\bar{\xi}). \quad (89)$$

The cross spectral density following amplification is therefore given by Eq. (81) as

$$\begin{aligned}&\mathrm{NPS}_{AB}(\nu) \\ &= \bar{\xi}(1-\bar{\xi})\bar{k}^A\bar{k}^B\,\mathrm{T}^A(\nu)\mathrm{T}^{B*}(\nu)\Big[\mathrm{NPS}_{in}(\nu) - \bar{q}_{in}\Big] \quad (90)\end{aligned}$$

showing that there is correlation between paths A and B only if quanta in the input image are statistically correlated. That is, when $\mathrm{NPS}_{in}(\nu) - \bar{q}_{in} \neq 0$. If the quanta are uncorrelated and $\mathrm{NPS}_{in}(\nu) = \bar{q}_{in}$, there is no cross term.

2. Cascade Fork

The cascade fork with amplification is shown in Fig. 9 where every quantum in the input is selected for both paths A and B. This again is a special case of the general point selection process described in Fig. 2 where $\tilde{\xi}_n = \tilde{\zeta}_n = 1$, modeled as deterministic unit factors. The cross covariance of $\tilde{\xi}_n$ and $\tilde{\zeta}_n$, is therefore

$$\mathrm{K}_{\xi\zeta} = \mathrm{E}\Big\{\tilde{\xi}_n\tilde{\zeta}_n\Big\} - \mathrm{E}\Big\{\tilde{\xi}_n\Big\}\mathrm{E}\Big\{\tilde{\zeta}_n\Big\} = 0, \quad (91)$$

and the cross spectral density term for the cascade fork based on Eq. (81) is given by

$$\mathrm{NPS}_{AB}(\nu) = \bar{k}^A\bar{k}^B\,\mathrm{T}^A(\nu)\mathrm{T}^{B*}(\nu)\mathrm{NPS}_{in}(\nu), \quad (92)$$

which is always non-zero if the input is a random point process, and therefore there is always a cross term between paths A and B.

B. Degradation of the NPS due to Reabsorption

The NPS in the distribution of optical quanta from each path in isolation is obtained by cascading appropriate combinations of the elementary processes described in Appendix A, giving

$$\mathrm{NPS}_A(\nu) = m^2(1-\varsigma\omega)\eta\,\bar{q}, \quad (93)$$

$$\mathrm{NPS}_B(\nu) = (1-\psi)^2m^2\varsigma\omega\eta\,\bar{q}, \quad (94)$$

$$\mathrm{NPS}_C(\nu) = \psi^2m^2f_k\varsigma\omega\eta\,\bar{q}, \quad (95)$$

where we have used $\mathrm{NPS}(\nu) = \bar{q}$ since the input quanta are Poisson distributed. Quanta in the input image are statistically uncorrelated, therefore there is no cross term between paths separated by the Bernoulli branch. That is,

$$\mathrm{NPS}_{AB}(\nu) = \mathrm{NPS}_{BA}(\nu) = 0,$$
$$\mathrm{NPS}_{AC}(\nu) = \mathrm{NPS}_{CA}(\nu) = 0.$$

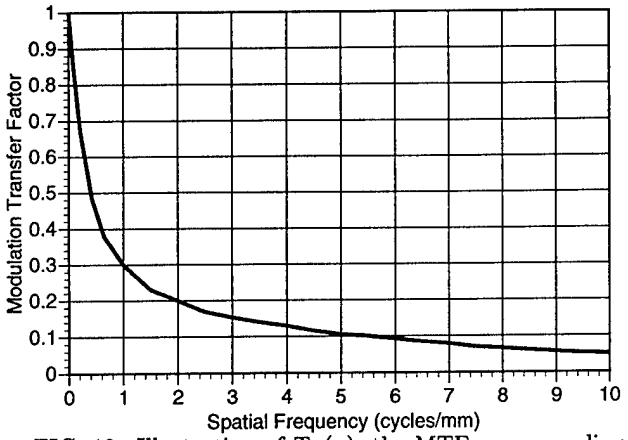

FIG. 10. Illustration of $T_k(\nu)$, the MTF corresponding to reabsorption in the film-screen system (adapted from Metz and Vyborny).

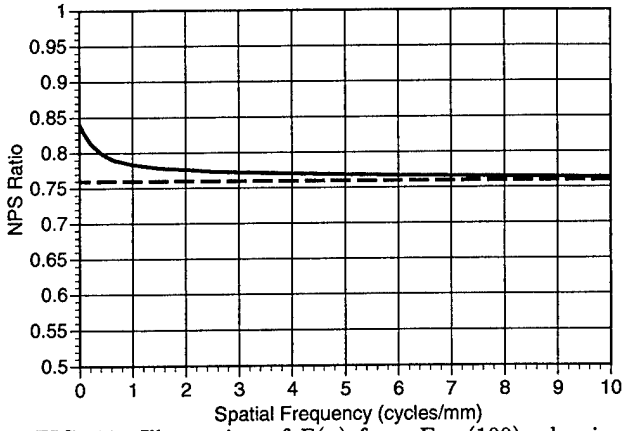

FIG. 11. Illustration of $\Gamma(\nu)$ from Eq. (100), showing contributions from the uncorrelated and correlated components (adapted from Metz and Vyborny).

The cross terms $\mathrm{NPS}_{BC}(\nu)$ and $\mathrm{NPS}_{CB}(\nu)$, based on Eq. (92), are given by

$$\mathrm{NPS}_{BC}(\nu) = (1-\psi)\psi m^2 f_K \mathrm{T}_K^*(\nu)\varsigma\omega\eta\,\bar{q}, \qquad (96)$$

and

$$\mathrm{NPS}_{CB}(\nu) = (1-\psi)\psi m^2 f_K \mathrm{T}_K(\nu)\varsigma\omega\eta\,\bar{q}, \qquad (97)$$

respectively, where $\mathrm{T}_K(\nu)$ is the characteristic transfer function describing the reabsorption probability density in terms of spatial frequencies and is equal to the Fourier transform of the reabsorption PSF, $p_K(r)$. It is known that the sum of two complex conjugates is equal to two times the real part. This leads to

$$\mathrm{NPS}_{BC}(\nu) + \mathrm{NPS}_{CB}(\nu) = 2\bar{q}\eta\varsigma\omega(1-\psi)\psi m^2 f_K \mathrm{Re}\Big\{\mathrm{T}_K(\nu)\Big\}, \qquad (98)$$

which is always real, where Re{ } denotes the real part of a complex quantity.

Combining the above results gives the NPS for the output optical image quanta, including the effect of the redistribution of light in the screen, as

$$\mathrm{NPS}_o(\nu) = \bar{q}\eta m^2\Big[(1-\varsigma\omega) + \varsigma\omega(1-\psi)^2 + \varsigma\omega f_K\psi^2 + 2\varsigma\omega f_K\psi(1-\psi)\mathrm{Re}\Big\{\mathrm{T}_K(\nu)\Big\}\Big]|\mathrm{T}_o(\nu)|^2 \qquad (99)$$

which is the Metz-Vyborny result for the NPS of light emitted from the screen.

Metz and Vyborny used Eq. (99) to describe the effect of reabsorption in a Dupont Par Speed calcium tungstate screen. Assuming a constant film density (fixed light output $\bar{q}_o$), the effect of reabsorption is obtained by considering the NPS just above and below the K-edge of tungsten at approximately 68.5 keV. Above the K-edge reabsorption takes place and $\bar{q}_o$ is given by Eq. (87). Below the K-edge, both the light output and the NPS are determined by setting $\psi = 0$ and $\varsigma\omega = 0$. Therefore, the ratio of the NPS just above the K-edge to just below, normalized to fixed total light output, is given by $\Gamma(\nu)$ where

$$\Gamma(\nu) = \frac{(1-\varsigma\omega) + \varsigma\omega(1-\psi)^2 + \varsigma\omega f_K\psi^2 + 2\varsigma\omega f_K\psi(1-\psi)\mathrm{Re}\Big\{\mathrm{T}_K(\nu)\Big\}}{1-\varsigma\omega\psi(1-f_K)}. \qquad (100)$$

Figure 10 illustrates $\mathrm{T}_K(\nu)$ as used by Metz and Vyborny. The corresponding degradation in the NPS, $\Gamma(\nu)$, is shown in Fig. 11 obtained using values listed in Table 1. The value of $\mathrm{NPS}(\nu)$ is decreased by approximately 10% at low frequencies, increasing to within a few percent of the uncorrelated value for frequencies above approximately 2 cycles/mm. While these results are specific to a calcium tungstate screen which has limited use at present, corresponding results for newer screens and other imaging systems can be obtained using the same formalism. The transfer-theory approach is sometimes more physically intuitive than a detailed statistical analysis, making an interpretation of the results more physically meaningful. For instance, it is clear from this analysis that the MTF describing reabsorption, $\mathrm{T}_K(\nu)$, appears in the cross-spectral density term since light emitted remotely is correlated with light emitted locally when a K x ray is produced. It appears in the first power since it appears in only one of two correlated paths.

IV. CONCLUSIONS

The DQE is an important indicator of the performance of medical imaging systems. Recent developments in understanding noise transfer in medical imaging systems has resulted in a generalized transfer-theory approach that can be used to describe the DQE and other metrics of system performance for many imaging systems.

TABLE I. Values used to determine $\Gamma(\nu)$ from Metz and Vyborny. $E_K = 59.3$ keV.

Variable	Value[a]	Physical Meaning
ς	0.85	probability that an interacting x rayundergoes a K-shell interaction
ω	0.93	fluorescent yield of K-shell photoelectricinteractions
ψ	0.866	fraction of incident x-ray energy transferredto K x ray, E_K/E_x
f_K	0.20	probability that a K x ray is reabsorbed in thescreen, depends on geometry

[a]See Ref. [34]

Until recently, the transfer-theory approach has been limited to the description of serial cascades of quantum gain and quantum scattering processes. As part of a program developing new transfer-theory relationships, we describe how parallel cascades of image-forming processes can be incorporated into the transfer-theory approach. Parallel cascades are required when more than one image-forming process combines to create the final image. It has been shown in this article that parallel cascades can be used with the introduction of the cross covariance between cascades. A general expression for the cross covariance of correlated point processes has been developed, and in particular, the cross covariance of two amplified point processes descending from randomly selected quanta in a common input image was examined which has particular importance for the analysis of medical imaging systems [Eq. (81) for WSS conditions]. It has been shown how a complete imaging system can be represented in terms of a schematic diagram describing relationships between elementary image-forming processes.

Under wide-sense stationary conditions, the Fourier transform of the cross covariance is the cross spectral density function. With it, transfer-theory models can be developed to describe the noise power spectrum in imaging systems that require the use of parallel cascades of image-forming processes. The example of reabsorption of K x rays in a radiographic screen was described in this article. It was shown that the transfer-theory approach gives the same result obtained by Metz and Vyborny using a sophisticated statistical analysis when the same assumptions are made. Other examples may include: a) double-emulsion film-screen systems where light may cross from one emulsion to the other; b) portal imaging systems where high-energy x rays may generate different kinds of secondary quanta in the detector such as electrons and light; and, c) flat-panel active matrix detectors where scattered light may contribute a non-negligible fraction of the image signal.

Extension of the transfer-theory approach to include parallel cascades increases the number of theoretical "tools" available to scientists and engineers in the transfer-theory "tool-box." We are currently developing additional tools for the analysis of new digital imaging systems. These new tools are required to describe noise transfer in the presence of other situations such as non-uniform detector-element gain and sensitivity, random errors in detector-element offset and gain corrections, polyenergetic x rays, thick phosphors with variable conversion factors due to Swank noise and the Lubberts effect, and detectors with lag.

ACKNOWLEDGEMENTS

The authors are grateful to the US Army Materiel Command Breast Cancer research program and the Canadian Institutes of Health Research for financial support. In addition, discussions with friends and associates including Drs. A. Fenster, R. Shaw, R.F. Wagner, A. Burgess, H.H. Barrett and G.E. Parraga have been very helpful.

APPENDIX A: ELEMENTARY PROCESSES

Medical x-ray imaging system modeling is based on three elementary processes. Under wide-sense stationary (WSS) conditions, the elementary processes, and the transfer properties of signal and noise, are summarized in this Appendix.

1. Quantum Gain and Selection

Rabbani *et al.* [13] described the transfer of signal and noise through a stochastic quantum gain stage, characterized by a random variable $\tilde{g}$ which has a mean value $\bar{g}$ and variance σ_g^2. Barrett *et al.* [19,20] considered this elementary process as the limiting case of amplified point process. They showed that the uniform mean value of distribution of quanta (i.e., mean number of quanta per unit area) and corresponding NPS are transferred according to

$$\bar{q}_{out} = \bar{g}\,\bar{q}_{in} \tag{A1}$$

and

$$\mathrm{NPS}_{out}(\nu) = \bar{g}^2\,\mathrm{NPS}_{in}(\nu) + \sigma_g^2\bar{q}_{in}, \tag{A2}$$

respectively. If $\tilde{g}$ is modeled as a deterministic gain factor, Eq. (A1) remains the same, but Eq. (A2) becomes

$$\mathrm{NPS}_{out}(\nu) = \bar{g}^2\,\mathrm{NPS}_{in}(\nu), \tag{A3}$$

which lacks the second term in Eq. (A2).

For the special case where $\tilde{g}$ represents a binary selection process such as the responsive quantum efficiency of the radiographic screen, $\tilde{g}$ can have a value of 0 or 1 only, $0 \le \bar{g} \le 1$, and $\sigma_g^2 = \bar{g}(1-\bar{g})$. In this case, it is also possible to express signal transfer as

$$q_{out}(\boldsymbol{r}) = \tilde{g}\, q_{in}(\boldsymbol{r}) \tag{A4}$$

where $q_{in}(\boldsymbol{r})$ and $q_{out}(\boldsymbol{r})$ are sample functions of the input and output random point processes.

2. Quantum Scatter (Relocation)

Quantum scatter is a translated point process [33] whereby a quantum is randomly relocated by the displacement vector $\boldsymbol{r}$ and where $p(\boldsymbol{r})$ is a point spread function (PSF) describing the translation probability density [13,38].

The transfer function through this process have been described by both Rabbani *et al.* [13] and Barrett *et al.* [19,20], given by

$$q_{out}(\boldsymbol{r}) = p(\boldsymbol{r}) *_s q_{in}(\boldsymbol{r}), \tag{A5}$$

where $*_s$ represents the scattering process and $p(\boldsymbol{r})$ has unity area. The statistics of signal and noise are transferred according to

$$\bar{q}_{out} = \bar{q}_{in}, \tag{A6}$$

and

$$\mathrm{NPS}_{out}(\nu) = \left[\mathrm{NPS}_{in}(\nu) - \bar{q}_{in}\right]|\mathrm{T}(\nu)|^2 + \bar{q}_{in} \tag{A7}$$

where $\mathrm{T}(\nu)$ is the Fourier transform of $p(\boldsymbol{r})$.

3. Linear Filter (Convolution)

The transfer relationships through a linear shift-invariant filter are described by the convolution integral, given by [2]

$$d_{out}(\boldsymbol{r}) = p(\boldsymbol{r}) * q_{in}(\boldsymbol{r}), \tag{A8}$$

$$\bar{d}_{out} = |\mathrm{T}(0)|\,\bar{q}_{in}, \tag{A9}$$

and

$$\mathrm{NPS}_{out}(\nu) = \mathrm{NPS}_{in}(\nu)|\mathrm{T}(\nu)|^2 \tag{A10}$$

where $*$ represents a convolution, $p(\boldsymbol{r})$ is the impulse response commonly referred to as the blur PSF and $\mathrm{T}(\nu)$ is the characteristic transfer function of the filter, given by the Fourier transform of $p(\boldsymbol{r})$. Unlike the scattering process, the ouput $d_{out}(\boldsymbol{r})$ from a linear filter is not a point process.

APPENDIX B: STATISTICS OF PARALLEL PROCESSES

When two random processes contribute to an output signal, the result is a random process that is the sum of two random processes. For example, consider a stochastic system described by $\tilde{c}(\boldsymbol{r}) = \tilde{a}(\boldsymbol{r}) + \tilde{b}(\boldsymbol{r})$. The autocorrelation of the sum process is [39]

$$\begin{aligned}
&\mathrm{R}_c(\boldsymbol{r},\boldsymbol{r}') = \mathrm{E}\Big\{\tilde{c}(\boldsymbol{r})\tilde{c}^*(\boldsymbol{r}')\Big\} \\
&= \mathrm{E}\Big\{[\tilde{a}(\boldsymbol{r}) + \tilde{b}(\boldsymbol{r})][\tilde{a}^*(\boldsymbol{r}') + \tilde{b}^*(\boldsymbol{r}')]\Big\} \\
&= \mathrm{E}\Big\{\tilde{a}(\boldsymbol{r})\tilde{a}^*(\boldsymbol{r}')\Big\} + \mathrm{E}\Big\{\tilde{b}(\boldsymbol{r})\tilde{b}^*(\boldsymbol{r}')\Big\} \\
&\qquad + \mathrm{E}\Big\{\tilde{a}(\boldsymbol{r})\tilde{b}^*(\boldsymbol{r}')\Big\} + \mathrm{E}\Big\{\tilde{b}(\boldsymbol{r})\tilde{a}^*(\boldsymbol{r}')\Big\} \\
&= \mathrm{R}_a(\boldsymbol{r},\boldsymbol{r}') + \mathrm{R}_b(\boldsymbol{r},\boldsymbol{r}') + \mathrm{R}_{ab}(\boldsymbol{r},\boldsymbol{r}') + \mathrm{R}_{ba}(\boldsymbol{r},\boldsymbol{r}'),
\end{aligned} \tag{B1}$$

where * denotes a complex conjugate. When $\tilde{a}(\boldsymbol{r})$ and $\tilde{b}(\boldsymbol{r})$ are both wide-sense stationary (WSS), $\tilde{c}(\boldsymbol{r})$ is also WSS, and the autocorrelation of $\tilde{c}(\boldsymbol{r})$ in Eq. (B1) can be written as

$$\mathrm{R}_c(\boldsymbol{\tau}) = \mathrm{R}_a(\boldsymbol{\tau}) + \mathrm{R}_b(\boldsymbol{\tau}) + \mathrm{R}_{ab}(\boldsymbol{\tau}) + \mathrm{R}_{ba}(\boldsymbol{\tau}). \tag{B2}$$

The autocovariance, $\mathrm{K}_c(\boldsymbol{r},\boldsymbol{r}')$, is similar to the autocorrelation but with the mean subtracted. Similar to above,

$$\begin{aligned}
&\mathrm{K}_c(\boldsymbol{r},\boldsymbol{r}') = \mathrm{E}\Big\{[\tilde{a}(\boldsymbol{r}) + \tilde{b}(\boldsymbol{r})][\tilde{a}^*(\boldsymbol{r}') + \tilde{b}^*(\boldsymbol{r}')]\Big\} \\
&\qquad - \mathrm{E}\Big\{\tilde{a}(\boldsymbol{r}) + \tilde{b}(\boldsymbol{r})\Big\}\mathrm{E}\Big\{\tilde{a}^*(\boldsymbol{r}') + \tilde{b}^*(\boldsymbol{r}')\Big\} \\
&= \mathrm{K}_a(\boldsymbol{r},\boldsymbol{r}') + \mathrm{K}_b(\boldsymbol{r},\boldsymbol{r}') + \mathrm{K}_{ab}(\boldsymbol{r},\boldsymbol{r}') + \mathrm{K}_{ba}(\boldsymbol{r},\boldsymbol{r}'),
\end{aligned} \tag{B3}$$

and for WSS processes

$$\mathrm{K}_c(\boldsymbol{\tau}) = \mathrm{K}_a(\boldsymbol{\tau}) + \mathrm{K}_b(\boldsymbol{\tau}) + \mathrm{K}_{ab}(\boldsymbol{\tau}) + \mathrm{K}_{ba}(\boldsymbol{\tau}). \tag{B4}$$

The corresponding NPS of $\tilde{c}(\boldsymbol{r})$ is therefore

$$\begin{aligned}
&\mathrm{NPS}_c(\nu) = \mathcal{F}\Big\{\mathrm{K}_c(\boldsymbol{\tau})\Big\} \\
&= \mathrm{NPS}_a(\nu) + \mathrm{NPS}_b(\nu) + \mathrm{NPS}_{ab}(\nu) + \mathrm{NPS}_{ba}(\nu),
\end{aligned} \tag{B5}$$

where each term in Eq. (B5) is the Fourier transform of the corresponding term in Eq. (B4). The terms $\mathrm{NPS}_{ab}(\nu)$ and $\mathrm{NPS}_{ba}(\nu)$ are cross spectral densities and reflect the spatial-frequency dependence of the auto-covariance.

By definition of the cross covariance for two random procesess, we have

$$\mathrm{K}_{ab}(\boldsymbol{r},\boldsymbol{r}') = \mathrm{K}_{ba}^*(\boldsymbol{r}',\boldsymbol{r}). \tag{B6}$$

Under WSS conditions, Eq. (B6) becomes

$$\mathrm{K}_{ab}(\tau) = \mathrm{K}^*_{ba}(-\tau), \tag{B7}$$

where $\tau = r - r'$. The cross spectral density $\mathrm{NPS}_{ab}(\nu)$ is the Fourier transform of $\mathrm{K}_{ab}(\tau)$ given by

$$\mathrm{NPS}_{ab}(\nu) = \mathcal{F}\Big\{\mathrm{K}_{ab}(\tau)\Big\} = \int_\infty \mathrm{K}_{ab}(\tau) e^{-j2\pi\nu\tau} d\tau. \tag{B8}$$

Substituting Eq. (B7) into Eq. (B8), we have

$$\begin{aligned}\mathrm{NPS}_{ab}(\nu) &= \int_\infty \mathrm{K}^*_{ba}(-\tau) e^{-j2\pi\nu\tau} d\tau \\ &= \int_\infty \mathrm{K}^*_{ba}(\tau) e^{j2\pi\nu\tau} d\tau \\ &= \left\{\int_\infty \mathrm{K}_{ba}(\tau) e^{-j2\pi\nu\tau} d\tau\right\}^* \\ &= \left\{\mathcal{F}\Big\{\mathrm{K}_{ba}(\tau)\Big\}\right\}^* = \mathrm{NPS}^*_{ba}(\nu). \end{aligned} \tag{B9}$$

Thus, we conclude that the cross spectral densities $\mathrm{NPS}_{ab}(\nu)$ and $\mathrm{NPS}_{ba}(\nu)$ are conjugate pairs, and the sum of $\mathrm{NPS}_{ab}(\nu) + \mathrm{NPS}_{ba}(\nu)$ is always a real value, i.e.,

$$\begin{aligned}\mathrm{NPS}_{ab}(\nu) + \mathrm{NPS}_{ba}(\nu) &= 2\,\mathrm{Re}\Big\{\mathrm{NPS}_{ab}(\nu)\Big\} \\ &= 2\,\mathrm{Re}\Big\{\mathrm{NPS}_{ba}(\nu)\Big\}, \end{aligned} \tag{B10}$$

where Re{ } denotes the real part of a complex quantity.

APPENDIX C: STATISTICAL AVERAGES AND MARGINAL PROBABILITY DENSITIES

Consider a continuous random variable $\tilde{y} = f(\tilde{x})$, where $\tilde{x}$ is a continuous random variable with the probability density function $p_{\tilde{x}}(x)$. The function $f(x)$ is a single-valued function of x, and maps random variable $\tilde{x}$ into random variable $\tilde{y}$. We define the mean of the continuous random variable $\tilde{y}$ by the equation [2]

$$\bar{y} = \mathrm{E}\{\tilde{y}\} = \mathrm{E}\Big\{g(\tilde{x})\Big\} = \int_{-\infty} g(x) p_{\tilde{x}}(x) dx, \tag{C1}$$

which is the statistical average over random variable $\tilde{x}$. If the probability density function $p_{\tilde{y}}(y)$ is defined, then

$$\bar{y} = E\{\tilde{y}\} = \int_{-\infty} y p_{\tilde{y}}(y) dy. \tag{C2}$$

Eqs. (C1) and (C2) give the same result for the statistical average of $\tilde{y} = g(\tilde{x})$. Equation (C1) refers to the sample space of $\tilde{x}$ and Eq. (C2) refers to the sample space of $\tilde{y}$.

For a set of several random variables, the statistics of each are called marginal [2]. For example, $p_{\tilde{x}}(x)$ is the marginal probability density of $\tilde{x}$ and $p_{\tilde{y}}(y)$ the marginal probability density of $\tilde{y}$ for their joint density function $p_{\tilde{x},\tilde{y}}(x,y)$. The following relationships are satisfied [2] for $p_{\tilde{x}}(x)$ and $p_{\tilde{y}}(y)$,

$$p_{\tilde{x}}(x) = \int_{-\infty} p_{\tilde{x},\tilde{y}}(x,y) dy \tag{C3}$$

and

$$p_{\tilde{y}}(y) = \int_{-\infty} p_{\tilde{x},\tilde{y}}(x,y) dx, \tag{C4}$$

which are the property of marginal densities.

[1] J. C. Dainty and R. Shaw, *Image Science*, (Academic, New York, 1974).

[2] A. Papoulis, *Probability, Random Variables, and Stochastic Processes*, 3rd ed. (McGraw Hill, New York, 1991).

[3] G. M. Jenkins and D. G. Watts, *Spectral Analysis and its Applications*, (Holden-Day, San Francisco, 1968).

[4] R. Shaw, "The equivalent quantum efficiency of the photographic process," J. Photogr. Sci. **11**, 199–204 (1963).

[5] "Medical imaging—the assessment of image quality," ICRU Rep. No. 54, (International Commission of Radiation Units and Measurements, Bethesda, Md., 1995).

[6] R. Shaw, "Some fundamental properties of xeroradiographic images," SPIE Proc. **70**, 359–363 (1975).

[7] R. F. Wagner and E. P. Muntz, "Detective quantum efficiency (DQE) analysis of electrostatic imaging and screen-film imaging in mammography," SPIE Proc. **173**, 162–165 (1979).

[8] M. J. Tapiovaara and R. F. Wagner, "A generalized detective quantum efficiency (DQE) approach to the analysis of x-ray imaging," Proc. Soc. Photo-Opt. Instrum. Eng. **454**, 540–549 (1984).

[9] M. J. Tapiovaara and R. F. Wagner, "SNR and DQE analysis of broad spectrum x-ray imaging," Phys. Med. Biol. **30**, 519–529 (1985).

[10] K. Rossmann, "Point spread-function, line spread-function, and modulation transfer function," Radiology **93**, 257–272 (1969).

[11] C. E. Metz and K. Doi, "Transfer function analysis of radiographic imaging systems," Phys. Med. Biol. **24**, 1079–1106 (1979).

[12] H. H. Barrett and W. Swindell, *Radiological imaging—the theory of image formation, detection, and processing*, (Academic, New York, 1981).

[13] M. Rabbani, R. Shaw, and R. Van Metter, "Detective quantum efficiency of imagin systems with amplifying and scattering mechanisms," J. Opt. Soc. Am. A **4**, 895–901 (1987).

[14] M. Rabbani and R. Van Metter, "Analysis of signal and noise propagation for several imaging mechanisms," J. Opt. Soc. Am. A **7**, 1156–1164 (1989).

[15] P. L. Dillon, J. F. Hamilton, M. Rabbani, R. Shaw, and R. Van Metter, "Principles governing the transfer of signal modulation and photon noise by amplifying and scattering mechanisms," SPIE Proc. **535**, 130–139 (1985).

[16] I. A. Cunningham, "Linear-systems modeling of parallel cascaded stochastic processes: the NPS of radiographic screens with reabsorption of characteristic x radiation," SPIE Proc. **3336**, 220–230 (1998).

[17] I. A. Cunningham and R. Shaw, "Signal-to-noise optimization of medical imaging systems," J. Opt. Soc. Am. A **16**, 621–632 (1999).

[18] I. A. Cunningham, "Applied linear-systems theory," in *Handbook of Medical Imaging, Vol. 1: Physics and Psychophysics*, edited by J. Beutel, H. L. Kundel, and R. Van Metter, (SPIE press, Bellingham, 2000), pp. 79–160.

[19] H. H. Barrett, R. F. Wagner, and K. J. Myers, "Correlated point processes in radiological imaging," SPIE Proc. **3032**, 110–125 (1997).

[20] H. H. Barrett and K. J. Myers, *Foundations of Image Science*, (Wiley, New York, in preparation for publication in 2001).

[21] P. C. Bunch, K. E. Huff, and R. Van Metter, "Analysis of the detective quantum efficiency of a radiographic screen-film combination," J. Opt. Soc. Am. A **4**, 902–909 (1987).

[22] R. M. Nishikawa and M. J. Yaffe, "Effect of various noise sources on the detective quantum efficiency of phosphor screens," Med. Phys. **17**, 887–893 (1990).

[23] R. M. Nishikawa and M. J. Yaffe, "Model of the spatial-frequency-dependent detective quantum efficiency of phosphor screens," Med. Phys. **17**, 894–904 (1990).

[24] J. H. Siewerdsen, L. E. Anonuk, Y. El-Mohri, J. Yorkston, W. Huang, J. M. Boudry, and I. A. Cunningham, "Empirical and theoretical investigation of the noise performance of indirect detection, active matrix flat-panel imagers (AMFPIs) for diagnostic radiology," Med. Phys. **24**, 71–89 (1997).

[25] J. H. Siewerdsen, L. E. Anonuk, Y. El-Mohri, J. Yorkston, W. Huang, and I. A. Cunningham, "Signal, noise power spectrum and detective quantum efficieney of indirect-detertion flat-panel imagers for diagnostic radiology," Med. Phys. **25**, 614–628 (1998).

[26] W. Zhao and J. A. Rowlands, "Digital radiology using active matrix readout of amorphous selenium: theoretical analysis of detective quantum efficiency," Med. Phys. **24**, 1819–1833 (1997).

[27] J. P. Bissonnette, I. A. Cunningham, D. A. Jaffray, A. Fenster, and P. Munro, "A quantum accounting and detective quantum efficiency analysis for video-based portal imaging," Med. Phys. **24**, 815–826 (1997).

[28] T. Falco and B. G. Fallone, "Characteristics of metal-plate/film detectors at therapy energies. II. Detective quantum efficiency," Med. Phys. **25**, 2463–2468 (1998).

[29] R. N. Cahn, B. Cederstrom, M. Danielsson, A. Hall, M. Lundqvist, and D. Nygren, "Detective quantum efficiency dependence on x-ray energy weighting in mammography," Med. Phys. **26**, 2680–2683 (1999).

[30] H. Liu, L. L. Fajardo, and B. C. Penny, "Signal-to-noise ratio and detective quantum efficiency analysis of optically coupled CCD mammography imaging systems," Acad. Radiol. **3**, 799–805 (1996).

[31] D. Mah, J. A. Rawlinson, and J. A. Rowlands, "Detective quantum efficiency of an amorphous selenium detector to megavoltage radiation," Phys. Med. Biol. **44**, 1369–1384 (1999).

[32] M. B. Williams, P. U. Simoni, L. Smilowitz, M. Stanton, W. Phillips, and A. Stewart, "Analysis of the detective quantum efficiency of a developmental detector for digital mammography," Med. Phys. **26**, 2273–2285 (1999).

[33] D. L. Snyder and M. I. Miller, *Random Point Processes, in Time and Space*, (Springer Verlag, New York, 1991).

[34] C. E. Metz and C. J. Vyborny, "Wiener spectral effects of spatial correlation between the sites of characteristic x-ray emission and reabsorption in radiographic screen-film systems," Phys. Med. Biol. **28**, 547–564 (1983).

[35] K. Rossmann, "Measurement of the modulation transfer function of radiographic systems containing fluorescent screens," Phys. Med. Biol. **9**, 551–557 (1964).

[36] K. Rossmann, "The spatial frequency spectrum: a means for studying the quality of radiographic imaging systems," Radiology, **90**, 1–13 (1968).

[37] F. A. Haight, *Handbook of the poisson distribution*, (Wiley, New York, 1967).

[38] I. A. Cunningham, M. S. Westmore, and A. Fenster, "Unification of image blur and noise in linear-systems transfer theory using a stochastic scattering operator," Med. Phys. (accepted) **27**, (2000).

[39] W. B. Davenport and W. L. Root, *Introduction to the Theory of Random Signals and Noise*, (McGraw Hill, New York, 1958).

Appendix II: Scatter Operator

This appendix consists of a manuscript completed this year describing how x-ray scatter can be incorporated into the linear-systems approach as a "scatter operator." It has been submitted to Medical Physics for publication.

Unified representation of image blur and noise in linear-systems transfer theory with a scatter operator

I.A. Cunningham,[1,2] M.S. Westmore[1] and A. Fenster[1]
[1]*Imaging Research Laboratories, The John P. Robarts Research Institute, P.O. Box 5015, 100 Perth Drive, London, Ontario, N6A 5K8 Canada; and,*
[2]*Diagnostic Radiology, London Health Sciences Centre*

Submitted for publication in Medical Physics, 2000.

ABSTRACT

Rabbani, Shaw and Van Metter described the transfer of the auto-covariance and image noise-power spectrum through a photon scattering (image blurring) process. We incorporate their result into a linear-systems transfer-theory framework by describing a generalized scatter operator acting with an associated point-spread function. Scatter is a translated point-process, and it is shown that this operator is not distributive over addition or multiplication. While in general it does not commute with addition or multiplication, it does commute with itself and with a binomial selection process (as might represent the quantum efficiency of a detector). Strictly speaking it is not associative, although a similar property that is true is described. This formalism is used to explain the degradation of the detective quantum efficiency (DQE) caused by both the x-ray focal-spot size and optical blur in a radiographic screen as illustrative examples. It is shown that for quantum-noise limited systems in general, the frequency dependence of the system DQE is a direct consequence of the statistical properties of image quanta as represented by the scatter operator. This extended linear-systems approach has wide application for the description of imaging systems in general.

Keywords: linear-systems, transfer theory, detective quantum efficiency, DQE, convolution, modulation-transfer function, MTF, noise-power spectrum, NPS, cascaded systems

I. INTRODUCTION

The design and analysis of medical imaging systems requires a mathematical understanding of important principles and processes that contribute to image formation. Linear-systems transfer theory is an approach used by many authors to describe the performance of linear and shift-invariant (LSI) imaging systems in both the spatial and spatial-frequency domains.[1–4] Image-blurring mechanisms are described in terms of linear filters[1,5,6] as a convolution with a specified point-spread function (PSF) in the spatial domain, or alternatively by multiplication with the modulation-transfer function (MTF) in the spatial-frequency domain.[7,8] Complex systems can be represented as a serial cascade of simple processes, or stages, where the output from one stage forms a virtual input to the next. Excellent early review papers on this topic have been written by Doi, Rossmann and Haus,[9] and Metz and Doi.[2]

This linear-filter approach describes only the expectation (noise-free) effect of image-blurring mechanisms since it represents blur as a deterministic process. In reality, blur generally results from the random scattering of individual image quanta, and the effect of this scatter on image noise must be described separately using stochastic-process theories.[2,10] For the special case of wide-sense-stationary (WSS) noise processes,[11] this noise can be characterized in terms of the auto-covariance, or its Fourier transform, the noise-power spectrum (NPS). Dainty and Shaw,[8] Barrett and Swindell,[1] Macovski,[5] Parker[6] and others have used this approach extensively in their texts to describe important principles and fundamental properties of many system designs.

The distinction between scatter and deterministic blur has been recognized by many investigators, including Dainty and Shaw,[8] Wagner,[12] Metz and Doi,[2] Sandrik and Wagner,[13] Metz and Vyborny,[14] and Barrett and Swindell.[1] The NPS of a random process undergoing a deterministic blur is "passed through" the square of the blur MTF (e.g. Barrett and Swindell[1] Eq. 3.200, Parker[6] Eq. 24.28). More recently, transfer of the NPS through a scattering process was described by Shaw and Van Metter,[15] derived theoretically by Rabbani et al.[16] using moment-generating functions, and later by Barrett et al.[17] using point-process theory. They note that the correlated component of the NPS is passed through the squared scatter MTF while the uncorrelated component is not.[15,16] Their result has been experimentally demonstrated by Maidment and Yaffe,[18] and derived in a different form by Mulder.[19]

The scatter result[16] has been used by Nishikawa et al.[20,21] and others in a small number of applications, but its implications are of a more general nature. We incorporate scatter into the linear-systems approach by describing a generalized scatter operator as an alternative to the convolution operation that is used to describe deterministic blur. The word "convolution" means to fold or roll together (Webster), and is used to represent the blur of a linear filter when the filter PSF is "folded into" the image signal. In some sense, scatter can be interpreted as a "stochastic convolution," as this folding together is a consequence of the random relocating of individual image quanta. Use of the scatter operator (and hence the Rabbani NPS) as a substitute for the convolution integral to describe image blurring processes means that linear-systems transfer theory can be used to describe both image-signal and image-noise (second order) transfer characteristics in a cascaded-systems analysis.

Under certain circumstances, the difference between scatter and deterministic blurring is insignificant. For instance, Barrett and Swindell[22] note that when x rays are converted to light in a radiographic screen, the statistical nature of the light photons can be ignored if a large number of photons are generated and hence each x ray produces light that is adequately described by the deterministic PSF. The work described here discusses this in more detail, and extends this observation to show that it is spatial-frequency dependent. In addition, if the light is subsequently collected by an inefficient optical system, the statistical nature of the optical photons cannot be ignored. This will occur, for example, if only a few light quanta are detected per interacting x ray since it is not possible to know where, within each PSF distribution, the detected quanta originated. Thus, when assessing new systems or system designs, it is necessary to correctly account for these statistical properties. Ignoring them can result in much wasted effort in designing new systems that have no chance of achieving a sufficiently high detective quantum efficiency (DQE).

II. BACKGROUND

Linear systems can be described in terms of the transfer of image signal and noise from input to output. In this context, an image is a spatial distribution of quanta (e.g. x rays or light). Signal transfer corresponds to the transfer of the expected distribution of image quanta. Noise transfer corresponds to the transfer of parameters that describe image noise, such as the autocovariance or NPS. In this article, a third type of transfer relationship will be used that we call the sample transfer, describing the transfer of a particular sample distribution of image quanta.

Quanta have negligible spatial extent, and one way of describing a sample distribution of quanta is as $q(\boldsymbol{r})$, a superposition of many δ-functions where each δ-function represents one quantum. While this approach is often convenient, δ-functions are generalized functions[3,23] and must be treated with care. In addition, it is convenient to write the ensemble average, or expectation, of $q(\boldsymbol{r})$ as $\mathrm{E}\{q(\boldsymbol{r})\}$. Thus, while $q(\boldsymbol{r})$ is a sample distribution of quanta representing a particular image, $\mathrm{E}\{q(\boldsymbol{r})\}$ describes the expectation number of quanta per unit area as a function of position, and can be viewed as a "noise-free" image. Both have dimension of quanta per unit area.

The generalized function $q(\boldsymbol{r})$ is not directly measurable. Measurable quantities, such as the output

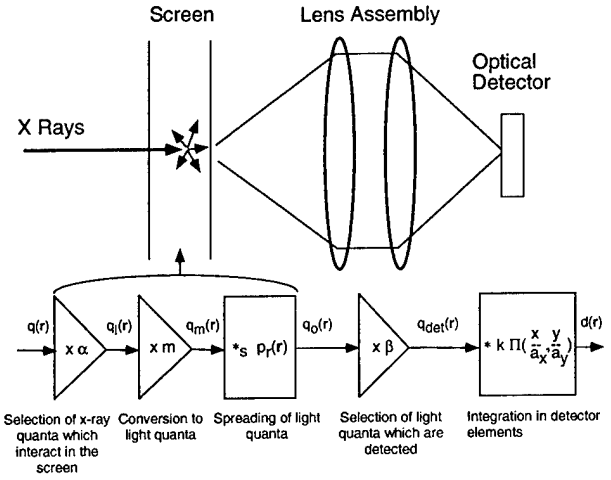

Figure 1: The hypothetical system represented as a cascade of linear stages.

from a detector element (see Appendix I) are expressed as d given by

$$d = g_o \int_{A_d} q(\boldsymbol{r}')\, \mathrm{d}^2\boldsymbol{r}' \tag{1}$$

where A_d is the area of the detector element and g_o is a conversion factor relating the number of interacting quanta to the detector signal. When A_d is expressed as $A_d(\boldsymbol{r})$, the area of a hypothetical element centered at position $\boldsymbol{r}$, the signal d is written as $d(\boldsymbol{r})$ and has been called the "presampling" detector signal as it is a function that describes the detector signals when evaluated ("sampled") at positions corresponding to the centers of the detector elements. In the following, we use q to represent a distribution of quanta and d to represent a physically measured - or measurable - detector signal in terms of an analog-to-digital converter (ADC) value. Image noise is defined in terms of the noise-power spectrum (NPS) in $q(\boldsymbol{r})$ for the special case of $\mathrm{E}\{q(\boldsymbol{r})\}$ equal to a constant throughout the image to satisfy the requirement for wide-sense stationary noise processes where the mean and autocorrelation are invariant with $\boldsymbol{r}$.[11]

The utility of the linear-systems approach is illustrated by analyzing the simplified hypothetical system shown in Fig. (1) to determine the presampling detector signal. The system consists of a thin radiographic screen coupled to a CCD camera through a lens assembly. All components are assumed to be linear and shift invariant. The screen quantum efficiency is α (assumed to be unity for the moment) and each interacting x ray generates exactly m optical quanta at some point of interaction in the screen. The optical quanta are scattered (i.e. spread) before leaving the screen according to a PSF $\mathrm{p}_r(\boldsymbol{r})$. The optical quanta are coupled to the CCD camera with a lens having a collection efficiency β. The camera integrates incident optical quanta in discrete detector elements and the signals from all elements are combined to generate a digital image. This model does not describe the effect of such things as variable x-ray energy, or variable interaction depth or gain in the screen. As such, it is a simplified model and is chosen primarily to highlight the difference between use of the conventional and "stochastic" convolutions in linear-systems theory.

The serial nature of the model is illustrated in Fig. (1) where $q(\boldsymbol{r})$ represents the distribution of x-ray quanta incident on the screen. The distribution of interacting quanta is $q_I(\boldsymbol{r})$ and the distribution of optical quanta as generated in the screen is $q_m(\boldsymbol{r})$ where

$$\mathrm{E}\{q_m(\boldsymbol{r})\} = \mathrm{E}\{q_I(\boldsymbol{r})\}m = \mathrm{E}\{q(\boldsymbol{r})\}\alpha m. \tag{2}$$

The two-dimensional NPS in the distribution of optical quanta is $\mathrm{NPS}_m(\boldsymbol{k})$ given by[16]

$$\mathrm{NPS}_m(\boldsymbol{k}) = m^2\mathrm{NPS}_I(\boldsymbol{k}) = m^2\bar{q}_I \tag{3}$$

where $\boldsymbol{k}$ is a two-dimensional frequency vector (with units cycles per unit length) in the direction of $\boldsymbol{r}$ and the NPS of $q_I(\boldsymbol{r})$ is[3] $\mathrm{NPS}_I(\boldsymbol{k}) = \bar{q}_I$. The assumption of a deterministic gain m is not always a valid assumption, and is discussed below.

If it can further be assumed that each interacting x-ray quantum produces exactly the same distribution of light at the screen surface, and that no optical quanta are lost or absorbed in the screen, then the expectation distribution of $q_o(\boldsymbol{r})$, the optical quanta that exit from the screen, can be expressed using linear-systems theory as

$$\mathrm{E}\{q_o(\boldsymbol{r})\} = \mathrm{E}\{q_m(\boldsymbol{r})\} ** \mathrm{p}_r(\boldsymbol{r}) = \int_{-\infty}^{\infty} \mathrm{E}\{q_m(\boldsymbol{r}')\}\mathrm{p}_r(\boldsymbol{r}-\boldsymbol{r}')\,\mathrm{d}^2\boldsymbol{r}' \tag{4}$$

where $**$ represents a two-dimensional convolution integral.[3] A pure scattering process neither creates nor destroys quanta, and hence $\mathrm{p}_r(\boldsymbol{r})$ must necessarily be normalized to unity area. Thus, as shown in Eq. (4), the expectation blurred optical image $\mathrm{E}\{q_o(\boldsymbol{r})\}$ can be expressed as a convolution of an expectation "pre-blurring" optical image $\mathrm{E}\{q_m(\boldsymbol{r})\}$ with the appropriate PSF.

The relationship described by Eq. (4) can be expressed in the spatial-frequency domain as

$$\mathrm{E}\{Q_o(\boldsymbol{k})\} = \mathrm{E}\{Q_I(\boldsymbol{k})\}m\mathrm{T}_r(\boldsymbol{k}) \tag{5}$$

where $\mathrm{E}\{Q_o(\boldsymbol{k})\}$, $\mathrm{E}\{Q_I(\boldsymbol{k})\}$ and $\mathrm{T}_r(\boldsymbol{k})$ are the two-dimensional Fourier transforms of $\mathrm{E}\{q_o(\boldsymbol{r})\}$, $\mathrm{E}\{q_I(\boldsymbol{r})\}$ and $\mathrm{p}_r(\boldsymbol{r})$ respectively. The two-dimensional MTF for this system is therefore given by

$$\mathrm{MTF}(\boldsymbol{k}) = |\mathrm{T}_r(\boldsymbol{k})| \tag{6}$$

which has a value of unity when $\boldsymbol{k} = 0$ since $\mathrm{p}_r(\boldsymbol{r})$ is required to have unity area.

The next stage in the model is propagation of the optical quanta and integration in the digital detector. In Appendix I it is shown that the presampling detector signal $d(\boldsymbol{r})$ can be represented as a convolution of the distribution of interacting quanta with an appropriate rectangular aperture function having unity height. An overall expression for the expectation presampling detector signal in Cartesian coordinates can therefore be written as

$$\mathrm{E}\{d(\boldsymbol{r})\} = \mathrm{E}\{d(x,y)\} = g_o\left[[\mathrm{E}\{q_I(x,y)\}m ** \mathrm{p}_r(x,y)]\,\beta ** \Pi\left(\frac{x}{a_x},\frac{y}{a_y}\right)\right] \tag{7}$$

where β describes the fraction of optical quanta leaving the screen that are integrated in the detector, a_x and a_y are the x- and y-direction dimensions of the active regions of individual detector elements.

The convolution operator commutes with both itself and multiplication,[3] and hence

$$\mathrm{E}\{d(x,y)\} = g_o m\beta \mathrm{E}\{q_I(x,y)\} ** \left[\mathrm{p}_r(x,y) ** \Pi\left(\frac{x}{a_x},\frac{y}{a_y}\right)\right]. \tag{8}$$

This relationship can be written in the spatial-frequency domain as

$$\mathrm{E}\{D(u,v)\} = g_o m\beta a_x a_y\, \mathrm{E}\{Q_I(u,v)\}\, \mathrm{T}_r(u,v)\, \mathrm{sinc}(\pi a_x u)\, \mathrm{sinc}(\pi a_y v) \tag{9}$$

where $\mathrm{E}\{D(u,v)\}$ is the (complex) expected value of the Fourier transform of $d(x,y)$, u and v are spatial frequencies in the x- and y-directions respectively, and $\mathrm{sinc}(\theta) = \sin(\theta)/\theta$. The product $g_o a_x a_y \mathrm{sinc}(\pi a_x u)\mathrm{sinc}(\pi a_y v)$ has been called the sampling aperture optical transfer function by Giger and Doi.[24] The two-dimensional MTF for this system including the effect of integration in detector elements is therefore given by

$$\mathrm{MTF}(u,v) = |\mathrm{T}_r(u,v)\ \mathrm{sinc}(\pi a_x u)\ \mathrm{sinc}(\pi a_y v)|. \tag{10}$$

While x-ray quanta are always Poisson distributed when distributed with a uniform mean, this is not generally so with other image quanta such as light from a screen. Therefore, Eq. (7) cannot be used directly to determine the NPS in $d(x,y)$. This is in part because the convolution integral correctly describes the transfer of mean values, but not noise, through a stochastic system. In the following sections, the "stochastic convolution" representation of scatter is suggested as a means of bringing the Rabbani result to this type of analysis.

III. THEORY

The blurring of an image when described by the convolution integral is given by Eq. (4) for LSI systems. In this expression, $p_r(\boldsymbol{r}-\boldsymbol{r}')$ describes the fraction of the signal in an infinitesimal element $d^2\boldsymbol{r}$ that is "mis-located" to the new position $\boldsymbol{r}$ as a result of the optical blurring process. The NPS is transferred through a convolution integral according to[3]

$$\mathrm{NPS}_d(\boldsymbol{k}) = \mathrm{NPS}(\boldsymbol{k})\,|\mathrm{T}(\boldsymbol{k})|^2 \tag{11}$$

where $\mathrm{NPS}(\boldsymbol{k})$ is the initial NPS and $\mathrm{T}(\boldsymbol{k})$ is the characteristic transfer function of the blurring process. We will call this process "deterministic blur," as indicted by the subscript d, to emphasize the deterministic nature of the convolution. However, this result is not generally used to describe the NPS transfer through imaging systems because it does not accommodate the discrete nature and statistical properties of the image quanta responsible for blurring processes.

Rabbani et al.[16] developed a theoretical description of the resulting NPS when independent quanta are scattered according to a probability density distribution $p_r(\boldsymbol{r})$ that specifically accounts for the statistical properties of these quanta. When $p_r(\boldsymbol{r})$ is shift invariant, a general expression for the resulting NPS $\mathrm{NPS}_s(\boldsymbol{k})$ is given by

$$\mathrm{NPS}_s(\boldsymbol{k}) = [\mathrm{NPS}(\boldsymbol{k}) - \bar{q}]\,|\mathrm{T}(\boldsymbol{k})|^2 + \bar{q} \tag{12}$$

where $\bar{q}$ is the average distribution of image quanta before the blur. We will call this "stochastic blur" as indicated by the subscript s. This result shows that the correlated component of the NPS, $\mathrm{NPS}(\boldsymbol{k}) - \bar{q}$, is passed though the squared MTF while the uncorrelated component, $\bar{q}$, is not.[16] A correlated component can result from a conversion with gain from one form of quanta to another as described in Sec. III.B. The NPS resulting from stochastic blur can also be expressed in terms of the NPS resulting from deterministic blur [Eq. (11)] as

$$\mathrm{NPS}_s(\boldsymbol{k}) = \mathrm{NPS}_d(\boldsymbol{k}) + \left[1 - |\mathrm{T}(\boldsymbol{k})|^2\right]\bar{q} \tag{13}$$

showing that at low frequencies where $|\mathrm{T}(\boldsymbol{k})|^2 \approx 1$, $\mathrm{NPS}_d(\boldsymbol{k})$ and $\mathrm{NPS}_s(\boldsymbol{k})$ are similar and hence the deterministic and stochastic results are similar. They are also similar if the distribution of input quanta are statistically correlated, implying that $\mathrm{NPS}(\boldsymbol{k}) \gg \bar{q}$ (Sec. III.B), except at very high spatial frequencies. However, at non-zero frequencies where $|\mathrm{T}(\boldsymbol{k})| < 1$, the deterministic result in general underestimates image noise.

Use of linear-systems theory in general, and the convolution operator in particular, to describe image blurring processes is a very powerful technique. Thus, while the convolution integral results in an NPS described by Eq. (11), it seems appropriate to introduce a modified operator that will result in the NPS described by Eq. (12). It is intended that this modified operator unify the description of both image blur and image noise within a linear-systems framework. That is, relatively simple expressions similar to Eq. (7) can be developed to describe both image-signal and image-noise transfer characteristics of particular systems by using this scatter operator.

A. The Scatter Operator, $*_s$

The input to an imaging system is a distribution of quanta, $q(\boldsymbol{r})$, which may be written as[1]

$$q(\boldsymbol{r}) = \sum_{i=1}^{N} \delta(\boldsymbol{r} - \boldsymbol{r}_i) \tag{14}$$

where N is a Poisson random variable describing the total number of incident quanta and $\boldsymbol{r}_i$ is a vector describing the position of the ith quantum. Thus, $q(\boldsymbol{r})$ is a sample distribution of a random process generating image quanta with the appropriate statistical distribution.

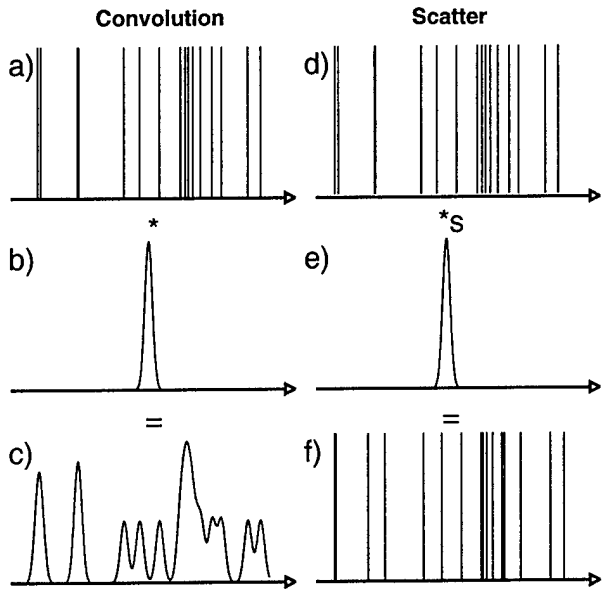

Figure 2: Deterministic blur represented with a convolution integral, and scatter, are shown in the left and right columns respectively. The convolution "smears" the input according to the PSF (a to c), while scatter "relocates" the input quanta according to the probability distribution given by the PSF (d to f).

Rabbani et al. derived Eq. (12) in terms of the set of transition probabilities $\{p_k^{(j)}\}$, where $p_k^{(j)}$ is the probability that a quantum in pixel j is scattered to pixel k. For LSI systems this transition probability is independent of position and hence the probability of being scattered to a pixel displaced by the vector $\Delta\boldsymbol{r}$ can be written $p_{\Delta\boldsymbol{r}}$. The distribution of quanta following a scattering process is described by $q_s(\boldsymbol{r})$ where

$$q_s(\boldsymbol{r}) = \sum_{i-1}^{N} \delta\left(\boldsymbol{r} - [\boldsymbol{r}_i + \Delta\boldsymbol{r}_i]\right) \tag{15}$$

and where $\Delta\boldsymbol{r}_i$ describes the scatter displacement of the ith quantum. The displacement $\Delta\boldsymbol{r}_i$ is a random vector variable with a set of probabilities $\{p_{\Delta\boldsymbol{r}_i}\}$ that describe the scatter PSF $\mathrm{p}(\boldsymbol{r})$ where

$$p_{\Delta\boldsymbol{r}_i} = \mathrm{p}(\boldsymbol{r})\,\mathrm{d}^2\boldsymbol{r}|_{\boldsymbol{r}=\Delta\boldsymbol{r}_i} \tag{16}$$

and where $\mathrm{d}^2\boldsymbol{r}$ is the area of an infinitesimal image element. Equation (15) describes the "stochastic convolution" of $q(\boldsymbol{r})$ with $\mathrm{p}(\boldsymbol{r})$, and is written in short form for two-dimensional scatter as

$$q_s(\boldsymbol{r}) = q(\boldsymbol{r}) *_s *_s \mathrm{p}(\boldsymbol{r}). \tag{17}$$

The scatter operator describes transfer of a sample distribution of image quanta. It is a translated point-process, similar to the translated Poisson-process described by Snyder and Miller,[10] although not restricted to Poisson processes.

Thus, while the convolution integral "smears" the input according to the PSF, scatter "mis-locates" input quanta according to a probability described by the PSF. This difference is illustrated in Fig. (2). In the column on the left, the input (2a) consists of randomly positioned quanta, each represented as a δ-function. This input is convolved with the PSF (2b) producing the result (2c) with a corresponding NPS described by Eq. (11). On the right, the same input undergoes a scatter resulting in a random relocation of all quanta (2f) according to the same PSF. The NPS of this result is described by Eq. (12).

1. Conditions of Use

The conditions of use of the scatter operator $*_s$ are essentially the assumptions described by Rabbani et al. in the derivation of Eq. (12). They include:

1. $q(\boldsymbol{r})$ must represent a distribution of independent quanta, with units of quanta per unit area (a one-dimensional form would have units of quanta per unit length);

2. the scattering process is shift invariant;

3. all scattering events are independent;

4. p($\boldsymbol{r}$) represents the probability (per unit area) that any given quantum is scattered (relocated) by a displacement vector $\boldsymbol{r}$; and,

5. quanta can be neither created nor destroyed by the scattering process [the integral of p($\boldsymbol{r}$) over all space is unity].

2. Numerical Implementation

It is intended that $*_s$ be used symbolically [e.g. Eq. (17)] to represent scattering processes, and the Rabbani equation be used to describe NPS transfer. However, a numerical implementation is also possible using simple Monte Carlo methods[25] should a numerical simulation of the blurring process be desired. The steps required in such a calculation are summarized below and must be repeated for each quantum being scattered:

1. Choose the scattering polar angle θ where $0 \leq \theta \leq 2\pi$. This will be a uniformly distributed random variable if the scattering process is isotropic. This step is not required for a one-dimensional geometry.

2. Choose the scatter displacement magnitude $|\Delta \boldsymbol{r}_i|$ which is a random variable with a probability distribution given by $p_{\Delta \boldsymbol{r}_i}$ [Eq. (16)].

3. Reassign the location of the quantum being scattered by the displacement $\Delta \boldsymbol{r}_i$ determined from the direction and distance calculated above.

Computation time is therefore dependent on the total number of quanta in the image at the scattering stage, but not on the size or number of pixels. Each image shown in the results section of this paper contain approximately 10^7 quanta in a 256 × 512-pixel matrix, requiring approximately 1 minute to implement the scatter on a Sun SPARC 10.

B. Scatter in a Cascaded Model

The operator $*_s$ represents a single scattering process. However, most real systems are better represented as a cascade of multiple scattering processes intermixed with quantum gain (conversion) processes as illustrated in Fig. (1). A consequence of the gain stages is that they can introduce spatial correlations into the distribution of image quanta and thereby influence how image noise is passed through scattering processes. This was described by Rabbani et al.,[16] who showed that an increase in the number of quanta representing the image by a gain stage having a mean $\bar{g}$ and variance σ_g^2 affects the NPS by

$$\mathrm{NPS}_g(\boldsymbol{k}) = \bar{g}^2 \mathrm{NPS}(\boldsymbol{k}) + \sigma_g^2 \bar{q}. \tag{18}$$

where NPS($\boldsymbol{k}$) and $\bar{q}$ are the NPS and mean respectively of the input distribution of image quanta $q(\boldsymbol{r})$. When the distribution of quanta after the gain is uncorrelated, the NPS is equal to the mean, i.e. $\mathrm{NPS}_g(\boldsymbol{k}) = \bar{g}\mathrm{NPS}(\boldsymbol{k}) = \bar{g}\bar{q}$. It is clear that the actual NPS given by Eq. (18) is always greater than this value for $\bar{g} > 1$ and non-deterministic gains ($\sigma_g^2 > 0$). Thus, the NPS of the distribution of quanta following a gain stage (in which the quanta are "clumped" according to the distribution of quanta before the gain) is always greater than the NPS of the same number of uncorrelated quanta. Equation (18) is an extension into the spatial-frequency domain of the effect of a stochastic gain on the signal variance.[1,26,27] The deterministic gain used in Eq. (3) corresponds to $\sigma_g^2 = 0$.

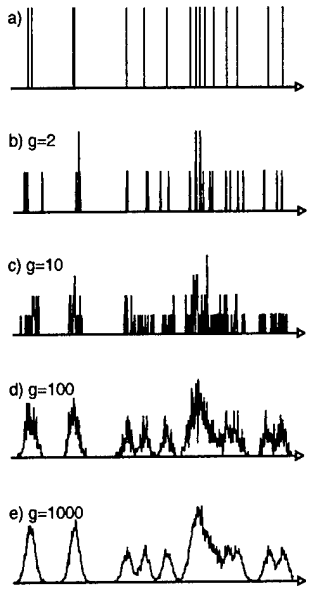

Figure 3: The statistical nature of light photons generated in a screen become less important, and stochastic and deterministic blurs merge, as the number of photons generated per x ray increases: (a) 1, (b) 2, (c) 10, (d) 100 and (e) 1000.

1. Cascading Gain and Scatter - a Radiographic Screen

In the radiographic screen example, each interacting x ray produces many light photons that are scattered before leaving the screen on the exit side. If the gain is assumed to be deterministic for simplicity with a value g, the resulting NPS, $\mathrm{NPS}_{g,s}(\boldsymbol{k})$, is obtained by combining Eqs. (18) and (12):

$$\mathrm{NPS}_{g,s}(\boldsymbol{k}) = \mathrm{NPS}_{g,d}(\boldsymbol{k}) + g\bar{q}[1 - |\mathrm{T}(\boldsymbol{k})|^2] \tag{19}$$

where $\mathrm{NPS}_{g,d}(\boldsymbol{k})$ is given by

$$\mathrm{NPS}_{g,d}(\boldsymbol{k}) = g^2\mathrm{NPS}(\boldsymbol{k})|\mathrm{T}(\boldsymbol{k})|^2 \tag{20}$$

and is the NPS that would be obtained if the blur were deterministic, obtained by combining Eqs. (18) and (11).

Equation (19) shows that in general $\mathrm{NPS}_{g,s}(\boldsymbol{k})$ is greater than $\mathrm{NPS}_{g,d}(\boldsymbol{k})$. They are similar only when the first term on the right side of Eq. (19) dominates which will occur when $g\mathrm{NPS}(\boldsymbol{k})|\mathrm{T}(\boldsymbol{k})|^2 \gg \bar{q}[1-|\mathrm{T}(\boldsymbol{k})|^2]$. This may occur when g is sufficiently large or when $|\mathrm{T}(\boldsymbol{k})|^2 \approx 1$ (i.e. $|\boldsymbol{k}| \approx 0$). At sufficiently high spatial frequencies for which $|\mathrm{T}(\boldsymbol{k})|^2 \ll \bar{q}/[g\mathrm{NPS}(\boldsymbol{k}) + \bar{q}]$ (a condition often true since g can be very large and $\mathrm{NPS}(\boldsymbol{k})$ can be no less than $\bar{q}$), the second term will dominate and the Rabbani NPS resulting from scatter is much greater than the NPS resulting from deterministic blur.

The above condition for large gain factors is illustrated in Fig. (3) where the distribution of light photons is calculated following a scatter and various gain values. Figure (3a) shows the same distribution of interacting quanta used in Fig. (2). The distribution of light photons following scatter (implemented using the Monte Carlo method) approaches the deterministic convolution result [Fig. (2c)] as g is increased from 2 [Fig. (3b)] to 1000 [Fig. (3e)]. This illustrates how similar the stochastic and deterministic blur results are when following a large gain stage as predicted by Eqs. (19) and (20).

2. Error Associated with the Deterministic-Blur Model

Equation (19) shows that the NPS of a system consisting of a noise-free gain followed by a blurring process is underestimated when the blur is represented as a convolution integral rather than as a scatter.

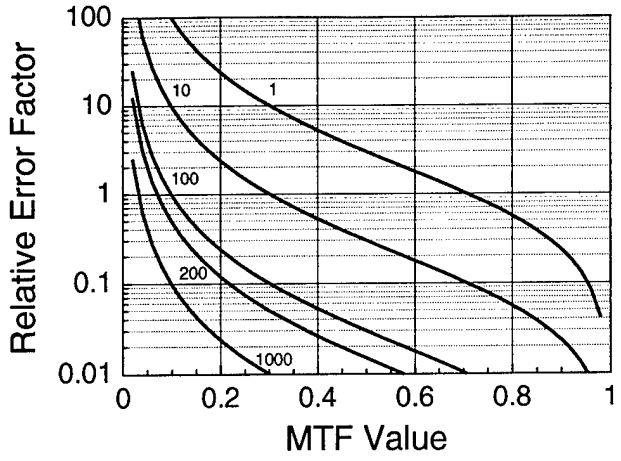

Figure 4: The relative error in the NPS following an amplification stage (such as generation of light photons in a radiographic screen) resulting from use of the conventional convolution for a Poisson-distributed input is shown as a function of the MTF value for gains of 1, 10, 100 and 200.

This relative error is given by the fraction $E(\boldsymbol{k})$ where

$$E(\boldsymbol{k}) = \frac{\mathrm{NPS}_{g,s}(\boldsymbol{k}) - \mathrm{NPS}_{g,d}(\boldsymbol{k})}{\mathrm{NPS}_{g,d}(\boldsymbol{k})} = \frac{1}{g}\left[\frac{1}{|\mathrm{T}(\boldsymbol{k})|^2} - 1\right] \tag{21}$$

for an uncorrelated Poisson-distributed input. Figure (4) shows this error increases dramatically as the MTF value decreases. In the absence of gain ($g = 1$), the error is approximately 56% when the MTF value is 0.8, and increases to a factor of 99 when the MTF value is 0.1. In a radiographic screen, a typical gain of $g = 200$ (the number of light quanta that exit the screen per interacting x ray) reduces this error to 0.5% and 46% respectively. In general, the error caused by use of the convolution integral depends on gains throughout the system, and hence cannot be determined without considering the entire system.

C. Properties of the Scatter Operator

1. Mean Value

The expectation result of scatter approaches the convolution integral (noise-free) result described by Eq. (4). This was shown by Rabbani et al. in Ref 16, Eq. (22):

$$\bar{y}_j = \sum_k \bar{x}_k p_{j-k} \tag{22}$$

indicating that the average number of quanta in pixel j after the scattering process, $\bar{y}_j$, is equal to the average number of quanta in pixel k before scattering, $\bar{x}_k$, multiplied by the transition probability p_{j-k} and summed over all pixels. Combining this with Eq. (16) and taking the limit of infinitesimally small pixels results in

$$\mathrm{E}\{q_s(\boldsymbol{r})\} = \int_{-\infty}^{\infty} \mathrm{E}\{q(\boldsymbol{r}')\}\mathrm{p}(\boldsymbol{r} - \boldsymbol{r}')\,\mathrm{d}^2\boldsymbol{r} \tag{23}$$

which is recognized as being the two-dimensional convolution integral of the incident expectation distribution with the scatter PSF. This result indicates that the linear-filter approach describes the true mean (noise-free) image. The convolution integral may be used to describe the *expectation* distribution of quanta after a scatter process, but details of the actual *sample* distribution are dependent on the statistical properties of the quanta as represented by the scatter operator.

2. Other Properties

The following results are expressed using one-dimensional geometry. Corresponding results are obtained using two-dimensional geometry. In each case, $q(x)$ represents an actual sample distribution of quanta.

1. Unlike the convolution integral, the two terms do not commute, i.e.

$$q(x) *_s \mathrm{p}(x) \neq \mathrm{p}(x) *_s q(x) \tag{24}$$

although this is not a particularly meaningful observation as one term must be a distribution of quanta and the other a probability density distribution (a PSF), and the roles cannot be reversed.

2. In general, scatter does not commute with multiplication, i.e.

$$[gq(x)] *_s \mathrm{p}(x) \neq g\,[q(x) *_s \mathrm{p}(x)] \tag{25}$$

since the NPS of each side evaluated using Eq. (18) differ. An exception to this occurs when g represents a binomial selection process such as a quantum efficiency. In this special case, g is a random variable having a value 1 or 0 only where the value 1 occurs with a probability $\bar{g}$, $0 \leq \bar{g} \leq 1$, and $\sigma_g^2 = \bar{g}(1-\bar{g})$. The NPS of each side are then equal, and scatter *does* commute with multiplication. This means that the order of sequential binomial selection and scattering processes can be reversed without affecting the NPS of the outcome.

3. The scatter operator is not distributive under addition, i.e.

$$[q(x) *_s \mathrm{p}_1(x)] + [q(x) *_s \mathrm{p}_2(x)] \neq q(x) *_s [\mathrm{p}_1(x) + \mathrm{p}_2(x)] \tag{26}$$

since the PSF must have unity area and it is not possible for each of $\mathrm{p}_1(x)$ and $\mathrm{p}_2(x)$ as well as the sum $\mathrm{p}_1(x) + \mathrm{p}_2(x)$ to be so normalized. Nor is it distributive under multiplication for the same reason.

4. Scatter is not associative, i.e.

$$[q(x) *_s \mathrm{p}_1(x)] *_s \mathrm{p}_2(x) \neq q(x) *_s [\mathrm{p}_1(x) *_s \mathrm{p}_2(x)] \tag{27}$$

since it is not meaningful to write $\mathrm{p}_1(x) *_s \mathrm{p}_2(x)$ as one term must be a distribution of quanta.

A consequence of the above results is that it is generally not possible to re-group or re-arrange expressions that include a scatter operation in the same way that it is possible to re-arrange expressions involving a convolution. This is because transfer expressions for the NPS can be cascaded, but are generally not multiplicative.

5. An important property that does apply to the scatter operator is

$$[q(x) *_s \mathrm{p}_1(x)] *_s \mathrm{p}_2(x) = q(x) *_s [\mathrm{p}_1(x) * \mathrm{p}_2(x)] \tag{28}$$

which is shown by proving that the mean and NPS of each side are equivalent. The means are obtained by replacing scatter with a convolution, and hence they must be equal since the convolution integral is associative. The NPS of the left-hand side [using Eq. (12)] is

$$\mathrm{NPS}_L(u) = [\mathrm{NPS}(u) - \bar{q}]\,|\mathrm{T}_1(u)|^2|\mathrm{T}_2(u)|^2 + \bar{q} \tag{29}$$

and that of the right-hand side is

$$\mathrm{NPS}_R(u) = [\mathrm{NPS}(u) - \bar{q}]\,|\mathrm{T}_1(u)\mathrm{T}_2(u)|^2 + \bar{q}. \tag{30}$$

Thus, they are equal and Eq. (28) is true since $|\mathrm{T}_1(u)|^2|\mathrm{T}_2(u)|^2 = |\mathrm{T}_1(u)\mathrm{T}_2(u)|^2$ for any complex $\mathrm{T}_1(u)$ and $\mathrm{T}_2(u)$. This means that two cascaded scattering processes can be represented as a single scattering process and retain the same second-order statistics by using a PSF that is a convolution of the two individual PSFs. In addition, the order of the two scattering processes in Eq. (28) can be reversed without affecting the outcome, showing that scatter commutes with itself.

6. The total "energy" in $q(x)$ is given by W as

$$W = \int_{-\infty}^{\infty} |q(x)|^2 \, \mathrm{d}x = N \tag{31}$$

where N is the total number of quanta. This result is equal also to the total energy in $q_s(x)$ following a scatter and hence scatter conserves energy.

3. Scatter in the Fourier Domain

Scatter relocates individual quanta by a random vector $\Delta \boldsymbol{r}$. Application of the shift theorem[3] indicates that the Fourier transform of this operation therefore corresponds to multiplication of the Fourier transform of individual quanta by the factor $e^{-i2\pi \boldsymbol{k}\cdot\Delta\boldsymbol{r}}$ which introduces a random phase change and where $\cdot$ represents a vector dot-product operation ($\boldsymbol{k}\cdot\Delta\boldsymbol{r} = u\Delta x + v\Delta y$). If the Fourier transform of $q(\boldsymbol{r})$ is $Q(\boldsymbol{k})$, where

$$Q(\boldsymbol{k}) = \mathrm{F}\left\{q(\boldsymbol{r})\right\} = \mathrm{F}\left\{\sum_{i=1}^{N} \delta(\boldsymbol{r} - \boldsymbol{r}_i)\right\} = \sum_{i=1}^{N} e^{-i2\pi \boldsymbol{k}\cdot\boldsymbol{r}_i}, \tag{32}$$

then the Fourier transform after scatter is $Q_s(\boldsymbol{k})$ where

$$Q_s(\boldsymbol{k}) = \sum_{i=1}^{N} e^{-i2\pi \boldsymbol{k}\cdot(\boldsymbol{r}_i + \Delta\boldsymbol{r}_i)} \tag{33}$$

and where $\Delta \boldsymbol{r}_i$ is a random vector variable describing the displacement of the ith quantum. It is clear that unlike the convolution integral, the effect of scatter is not multiplicative in the spatial-frequency domain.

D. Relationship to the Detective Quantum Efficiency

The detective quantum efficiency (DQE) describes the transfer through an imaging system of the image NPS weighted by the squared system transfer function, and can be expressed as[28]

$$\mathrm{DQE}(\boldsymbol{k}) = \frac{\bar{G}^2 |\mathrm{T}(\boldsymbol{k})|^2 \mathrm{NPS}(\boldsymbol{k})}{\mathrm{NPS}_{out}(\boldsymbol{k})} \tag{34}$$

where $\bar{G}$ is the average overall system gain, $|\mathrm{T}(\boldsymbol{k})|$ is the system MTF, $\mathrm{NPS}(\boldsymbol{k})$ is the input NPS which is equal to $\bar{q}$ (the average incident quantum distribution) if the input quanta are uncorrelated,[8] and $\mathrm{NPS}_{out}(\boldsymbol{k})$ is the image NPS. Using this approach, the effect of scatter on the DQE is obtained by setting $G = 1$ and noting that the numerator is then equal to the NPS for deterministic blur $\mathrm{NPS}_d(\boldsymbol{k})$ [Eq. (11)]. Hence, the effect of scatter on the DQE can be expressed as the term $\mathrm{DQE}'(\boldsymbol{k})$, defined as the ratio of $\mathrm{NPS}_d(\boldsymbol{k})$ to the actual NPS, $\mathrm{NPS}_{out}(\boldsymbol{k})$:

$$\mathrm{DQE}'(\boldsymbol{k}) = \frac{\mathrm{NPS}_d(\boldsymbol{k})}{\mathrm{NPS}_{out}(\boldsymbol{k})} \tag{35}$$

A deterministic linear-filter blur therefore has no effect on the system DQE. The effect of scatter on the DQE, $\mathrm{DQE}'_s(\boldsymbol{k})$, is

$$\mathrm{DQE}'_s(\boldsymbol{k}) = \frac{\mathrm{NPS}_d(\boldsymbol{k})}{\mathrm{NPS}_s(\boldsymbol{k})} \tag{36}$$

$$= \frac{\mathrm{NPS}_d(\boldsymbol{k})}{\mathrm{NPS}_d(\boldsymbol{k}) + \bar{q}[1 - |\mathrm{T}(\boldsymbol{k})|^2]} = \frac{1}{1 + \dfrac{\bar{q}[1 - |\mathrm{T}(\boldsymbol{k})|^2]}{\mathrm{NPS}(\boldsymbol{k})|\mathrm{T}(\boldsymbol{k})|^2}} \tag{37}$$

and is always less than unity. For the special case of Poisson-distributed incident quanta, $\mathrm{NPS}(\boldsymbol{k}) = \bar{q}$, and $\mathrm{DQE}'_s(\boldsymbol{k})$ becomes

$$\mathrm{DQE}'_s(\boldsymbol{k}) = \frac{1}{1 + \dfrac{1 - |\mathrm{T}(\boldsymbol{k})|^2}{|\mathrm{T}(\boldsymbol{k})|^2}} = |\mathrm{T}(\boldsymbol{k})|^2. \tag{38}$$

Thus, blur described with a convolution does not result in a degradation of the DQE, while blur due to scatter does. This result must be interpreted with caution as in general the DQE of a cascaded system is not simply a product of DQE factors.[29]

Using this type of linear-systems approach, a more general form of Eq. (38) has been derived elsewhere,[29] giving the DQE of a system consisting of an arbitrary cascade of M scattering and gain processes as

$$\mathrm{DQE}(\boldsymbol{k}) = \frac{1}{1 + \displaystyle\sum_{i=1}^{M} \frac{1 + \epsilon_{g_i}|\mathrm{T}_i(\boldsymbol{k})|^2}{\mathrm{P}_i(\boldsymbol{k})}}; \mathrm{P}_i(\boldsymbol{k}) = \prod_{j=1}^{i} g_j |\mathrm{T}_j(\boldsymbol{k})|^2 \tag{39}$$

where each stage may be either a scatter or a gain stage, but not both; g_i is the gain of the ith stage having a gain variance of $\sigma^2_{g_i}$ which can also be expressed in terms of a gain Poisson excess, $\epsilon_{g_i} = (\sigma^2_{g_i}/g_i - 1)$; and $\mathrm{P}_i(\boldsymbol{k})$ is the product of the gains and squared MTFs of all stages up to and including the ith stage. For scattering stages, $g_i = 1$, $\sigma^2_{g_i} = 0$, and $\epsilon_{g_i} = -1$. For gain stages, $\mathrm{T}_i(\boldsymbol{k}) = 1$. Equation (39) describes the DQE following a cascade of stochastic gains and scatters only. Linear-filter blurs, such as the stage representing integration of quanta in the detector elements as a convolution with $\Pi(x/a_x, y/a_y)$, would not normally be included in Eq. (39) since the convolution integral does not affect the DQE.

	CONVOLUTION	SCATTER
Notation:	$q_d(\boldsymbol{r}) = q(\boldsymbol{r}) ** \mathrm{p}(\boldsymbol{r})$	$q_s(\boldsymbol{r}) = q(\boldsymbol{r}) *_s *_s \mathrm{p}(\boldsymbol{r})$
Definition:	$q_d(\boldsymbol{r}) = \int_{-\infty}^{\infty} q(\boldsymbol{r}')\mathrm{p}(\boldsymbol{r} - \boldsymbol{r}')\,\mathrm{d}^2\boldsymbol{r}'$	$q_s(\boldsymbol{r}) = \sum_{i=1}^{N} \delta(\boldsymbol{r} - [\boldsymbol{r}_i + \Delta\boldsymbol{r}_i])$
Fourier Transform:	$\mathrm{F}\{q_d(\boldsymbol{r})\} = \mathrm{F}\{q(\boldsymbol{r})\}\mathrm{T}(\boldsymbol{k})$	$\mathrm{F}\{q_s(\boldsymbol{r})\} = \sum_{i=1}^{N} e^{-i2\pi\boldsymbol{k}\cdot(\boldsymbol{r}_i + \Delta\boldsymbol{r}_i)}$
Commutative:	terms; self; addition; multiplication	self; binomial selection
Distributive:	addition; multiplication	No
Associative:	Yes	No
Expectation Value:	$\mathrm{E}\{q_d(\boldsymbol{r})\} = \mathrm{E}\{q(\boldsymbol{r})\} ** \mathrm{p}(\boldsymbol{r})$	$\mathrm{E}\{q_s(\boldsymbol{r})\} = \mathrm{E}\{q(\boldsymbol{r})\} ** \mathrm{p}(\boldsymbol{r}) = \mathrm{E}\{q_d(\boldsymbol{r})\}$
MTF:	$\mathrm{MTF}(\boldsymbol{k}) = \dfrac{\lvert\mathrm{T}(\boldsymbol{k})\rvert}{\mathrm{T}(0)}$	$\mathrm{MTF}(\boldsymbol{k}) = \lvert\mathrm{T}(\boldsymbol{k})\rvert$
NPS:	$\mathrm{NPS}_d(\boldsymbol{k}) = \mathrm{NPS}(\boldsymbol{k})\lvert\mathrm{T}(\boldsymbol{k})\rvert^2$	$\mathrm{NPS}_s(\boldsymbol{k}) = [\mathrm{NPS}(\boldsymbol{k}) - \bar{q}]\lvert\mathrm{T}(\boldsymbol{k})\rvert^2 + \bar{q} = \mathrm{NPS}_d(\boldsymbol{k}) + \bar{q}[1 - \lvert\mathrm{T}(\boldsymbol{k})\rvert^2]$ (Rabbani et al.)
Effect on DQE:	none	system dependent

Table 1: Summary of the properties of the (deterministic) convolution ($*$) and scatter ($*_s$) operators for an input image $q(\boldsymbol{r}) = \sum_{i=1}^{N} \delta(\boldsymbol{r} - \boldsymbol{r}_i)$, where $\mathrm{T}(\boldsymbol{k})$ is the Fourier transform of $\mathrm{p}(\boldsymbol{r})$.

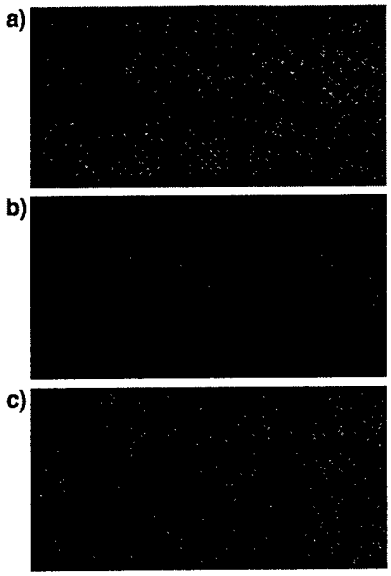

Figure 5: Simulated images showing: a) initial "pre-blurring" image; b) blurred image using the convolution integral; and c) blurred image using the scatter operator with the same PSF as b).

These characteristics of the scatter operator are summarized and compared with those of the convolution integral in Table I.

IV. RESULTS

A. Simulated Images

The visual effect of scatter is illustrated by simulating images of sinusoidal patterns of various frequencies[30] where image blur is described first as a convolution and second as a scatter. It is not intended that this calculation describe a particular physical situation; rather, it is presented as a visual comparison.

A "pre-blurring" image was generated assuming an average of 100 detected quanta per 0.025- × 0.025-mm^2 pixel. An isotropic Gaussian-shaped PSF, p($\boldsymbol{r}$), with a standard deviation width $\sigma = 4$ pixels (0.1 mm) was used to represent the blur, where

$$\mathrm{p}(\boldsymbol{r}) = \frac{1}{2\pi\sigma^2} e^{-\boldsymbol{r}^2/2\sigma^2} \tag{40}$$

and where $\boldsymbol{r}^2 = x^2 + y^2$. The resulting MTF associated with this blur is

$$|\mathrm{T}(\boldsymbol{k})| = e^{-2\pi^2\sigma^2\boldsymbol{k}^2}. \tag{41}$$

Figure (5a) is the simulated pre-blurring image on a 256- x 512-pixel matrix. All 10 sinusoidal patterns can be seen, although the image noise obscures some image detail. Figure (5b) is the result of a conventional convolution of the pre-blurring image with the PSF described by Eq. (40). It is shown that only approximately 7 patterns can be seen, and that image noise has also been reduced significantly. Figure (5c) is the result of a "stochastic convolution" of the pre-blurring image with the same PSF. Approximately 7 patterns can still be seen, similar to Fig. (5b), although the noise in Fig. (5c) is significantly greater. Theoretically one would expect both Figs. (5b) and (5c) to have the same spatial resolution (same MTF) but very different noise properties. The difference between Figs. (5b) and (5c) illustrates the difference between convolution and scatter for an input image with Poisson-distributed quanta.

The NPS measured from each image in Fig. (5) are shown in Fig. (6). Subsequent to convolution with the PSF, the NPS decreases rapidly with increasing frequency, and shows excellent agreement with the

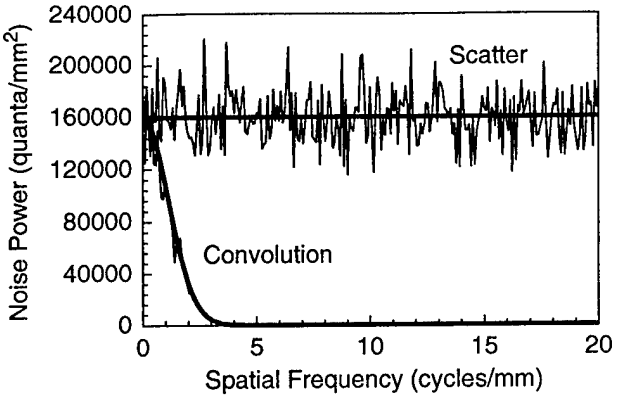

Figure 6: The NPS measured from the image data used in Fig. (5) (thin lines) are compared with theoretical predictions (thick lines) for convolution (deterministic blur) and scatter operations.

theoretical NPS predicted by Eq. (11). Subsequent to scatter, the NPS is uniform in frequencies, and shows excellent agreement with the theoretical NPS predicted by Eq. (12).

B. Scatter in a Cascaded-Systems Analysis

By extending the linear-systems approach to make use of scatter when appropriate, the linear-systems method can also be used to describe noise properties of these systems. In this section, illustrative examples of this approach are described.

1. Image Focal-Spot Blur

The effect of x-ray focal-spot blur on image sharpness has been described by Rossmann and Doi,[31,32] Burgess,[33,34] Barrett and Swindell[1] and others in terms of a convolution integral with the appropriate focal-spot PSF. This calculation is summarized in Appendix II where it is shown that

$$\mathrm{E}\{q(\boldsymbol{r})\} \approx \mathrm{E}\{\hat{q}(\boldsymbol{r})\} ** \mathrm{p}_f(\boldsymbol{r}) \tag{42}$$

where $\mathrm{E}\{\hat{q}(\boldsymbol{r})\}$ and $\mathrm{E}\{q(\boldsymbol{r})\}$ represent the expectation (noise-free) pre- and post-blurring images respectively, and $\mathrm{p}_f(\boldsymbol{r})$ is the normalized focal-spot PSF projected onto the image plane. If we instead omit the expectation operator and represent the pre-blurring image as $\hat{q}(\boldsymbol{r})$, an actual sample distribution of quanta, then second-order statistics of the blurred image $q(\boldsymbol{r})$ are preserved if we write

$$q(\boldsymbol{r}) \approx \hat{q}(\boldsymbol{r}) *_s *_s \mathrm{p}_f(\boldsymbol{r}). \tag{43}$$

The distribution $\hat{q}(\boldsymbol{r})$ is Poisson distributed and hence the DQE associated with the finite size of the source is given by Eq. (38) as

$$\mathrm{DQE}_f(\boldsymbol{k}) = |\mathrm{T}_f(\boldsymbol{k})|^2 \tag{44}$$

where $|\mathrm{T}_f(\boldsymbol{k})|$ is the focal-spot MTF. An additional consequence is that while image sharpness is degraded, image noise (NPS) is unaffected by focal-spot size. Although this result has been known for some time (e.g. Sandrik and Wagner[13]), it is presented as an illustrative example to show that this result can also be obtained using a linear-systems approach with the scatter operator.

Off-focal radiation is also a source of image quality degradation. If the source PSF is calculated to include the distribution of any off-focal radiation contributing to image formation, the NPS and DQE obtained with this approach will describe the corresponding image quality degradation.

2. Hypothetical Radiographic System

The hypothetical system illustrated in Fig. (1) is now analyzed using the extended linear-systems approach. Screen blur is represented with the scatter operator while integration of light quanta in the detector elements remains a convolution integral. The presampling detector signal therefore becomes

$$d(x,y) = g\left[\left[q_I(x,y)m *_s *_s \mathrm{p}_r(x,y)\right]\beta ** \Pi\left(\frac{x}{a_x},\frac{y}{a_y}\right)\right]. \tag{45}$$

This expression cannot be rearranged significantly because scatter does not commute with multiplication by m (Sec. III.C.2.ii).

The corresponding NPS is obtained by cascading the NPS of each individual step as summarized in Table II, where the signal and NPS following each stage are determined by cascading appropriate combinations of Eqs. (12) and (18). The DQE of the system can then be obtained using Eq. (34). Equivalently, Eq. (39) can be used directly to obtain

$$\mathrm{DQE}_s(\boldsymbol{k}) = \frac{1}{1+\frac{1+\epsilon_m}{m}+\frac{1-|\mathrm{T}_r(\boldsymbol{k})|^2}{m|\mathrm{T}_r(\boldsymbol{k})|^2}+\frac{1-\beta}{m\beta|\mathrm{T}_r(\boldsymbol{k})|^2}} \tag{46}$$

$$= \frac{1}{1+\frac{\epsilon_m}{m}+\frac{1}{m\beta|\mathrm{T}_r(\boldsymbol{k})|^2}} \tag{47}$$

which is the accepted result.[16,35]

It should be noted that if the convolution integral had been (incorrectly) used to describe image blur, the DQE would have been

$$\mathrm{DQE}_d(\boldsymbol{k}) = \frac{1}{1+\frac{\epsilon_m}{m}+\frac{1}{m\beta}} \tag{48}$$

which is a similar result but lacks any spatial-frequency dependence. The difference between scatter and deterministic blur is fully responsible for the frequency dependence of the DQE.

STAGE	IMAGE QUANTA	NPS
X Rays Interacting	$q_I(\boldsymbol{r})$	$\mathrm{NPS}_I(\boldsymbol{k}) = \bar{q}_I$
Optical Photons Generated	$q_m(\boldsymbol{r}) = q_I(\boldsymbol{r})m$	$\mathrm{NPS}_m(\boldsymbol{k}) = \bar{m}^2\mathrm{NPS}_I(\boldsymbol{k}) + \sigma_m^2\bar{q}_I$ $= \bar{q}_I\bar{m}^2(1+\frac{\sigma_m^2}{\bar{m}^2})$
Optical Photons Scattered	$q_s(\boldsymbol{r}) = q_m(\boldsymbol{r}) *_s *_s \mathrm{p}_r(\boldsymbol{r})$	$\mathrm{NPS}_s(\boldsymbol{k}) = [\mathrm{NPS}_m(\boldsymbol{k}) - \bar{q}_m]\lvert\mathrm{T}_r(\boldsymbol{k})\rvert^2 + \bar{q}_m$ $= \bar{q}_I\bar{m}^2(1+\frac{\sigma_m^2}{\bar{m}^2}-\frac{1}{\bar{m}})\lvert\mathrm{T}_r(\boldsymbol{k})\rvert^2 + \bar{q}_I\bar{m}$
Optical Photons Detected	$q_{det}(\boldsymbol{r}) = q_s(\boldsymbol{r})\beta$	$\mathrm{NPS}_{det}(\boldsymbol{k}) = \beta^2\mathrm{NPS}_s(\boldsymbol{k}) + \beta(1-\beta)\bar{q}_s$ $= \bar{q}_I\bar{m}^2(1+\frac{\sigma_m^2}{\bar{m}^2}-\frac{1}{\bar{m}})\beta^2\lvert\mathrm{T}_r(\boldsymbol{k})\rvert^2 + \bar{q}_I\bar{m}\beta$
Presampling Detector Signal	$d_s(x,y) =$ $g_o q_{det}(x,y) ** \Pi(\frac{x}{a_x},\frac{y}{a_y})$	$\mathrm{NPS}_s(u,v) =$ $\mathrm{NPS}_{det}(u,v)g_o^2a_x^2a_y^2\mathrm{sinc}^2(\pi u a_x)\mathrm{sinc}^2(\pi v a_y)$

Table 2: Expressions describing the distribution of image quanta and the NPS at each stage of the hypothetical system.

In the absence of additive noise, the DQE of the entire system including the effect of focal-spot blur and screen quantum efficiency can be obtained by extending the model with additional stages:

$$d(x,y) = g_o \left[\left[\left\{ \hat{q}(x,y) *_s *_s \mathrm{p}_f(\boldsymbol{r}) \right\} \alpha m *_s *_s \mathrm{p}_r(x,y) \right] \beta * * \Pi\left(\frac{x}{a_x}, \frac{y}{a_y}\right) \right] \tag{49}$$

where $\hat{q}(x,y)$ represents the sample distribution of x-ray quanta that would have been obtained had there been no focal-spot blur (Appendix II). The DQE obtained using Eq. (39) is

$$\begin{aligned} &\mathrm{DQE}_s(\boldsymbol{k}) \\ &= \left[1 + \frac{1-|\mathrm{T}_f(\boldsymbol{k})|^2}{|\mathrm{T}_f(\boldsymbol{k})|^2} + \frac{1-\alpha}{\alpha|\mathrm{T}_f(\boldsymbol{k})|^2} + \frac{1+\epsilon_m}{\alpha m|\mathrm{T}_f(\boldsymbol{k})|^2} + \frac{1-|\mathrm{T}_r(\boldsymbol{k})|^2}{\alpha m|\mathrm{T}_f(\boldsymbol{k})\mathrm{T}_r(\boldsymbol{k})|^2} + \frac{1-\beta}{\alpha m\beta|\mathrm{T}_f(\boldsymbol{k})\mathrm{T}_r(\boldsymbol{k})|^2} \right]^{-1} \\ &= \frac{\alpha|\mathrm{T}_f(\boldsymbol{k})|^2}{1 + \frac{\epsilon_m}{m} + \frac{1}{m\beta|\mathrm{T}_r(\boldsymbol{k})|^2}} \end{aligned} \tag{50}$$

which includes the effect of focal-spot blur.

V. DISCUSSION

The scatter operator described in this article is a translated point-process,[10] and represents the physical mechanism giving rise to the Rabbani, Shaw and Van Metter NPS. It is described as a "stochastic convolution" in which the blur PSF is "folded" into the image signal through a stochastic mechanism. It is used as an alternative to the convolution integral (linear filter) description of blur in a linear-systems analysis. Convolution describes a deterministic cascading of weights, while the scatter operator describes a cascading of probabilities.

A deterministic system is one in which the output depends only on the input (Papoulis[11]) and where Eq. (11) describes the NPS transfer through a blurring mechanism. In contrast to this, a stochastic system is one in which the system transfer function contains a stochastic element.[11] In the context of this article, this is due to the statistical nature of quanta transferring image information through the system. Physical imaging systems are almost universally stochastic systems, and thus the Rabbani results [Eqs. (12) and (18)] should generally be used to describe the NPS transfer through blur and gain processes in these systems.

In the simplistic hypothetical system discussed here, it was assumed that none of the optical quanta were absorbed in the screen. When this is not a good assumption, an additional stage must be introduced to describe the fraction of generated optical quanta that are emitted. This is represented as a binomial selection stage (a gain less than unity). Since the scatter operator commutes with binomial selection (Sec. III.C.2), the relative order of this selection and the scatter stage is unimportant.

A deterministic blurring process has no effect on the DQE of a system. That is, both the square of the signal and the NPS are passed through the square of the blur MTF. This is not the case for a scatter, where the DQE decreases according to Eq. (12) and hence it can be concluded that the frequency-dependence of the DQE is a direct consequence of the scatter of image quanta. In the absence of additive noise, these statistical properties - as described by the Rabbani NPS and hence the scatter operator - fully account for this frequency dependence. This observation would suggest that at sufficiently high spatial frequencies, where the MTF of a system is necessarily much less than unity, scatter is always the dominant factor responsible for degradation of the DQE.

The impact on the DQE of scatter in a cascaded system can only be determined when expressed in the context of the complete system. For instance, in the hypothetical system the DQE [Eq. (50)] is degraded by scatter only when both the terms $|\mathrm{T}_r(\boldsymbol{k})|^2$ and $m\beta|\mathrm{T}_r(\boldsymbol{k})|^2$ are less than unity. The second term describes the effective number of secondary optical quanta at a particular frequency that are detected by

the detector array. A value less than unity indicates the presence of a secondary "quantum sink". Thus, it is the secondary quantum sink that is responsible for making scatter a significant degrading factor in the DQE. If the squared MTF term is not small also, then the secondary quantum sink exists due to inadequate gain rather than to scatter. A more general comment can therefore be made that for any specified frequency, *a scattering process degrades the system DQE significantly if the squared MTF of that process is significantly less than unity, and the system has a subsequent secondary quantum sink at any specified frequency [$P_i(\boldsymbol{k}) < 1$ in Eq. (39)].*

VI. CONCLUSION

The convolution operator often used to describe image blurring processes in linear-systems theory passes first-order statistics (mean values) but not second-order statistics when applied to imaging systems. As a consequence, image noise is generally not analyzed using linear-systems theory, but rather with stochastic process theory. A scatter operator is described here which represents the physical process giving rise to the Rabbani NPS, and passes first- and second-order statistics thereby unifying image blur and image noise calculations within a linear-systems framework. A convolution blurs the input in a deterministic way according to the PSF, while scatter relocates quanta according to a probability given by the same PSF. The scatter operator is expressed in terms of random variables and is consistent with a linear-systems approach to modeling linear and shift-invariant imaging systems, allowing for the use of Fourier-domain mathematics.

Several properties of the scatter operator are described. It is shown that it commutes with itself and with a binomial selection process (representing a quantum efficiency). Strictly speaking it is not associative, although a similar property that is true is described. The input and output must necessarily be expressed in units of quanta per unit area, and the associated PSF must necessarily be normalized to unity area. It is shown that for LSI systems in general (in the absence of additive noise), the transfer of second-order statistics through scattering processes is fully responsible for the spatial-frequency dependence of the system DQE.

ACKNOWLEDGMENT

The financial assistance of The Whitaker Foundation, the US Army Medical Research and Materiel Command breast cancer research program, and the Canadian Institutes of Health Research is gratefully acknowledged. The second author acknowledges the support of a Medical Research Council of Canada Studentship. In addition, J.-P. Bissonnette, H.N. Cardinal, D. Holdsworth, D. Jaffray, H. Lai, T.-Y. Lee and C. Maier are acknowledged for contributions made during discussions of this work. The assistance of S. Sherebrin with the Monte Carlo code and M. Mcbain with LaTeX programming is also gratefully acknowledged.

APPENDIX I: Detector Presampling Signal

In this appendix it is shown that the operation of integrating image quanta in discrete detector elements of a detector array can be described with a convolution operation. The resulting "presampling" detector signal includes the smoothing effect caused by the finite width of detector-element apertures, but does not include aliasing artifacts. This approach of using a presampling signal is equivalent to the presampling optical transfer function described by Sones and Barnes[36] and Giger and Doi[24] among others.

It is assumed that the distribution of quanta that interact in the detector can be represented as $q(x,y)$, a generalized function consisting of the superposition of δ-functions where each δ-function represents a single interacting quantum. Thus, the signal from a rectangular detector element centered at position x_n, y_n and having dimensions $a_x \times a_y$ is given by

$$d_n = g_o \int_{x_n-\frac{a_x}{2}}^{x_n+\frac{a_x}{2}} \int_{y_n-\frac{a_y}{2}}^{y_n+\frac{a_y}{2}} q(x,y)\,\mathrm{d}x\,\mathrm{d}y \qquad \text{(A-1)}$$

where g_o relates the detector signal (in detector-signal units) to the number of interacting quanta. Inspection of Eq. (A-1) shows that this integral can also be expressed as the integral of $q(x,y)$ multiplied by a rectangular function having unity height and dimensions a_x and a_y that describe the element aperture:

$$d_n = g_o \int_{-\infty}^{\infty} \int_{-\infty}^{\infty} q(x,y) \Pi\left(\frac{x-x_n}{a_x}, \frac{y-y_n}{a_y}\right) \mathrm{d}x\,\mathrm{d}y. \qquad \text{(A-2)}$$

Equation (A-2) is recognized as being the two-dimensional cross-correlation integral[11] of $q(x,y)$ with $\Pi(x/a_x, y/a_y)$, evaluated at position x_n, y_n. Therefore, we can express the signal from the nth detector element as

$$d_n = d(x,y)|_{x,y=x_n,y_n} \qquad \text{(A-3)}$$

where $d(x,y)$ is the presampling detector signal that provides the detector element values for all possible element positions. When evaluated ("sampled") at positions corresponding to the centers of the actual elements, it provides the set of actual detector-element values. The function $d(x,y)$ is given by

$$d(x,y) = g_o \int_{-\infty}^{\infty} \int_{-\infty}^{\infty} q(x',y') \Pi\left(\frac{x'-x}{a_x}, \frac{y'-y}{a_y}\right) \mathrm{d}x'\,\mathrm{d}y' = k\; q(x,y) \star\star\, \Pi\left(\frac{x}{a_x}, \frac{y}{a_y}\right) \qquad \text{(A-4)}$$

in terms of the two-dimensional cross-correlation operator $\star\star$, or as

$$d(x,y) = g_o\; q(x,y) * * \Pi\left(\frac{-x}{a_x}, \frac{-y}{a_y}\right) \qquad \text{(A-5)}$$

in terms of the two-dimensional convolution[3] operator $**$. The aperture profile is symmetric and hence the negative signs in Eq. (A-5) can be omitted.

APPENDIX II: Focal Spot Blur as a Convolution

In this appendix, a calculation showing that the average effect of focal-spot blur can be expressed as a convolution is summarized following Barrett and Swindell.[1] In Fig. (7), $\boldsymbol{r}''$ is a two-dimensional coordinate in the source plane, $\boldsymbol{r}'$ is in the object plane, and $\boldsymbol{r}$ is in the image plane ($\boldsymbol{r}''$ and $\boldsymbol{r}$ have been exchanged relative to Barrett and Swindell's use. Care must be taken because $\boldsymbol{r}$, $\boldsymbol{r}'$ and $\boldsymbol{r}''$ lie in three parallel but different planes. If $s(\boldsymbol{r}'')$ is an emission function describing the emission of x rays (photons emitted per unit area) from the source, $s(\boldsymbol{r}'')\,\mathrm{d}^2\boldsymbol{r}''$ is the mean number of x-ray photons emitted into all space from an elemental area $\mathrm{d}^2\boldsymbol{r}''$. If the x rays are emitted uniformly in all directions from the source and $t(\boldsymbol{r}')$ is

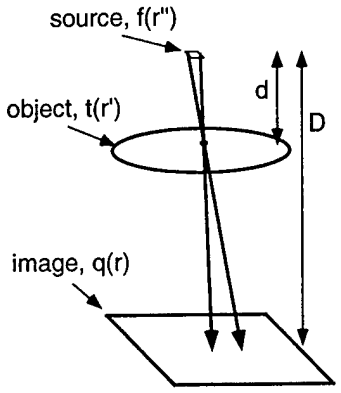

Figure 7: Calculation of the focal spot MTF.

the transmission factor through a planar object at position $\boldsymbol{r}'$, then the expectation x-ray photon density reaching the image at position $\boldsymbol{r}$ can be written as[1]

$$\mathrm{E}\{q(\boldsymbol{r})\} = \frac{1}{4\pi D^2}\int_{source} s(\boldsymbol{r}'')\cos^3(\theta)t(\boldsymbol{r}')\,\mathrm{d}^2\boldsymbol{r}'' \qquad \text{(A-6)}$$

where θ is the angle of the x-ray beam with respect to the source-image direction, and D is the source-image distance. Barrett and Swindell then show that if D is large with respect to the source dimensions,

$$\mathrm{E}\{q(\boldsymbol{r})\} \approx \frac{1}{(1-m)^2 4\pi D^2}\int_{-\infty}^{\infty} s(\frac{\boldsymbol{r}_o}{1-m})t(\frac{\boldsymbol{r}-\boldsymbol{r}_o}{m})\,\mathrm{d}^2\boldsymbol{r}_o \qquad \text{(A-7)}$$

where $m = D/d$ is the geometric magnification factor and d is the source-object distance. It is more convenient to work with the projection of s and t onto the image plane. Therefore, $t([\boldsymbol{r}-\boldsymbol{r}_o]/m)$ is replaced with $t_i(\boldsymbol{r}-\boldsymbol{r}_o)$ where the subscript i indicates projection onto the image plane. The integral of $s(\boldsymbol{r}'')$ over all space gives $\mathrm{E}\{N\}$, the expectation total number of x rays emitted from the source. As a result, $[1-m]^{-2}s(\boldsymbol{r}_o/[1-m])$ is replaced with $\mathrm{E}\{N\}\mathrm{p}_f(\boldsymbol{r}_o)$ where $\mathrm{p}_f(\boldsymbol{r}_o)$ is the focal-spot PSF projected on to the image plane (normalized to unity area). Therefore,

$$\mathrm{E}\{q(\boldsymbol{r})\} \approx \frac{\mathrm{E}\{N\}}{4\pi D^2}\int_{-\infty}^{\infty}\mathrm{p}_f(\boldsymbol{r}_o)t_i(\boldsymbol{r}-\boldsymbol{r}_o)\,\mathrm{d}^2\boldsymbol{r}_o \qquad \text{(A-8)}$$

$$\approx \frac{\mathrm{E}\{N\}}{4\pi D^2}\mathrm{p}_f(\boldsymbol{r}) ** t_i(\boldsymbol{r}). \qquad \text{(A-9)}$$

This result shows that the average blurring effect of the focal spot can be represented as a convolution of the source profile with the object transmission function. The commutative property of the conventional convolution operator means that Eq. (A-9) can also be written as

$$\mathrm{E}\{q(\boldsymbol{r})\} \approx \frac{\mathrm{E}\{N\}}{4\pi D^2}t_i(\boldsymbol{r}) ** \mathrm{p}_f(\boldsymbol{r}) \qquad \text{(A-10)}$$

$$\approx \mathrm{E}\{\hat{q}(\boldsymbol{r})\} ** \mathrm{p}_f(\boldsymbol{r}). \qquad \text{(A-11)}$$

where $\mathrm{E}\{\hat{q}(\boldsymbol{r})\} = \mathrm{E}\{N\}/(4\pi D^2)t_i(\boldsymbol{r})$ represents an expectation image that has not been blurred by the focal spot. The expectation blurred image is therefore represented as the expectation "pre-blurring" image convolved with the focal-spot PSF.

References

1. Barrett,H.H. and Swindell,W., "Radiological Imaging - The Theory of Image Formation, Detection, and Processing," (Academic Press, New York, 1981).

2. Metz,C.E. and Doi,K., "Transfer function analysis of radiographic imaging systems," Phys Med Biol 24, 1079-1106 (1979).

3. Bracewell,R.N., "The Fourier Transform and its Applications," 2 edition (McGraw-Hill Book Company, New York, 1978).

4. Cunningham,I.A. and Shaw,R., "Signal-to-noise optimization of medical imaging systems," J Opt Soc Am A 16, 621-632 (1999).

5. Macovski,A., "Medical Imaging Systems," (Prentice-Hall, Inc., Englewood Cliffs, N.J., 1983).

6. Parker,J.A., "Image Reconstruction in Radiology," (CRC Press, Boca Raton, 1991).

7. Rossmann,K., "Point Spread-Function, Line Spread-Function, and Modulation Transfer Function," Radiol 93, 257-272 (1969).

8. Dainty,J.C. and Shaw,R., "Image Science," (Academic Press, New York, 1974).

9. Doi,K., Rossmann,K., and Haus,A.G., "Image quality and patient exposure in diagnostic radiology," Photographic Science and Engineering 21, 269-277 (1977).

10. Snyder,D.L. and Miller,M.I., "Random Point Processes in Time and Space," (Springer Verlag, New York, 1991).

11. Papoulis,A., "Probability, random variables, and stochastic processes," 3 edition (McGraw Hill, New York, 1991).

12. Wagner,R.F., "Toward a unified view of radiological imaging systems. Part II: Noise images," Med Phys 4, 279-296 (1977).

13. Sandrik,J.M. and Wagner,R.F., "Absolute measures of physical image quality: measurement and application to radiographic magnification," Med Phys 9, 540-549 (1982).

14. Metz,C.E. and Vyborny,C.J., "Wiener spectral effects of spatial correlation between the sites of characteristic x-ray emission and reabsorption in radiographic screen-film systems," Phys Med Biol 28, 547-564 (1983).

15. Shaw,R. and Van Metter,R.L., "An analysis of the fundamental limitations of screen-film systems for x-ray detection I. General theory," in Application of Optical Instrumentation in Medicine XII, Schneider,R.H. and Dwyer,S.J., Editors, Proc SPIE 454, 128-132 (1984).

16. Rabbani,M., Shaw,R., and Van Metter,R.L., "Detective quantum efficiency of imaging systems with amplifying and scattering mechanisms," J Opt Soc Am A 4, 895-901 (1987).

17. Barrett,H.H., Wagner,R.F., and Myers,K.J., "Correlated point processes in radiological imaging," in Medical Imaging 1997: Physics of Medical Imaging, Van Metter,R.L. and Beutel,J., Editors, Proc SPIE 3032, 110-125 (1997).

18. Maidment,A.D. and Yaffe,M.J., "Analysis of the spatial-frequency-dependent DQE of optically coupled digital mammography detectors," Med Phys 21, 721-729 (1994).

19. Mulder,H., "Signal and noise transfer through imaging systems consisting of a cascade of amplifying and scattering processes," J Opt Soc Am A 10, 2038-2045 (1993).

20. Nishikawa,R.M. and Yaffe,M.J., "Effect of various noise sources on the detective quantum efficiency of phosphor screens," Med Phys 17, 887-893 (1990).

21. Nishikawa,R.M. and Yaffe,M.J., "Model of the spatial-frequency-dependent detective quantum efficiency of phosphor screens," Med Phys 17, 894-904 (1990).

22. Barrett,H.H. and Swindell,W., "Radiological Imaging," (Academic Press, New York, 1981).

23. Gaskill,J.D., "Linear Systems, Fourier Transforms, and Optics," (John Wiley & Sons, New York, 1978).

24. Giger,M.L. and Doi,K., "Investigation of basic imaging properties in digital radiography. 1. Modulation transfer function," Med Phys 11, 287-295 (1984).

25. Chan,H.-P. and Doi,K., "Monte Carlo simulation in diagnostic radiology," in Monte Carlo Simulation in the Radiological Sciences, Morin,R.L. editors, p103-192 (CRC Press, Boca Raton, Florida, 1988).

26. Shockley,W. and Pierce,J.R., "A theory of noise for electron multipliers," Proc.Inst.Radio.Eng. 26, 321-332 (1938).

27. Zweig,H.J., "Detective quantum efficiency of photodetectors with some amplifying mechanism," J Opt Soc Am 55, 525-528 (1965).

28. Shaw,R., "The equivalent quantum efficiency of the photographic process," J Photogr Sc 11, 199-204 (1963).

29. Cunningham,I.A., Westmore,M.S., and Fenster,A., "A spatial-frequency dependent quantum accounting diagram and detective quantum efficiency model of signal and noise propagation in cascaded imaging systems," Med Phys 21, 417-427 (1994).

30. Cunningham,I.A., Westmore,M.S., and Fenster,A., "Visual impact of the non-zero spatial frequency quantum sink," in Medical Imaging 1994: Physics of Medical Imaging, Shaw,R., Editors, Proc SPIE 2163, 274-283 (1994).

31. Rossmann,K., "The spatial frequency spectrum: A means for studying the quality of radiographic imaging systems," Radiology 90, 1-13 (1968).

32. Doi,K. and Rossmann,K., "Effect of focal spot distribution on blood vessel imaging in magnification radiography," Radiology 114, 435 (1975).

33. Burgess,A.E., "Focal spots: I. MTF separability," Invest Radiol 12, 36-43 (1977).

34. Burgess,A.E., "Effect of asymmetric focal spots in angiography," Med Phys 4, 21-25 (1977).

35. Van Metter,R.L. and Rabbani,M., "An application of multivariate moment-generating functions to the analysis of signal and noise propagation in radiographic screen-film systems," Med Phys 17, 65-71 (1990).

36. Sones,R.A. and Barnes,G.T., "A method to measure the MTF of digital x-ray systems," Med Phys 11, 166-171 (1984).